Title	Study of Quark Distributions using the Light-cone Wave Function based on the Chiral Quark Soliton Model
Author(s)	大西, 陽一
Citation	大阪大学, 2006, 博士論文
Version Type	VoR
URL	https://doi.org/10.18910/46475
rights	
Note	

Study of Quark Distributions using the Light-cone Wave Function based on the Chiral Quark Soliton Model

（カイラルクォーク・ソリトン模型に基づく光円錐波動関数を用いたクォーク分布の研究）

by

Yoichi Ohnishi

Dissertation submitted

to

Graduate School of Science

at

OSAKA UNIVERSITY

for

the Degree of Doctor of Philosophy

Acknowledgments

Abstract

We study the generalized parton distribution functions (GPDs) with the light-cone wave function derived from the chiral quark soliton model, which is an effective model of baryons maximally incorporating the spontaneously chiral symmetry breaking of the QCD vacuum. In the relativistic mean field approximation in this model, one obtains a quantitative picture of baryons as localized states of constituent quarks bound by a self-consistent chiral filed. Simultaneously, the negative Dirac sea is distorted by the same chiral field, leading to the presence of an indefinite number of additional quark-antiquark pairs in the baryons. Then the baryon wave functions can be constructed as a product of $N_c = 3$ valence quark wave functions and the coherent exponent of quark-antiquark pairs.

We present the expression of the GPDs in the light-cone frame using the light-cone wave function in this model. They are representated as the overlap integrals of the initial and final state Fock components. In the characteristic kinematical range in the representation of the GPDs, there arise non-diagonal Fock space matrix elements which never appear in the case of ordinary Feynman quark distribution functions. Consequently, GPDs contain quite new information about nucleon structure.

We numerically investigate the GPDs under various limiting conditions. In the forward limit, GPDs reduce to the ordinary Feynman parton distribution. When one leave the transverse momentum of the struck quark unintegrated, the transverse momentum dependent quark distribution function can be obtained. In the purely transverse momentum transfer case, GPDs become the probability density of both the longitudinal momentum direction and impact parameter space. We emphasize that the chiral symmetry breaking of the QCD plays a very important role in all kind of distribution functions.

Contents

I. INTRODUCTION

The fundamental particles which form hadrons are long known to be quarks and gluons, whose interactions are described by the Lagrangian of Quantum Chromo Dynamics (QCD):

$$\mathcal{L} = \sum_f \bar{\psi}_f \left(i\slashed{\partial} - m_f + g\slashed{A}\right)\psi_f - \frac{1}{4}F^a_{\mu\nu}F^{a\mu\nu}, \tag{1}$$

where the Minkowski metric is $g_{\mu\nu} = \text{diag}\{1, -1, -1, -1\}$. Thtoughout, we use the natural units $\hbar = c = 1$. A striking property of QCD is that of asymptotic freedom at short distances [1–3]. However, this knowledge is not sufficient (at the moment) for concluding that we are completely understanding QCD, since the mechanism of hadronization of quarks and gluons is governed by long-distance phenomena such as confinement and spontaneous chiral symmetry breaking. These long-distance phenomena are in turn related to the non-trivial structure of the QCD vacuum. It implies that the studies of hadronization processes provide us with valuable information on the fundamental questions of the vacuum structure of non-abelian gauge theories.

The spin structure of the nucleon reflects interesting nonperturbative physics in QCD [10–12]. From the EMC data on polarized deep-inelastic scattering, one finds that about $(30 \pm 7)\%$ of the nucleon spin is carried by quark spin or helicity [4–6]. Natural questions are then what carries the rest of the nucleon spin? How can it be measured or calculated?

Intuitively, the candidates for the missing spin are the quark and gluon orbital angular momenta and gluon helicity. In QCD, they can be identified with matrix elements of certain quark-gluon operators in the nucleon state [7]:

$$\vec{J}_q = \int d^3 x \psi^\dagger \left[\vec{\gamma}\gamma_5 + \vec{x} \times (-i\vec{\partial})\right]\psi,$$
$$\vec{J}_g = \int d^3 x \left[(\vec{E} \times \vec{A}) - E_i(\vec{x} \times \vec{\partial})A_i\right]. \tag{2}$$

The problem, however, is that these operators take free-field expressions and are not gauge invariant in an interacting gauge theory. Hence it is doubtful that their matrix elements have any experimental significance, although they can be calculated in some theoretical models. In 1997 Ji showed that there exists a gauge-invariant decomposition of the QCD angular momentum operator into quark and gluon contributions [8]:

$$\vec{J}_q = \int d^3 x \psi^\dagger \left[\vec{\gamma}\gamma_5 + \vec{x} \times (-i\vec{D})\right]\psi,$$
$$\vec{J}_g = \int d^3 x \left[\vec{x} \times (\vec{E} \times \vec{B})\right]. \tag{3}$$

The quark part can be separated into the usual quark helicity plus the gauge-invariant orbital contribution. There exists, however, no gauge-invariant separation of the gluon part into helicity and orbital contributions, although high-energy scattering favors such a separation in the light-like gauge and infinite momentum frame. The gauge-invariant expression for the angular momentum operator allows one to calculate meaningfully fractions of the nucleon spin carried by quarks and gluons. Furthermore, it allows them to be measured in deeply virtual Compton scattering (DVCS) in which the virtual photon momentum approaches the Bjorken limit. DVCS gives an access to a new class of nucleon observables the Generalized Parton Distributions (GPDs) [13–17].

GPDs are generalization of ordinary parton distributions and elastic form factors. Taking the n-th moment of the GPDs one obtains the form factors i.e., off-forward matrix elements of the spin-n, twist-two quark and gluon operators. On the other hand, in the forward limit the GPDs reduce to the usual quark, antiquark and gluon distributions. In other words, the GPDs interpolate between the traditional inclusive (parton distributions) and exclusive (form factors) characteristics of baryons and thus provide us with a considerable new amount of information on baryon structure. The most interesting aspect of the GPDs is that in addition to the parton intrinsic spin they also contain information on their orbital angular momenta [8]. Hence the measurement of GPDs would allow us to determine the quark orbital angular momentum contribution to the proton spin.

The clearest information about GPDs can be obtained in DVCS and in hard exclusive electroproduction of mesons,

$$\gamma^*(q) + N(p) \to \gamma(q') + N(p'), \quad \gamma^*(q) + N(p) \to M(q') + N(p'). \tag{4}$$

in which a photon γ^* with high energy and large virtuality $-q^2 = Q^2 > 0$ scatters off the hadoronic target N and produces a meson M or a real photon γ. The common important feature of hard reactions is the possibility to clearly separate the perturbative and nonperturbative stages of the interactions, this is the so-called factorization theorem [17]. The hard process-dependent parts are calculated according to perturbative QCD and the soft process-independent part is usually encoded in soft functions, GPDs. Usually, formal definition of soft part can be formulated in terms of definite quark and gluon matrix elements (here we show it for the quark operator only)

$$\int \frac{dz}{2\pi} e^{ixz} \langle N(p') | \bar{\psi}_\alpha(0) \, P \, e^{ig \int_0^z dx_\mu A^\mu} \, \psi_\beta(z) | N(p) \rangle, \tag{5}$$

2

where the operators are on the "*light cone*", i.e. $z^2 = 0$. The GPDs depend upon three variables $x = \bar{k}^+/\bar{P}^+, \xi = 2(p' - p)/\bar{P}^+$ and $t = (p' - p)^2$. In the Bjorken scaling limit, GPDs probe light-like correlations in the target.

In principle, any soft part can be expressed in terms of the hadron wave-function. The advantage of making use of the light-cone formalism is that only in that frame one can express GPDs probed in hard process as a ground state property of the nucleon. In all other frames the light-like correlation function involves correlations in the time direction and therefore knowledge of the ground state wave function of the target is not sufficient to describe GPDs. One also needs to know the time evolution of the target with one quark replaced by a quark that moves with nearly the speed of light along a straight line [18-24].

Unfortunately up to now, the light-cone wave functions of baryons in the low normalization point cannot be determined from the first principle of QCD. Perturbative theory is able to predict only the so-called asymptotic wave functions which are normalized at arbitrary high normalization point. For this reason, reliable models of the baryons become highly desirable.

Recently, Petrov and Polyakov calculated the light-cone wave function based on the Chiral Quark Soliton Model (CQSM) which is an effective model of baryons maximally incorporating the spontaneous chiral symmetry breaking of the QCD vacuum [25]. The CQSM has been derived from the instanton liquid model of the QCD vacuum, which provides a natural mechanism of chiral symmetry breaking and enables one to reproduce the dynamical quark mass M [26-29]. In the relativistic mean field approximation in the CQSM, one obtains a quantitative picture of baryons as localized states of constituent quarks bound by a self-consistent chiral filed. Simultaneously, the negative Dirac sea is distorted by the same chiral field, leading to the presence of an indefinite number of additional quark-antiquark pairs in the baryons. Petrov and Polyakov used the technique of the finite time evolution operator in order to obtain expressions for all Fock components describing the baryons [25]. Then the baryon wave functions can be constructed as a product of $N_c = 3$ valence quark wave functions and the coherent exponent of $Q\bar{Q}$ pairs. In the infinite momentum frame of baryon, the expansion of the coherent exponent is well defined, and light cone baryon wave functions are mainly represented by the $3Q$ and $5Q$ Fock components [30, 31]. Recently, Diakonov and Petrov developed the framework for calculating the static physical observable in terms of the light-cone wave functions obtained in the CQSM [32]. They showed that the

3

octet and decuplet baryons have non-negligible $5Q$ components in addition to their leading $3Q$ components, while $3Q$ component of exotic antidecuplet baryon is identically zero.

In this thesis, we numerically evaluate various structure functions using the light-cone baryon wave functions based on the CQSM. These include transverse momentum dependent parton distribution functions $q(x, \mathbf{k}_\perp)$, spin non-flip GPDs $H(x, \xi, \Delta^2), E(x, \xi, \Delta^2), \widetilde{H}(x, \xi, \Delta^2)$ and $\widetilde{E}(x, \xi, \Delta^2)$, and impact parameter space parton distribution functions $q(x, \mathbf{b}_\perp)$. The transverse momentum dependent PDF $q(x, \mathbf{k}_\perp)$ is the probability of finding a quark with longitudinal momentum xP^+ and transverse momentum $\mathbf{k}_\perp$ in a nucleon. Following the Ji's sum rule, the second moment of the combination $H^q(x, 0, 0)$ and $E^q(x, 0, 0)$ gives the total quark contribution to the nucleon spin

$$\int_{-1}^{1} dx\, x\, (H^q(x, 0, 0) + E^q(x, 0, 0)) = J^q. \tag{6}$$

Thus, a deep understanding of the spin structure of the nucleon can be achieved through the study of GPDs. The impact parameter space PDF $q(x, \mathbf{b}_\perp)$ is the Fourier transform of the GPD in the limit $\xi \to 0$

$$H(x, 0, -\Delta_\perp^2) = \int d^2 \mathbf{b}_\perp e^{i\mathbf{\Delta}_\perp \cdot \mathbf{b}_\perp} q(x, \mathbf{b}_\perp). \tag{7}$$

$q(x, \mathbf{b}_\perp)$ represents the momentum density to find a quark with momentum fraction x in the longitudinal direction and the spatial density in the transverse directions. All the quantities are represented by the overlap integral of the initial and final state Fock components sandwiching the matrix elements of corresponding operator. We emphasize that the chiral symmetry plays various important roles in the internal structure of the baryon. In particular, the region $0 < x < \xi/2$ where baryon emits a quark-antiquark pair, GPDs contain completely new information about baryon structure. In this region, the initial $5Q$ and final $3Q$ overlap are relevant, and the model prediction shows that the GPDs as functions of x exhibit discontinuity at $|x| = \xi/2$.

The plan of this thesis is as follows. In Sec. II we outline the QCD definition of the GPDs and their basic properties. Section III gives an introduction to the chiral quark soliton model of the nucleon and a derivation of the light-cone wave function based on this model. In Sec. IV we derive the expressions for the GPDs including the impact parameter space distribution and the transverse momentum dependent distribution in the chiral quark soliton model. We show that the contributions in the region $x < |\xi|/2$ to the GPDs can

4

be interpreted as the distribution amplitudes for the mesons convoluted with the valence wave functions of the baryon. Numerical estimates for the transverse momentum dependent $q(x, \mathbf{k}_\perp)$, spin non-flip GPDs $H(x, \xi, \Delta^2)$ and $\tilde{H}(x, \xi, \Delta^2)$, and impact parameter space parton distribution functions $q(x, \mathbf{b}_\perp)$ are presented in Sec. V. A summary and conclusions are given in Sec. VI.

II.   QCD DEFINITION OF GENERALIZED PARTON DISTRIBUTIONS

To start, consider the bilocal operator $\bar{\psi}(-\lambda n/2)\mathcal{L}\Gamma^\mu\psi(\lambda n/2)$, where λ is a scalar parameter, ψ is a quark field of a certain flavor, and $\Gamma^\mu = \gamma^\mu$ or $\gamma^\mu\gamma_5$. Throughout, we will use light-cone coordinate system,

$$x^\pm = \frac{1}{\sqrt{2}}(x^0 \pm x^3), \quad x_\perp = (x_1, x_2), \tag{8}$$

and all other vectors are treated in the same way. The light-like vector n is proportional to $(1,0,0,-1)$, with a coefficient depending on the choice of coordinates. The gauge link $\mathcal{L}$ is along a straight line segment extending on the choice from one quark field to the other, which makes the bilocal operator gauge invariant. In the following, we work in the light-like gauge, $A \cdot n = 0$, so that the gauge link can be ignored.

One can now proceed to the matrix element of the bilocal operator between the nucleon states with momenta P^μ and $P'^\mu = P^\mu + \Delta^\mu$, where Δ^μ is the four momentum transfer. The matrix element must be expressible in terms of nucleon spinors, Dirac matrices, and the four-vectors P^μ, Δ^μ and n^μ. Since we are only interested in the leading-twist contributions which are proportional to P^μ or P'^μ in the infinite momentum frame, we keep terms that are non-vanishing after multiplication by n^μ:

$$F_{\gamma^+}(x,\xi,t) = \int \frac{d\lambda}{4\pi}e^{ixM_B\lambda}\langle P'|\bar{\psi}(-\lambda n/2)\gamma^+\psi(\lambda n/2)|P\rangle = H(x,\xi,t)\frac{\bar{U}(P')\gamma^+U(P)}{2P^+} \tag{9}$$

$$+ E(x,\xi,t)\bar{U}(P')\frac{i\sigma^{+\nu}\Delta_\nu}{4P^+M_B}U(P)$$

$$+ \quad ,$$

$$F_{\gamma^+\gamma_5}(x,\xi,t) = \int \frac{d\lambda}{4\pi}e^{ixM_B\lambda}\langle P'|\bar{\psi}(-\lambda n/2)\gamma^+\gamma_5\psi(\lambda n/2)|P\rangle = \widetilde{H}(x,\xi,t)\frac{\bar{U}(P')\gamma^+\gamma_5U(P)}{2P^+} \tag{10}$$

$$+ \widetilde{E}(x,\xi,t)\bar{U}(P')\frac{\Delta^+\gamma_5}{4P^+M_B}U(P)$$

$$+$$

where $t \equiv \Delta^2$ and $\xi \equiv -n\ \Delta/2$, with $U(P)$ the nucleon spinor, the dots $(\cdots)$ denote higher-twist contributions, and M_B denotes the baryon mass. It is possible to construct other Dirac structures that appear to be leading-twist, however, using Gordon identities and throwing away sub-leading terms one can always reduce these to the form in Eqs.(9-10). The structures in Eqs.(9-10) are the same as those in the definition of the nucleon's elastic form factors. Examination of the helicity structure of quark-nucleon scattering shows

6

that there are exactly four independent amplitudes. The chiral-even distributions H and $\widetilde{H}$ survive in the forward limit in which the nucleon helicity is conserved, while the chiral-odd distributions E and $\widetilde{E}$ arise from the nucleon helicity flip associated with a finite momentum transfer.

A. Properties of GPDs

The GPDs are depicted graphically in Fig.1, where k^μ and k'^μ are the four-momenta of the active partons. The physical meaning of the distributions becomes clear if one introduces
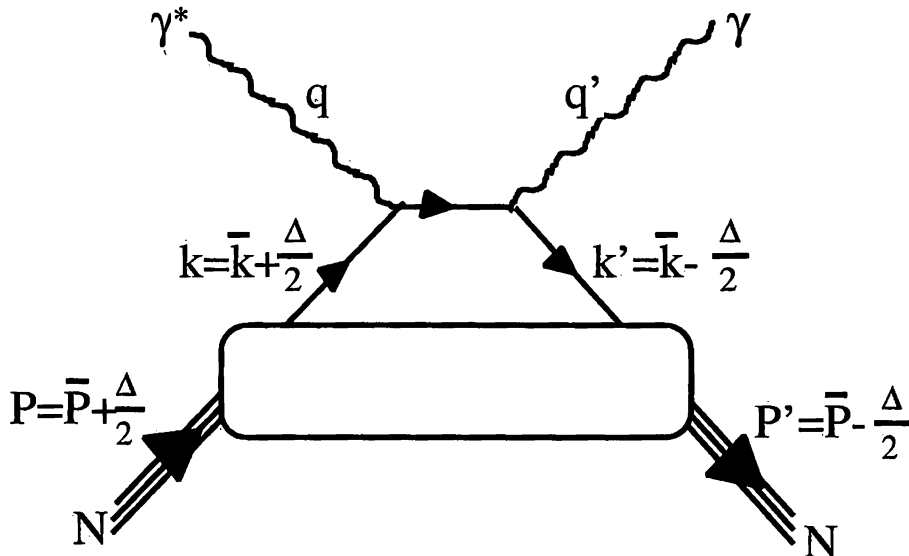
FIG. 1: "Handbag" diagram for DVCS.

a conjugate light-like vector p^μ of n^μ, with $p \cdot n = 1$. Expanding $\bar{P}^\mu = (P + P')^\mu/2$ and Δ^μ in terms of the vectors p^μ and n^μ then gives:

$$\bar{P}^\mu = p^\mu + \left(\overline{M}^2/2\right) n^\mu \tag{11}$$

$$\Delta^\mu = -\xi \left(p^\mu - \left(\overline{M}^2/2\right) n^\mu\right) + \Delta^\mu_\perp, \tag{12}$$

where $\overline{M}^2 = \bar{P}^2 = M_B^2 - t/4$, and the spatial components of $\bar{P}^\mu$ have been chosen along the z-direction. If we focus on the p^μ components of the momenta, the initial and final nucleons have longitudinal momenta $(1 + \xi/2)p^\mu$ and $(1 - \xi/2)p^\mu$, and the outgoing and incoming quarks carry $(x + \xi/2)p^\mu$ and $(x - \xi/2)p^\mu$, respectively. Since the nucleon cannot

have negative longitudinal momentum, the limit on ξ is obviously:

$$0 < \xi < \sqrt{-t}/M \tag{13}$$

On the other hand, since quarks cannot carry more longitudinal momentum than parent nucleon, one has the constraint on x:

$$-1 < x < 1 \tag{14}$$

The distribution in the negative x region should be interpreted as that of the antiquarks

$$H^q(-x,\xi,t) = -H^{\bar{q}}(x,\xi,t), \quad E^q(-x,\xi,t) = -E^{\bar{q}}(x,\xi,t) \tag{15}$$

and

$$\widetilde{H}^q(-x,\xi,t) = \widetilde{H}^{\bar{q}}(x,\xi,t), \quad \widetilde{E}^q(-x,\xi,t) = \widetilde{E}^{\bar{q}}(x,\xi,t). \tag{16}$$

With the phase conventions of the Brodsky-Lepage light-cone spinors in Appendix A, it is convenient to introduce the following decomposition for Eqs.(9) and (10) in terms of the light-cone helicities λ, λ'

$$\mathcal{H}_{\lambda\lambda'} \equiv F_{\gamma^+}(x,\xi,t), \tag{17}$$

$$\widetilde{\mathcal{H}}_{\lambda\lambda'} \equiv F_{\gamma^+\gamma_5}(x,\xi,t). \tag{18}$$

The spinor products in RHS of Eqs.(9) and (10) now read [23, 24]

$$\frac{1}{2\bar{P}^+}\bar{U}(P,\lambda)\gamma^+ U(P',\lambda') = \sqrt{1-\xi^2}\delta_{\lambda,\lambda'}, \tag{19}$$

$$\frac{1}{2\bar{P}^+}\bar{U}(P,\lambda)\frac{i\sigma^{+\nu}\Delta_\nu}{2M_B}U(P',\lambda') = -\frac{\xi^2}{\sqrt{1-\xi^2}}\delta_{\lambda,\lambda'} + \frac{1}{\sqrt{1-\xi^2}}\frac{-\lambda\Delta^1 - i\Delta^2}{2M_B}\delta_{\lambda,-\lambda'}, \tag{20}$$

$$\frac{1}{2\bar{P}^+}\bar{U}(P,\lambda)\gamma^+\gamma_5 U(P',\lambda') = \lambda\sqrt{1-\xi^2}\delta_{\lambda,\lambda'}, \tag{21}$$

$$\frac{1}{2\bar{P}^+}\bar{U}(P,\lambda)\frac{\Delta^+\gamma_5}{2M_B}U(P',\lambda') = -\frac{\xi}{\sqrt{1-\xi^2}}\delta_{\lambda,\lambda'} + \frac{1}{\sqrt{1-\xi^2}}\frac{-\lambda\Delta^1 - i\Delta^2}{2M_B}\delta_{\lambda,-\lambda'} \tag{22}$$

For the different helicity combinations we now find

$$\mathcal{H}_{++} \equiv \mathcal{H}_{--} = \sqrt{1-\xi^2}H(x,\xi,t) - \frac{\xi^2}{\sqrt{1-\xi^2}}E(x,\xi,t), \tag{23}$$

$$\mathcal{H}_{-+} \equiv -(\mathcal{H}_{+-})^* = \eta\frac{\sqrt{t_0-t}}{2M_B}E(x,\xi,t), \tag{24}$$

$$\widetilde{\mathcal{H}}_{++} \equiv -\widetilde{\mathcal{H}}_{--} = \sqrt{1-\xi^2}\widetilde{H}(x,\xi,t) - \frac{\xi^2}{\sqrt{1-\xi^2}}\widetilde{E}(x,\xi,t), \tag{25}$$

$$\widetilde{\mathcal{H}}_{-+} \equiv \left(\widetilde{\mathcal{H}}_{+-}\right)^* = \eta\xi\frac{\sqrt{t_0-t}}{2M_B}\widetilde{E}(x,\xi,t), \tag{26}$$

8

with t_0 defined as $t_0 = \xi^2 M_B^2/(1 - \xi^2/4)$ and a phase factor reading

$$\eta = \frac{\Delta^1 + \Delta^2}{|\Delta_\perp|}. \tag{27}$$

Evaluating $\mathcal{H}_{\lambda,\lambda'}$ and $\widetilde{\mathcal{H}}_{\lambda,\lambda'}$ for both helicity flip and non-flip, one obtains the usual GPDs H and E. In this study, we will calculate the helicity non-flip parts Eqs.(23) and (25) using the light-cone wave function based on the chiral quark soliton model.

1. Generalized form factors and polynomiality condition

The electromagnetic form factors are among the first measured and mostly studied observables of the nucleon [33]. They are defined as the matrix elements of the electromagnetic current between the nucleon states of different four momenta. Because the nucleon is a spin one-half particle, the matrix element defines two form factors

$$\langle p'|J^\mu(0)|p\rangle = \bar{U}(p') \left(F_1(t)\gamma^\mu + F_2(t)\frac{i\sigma^{\mu\nu}\Delta_\nu}{2M_B} \right) U(p), \tag{28}$$

where F_1 and F_2 are the well-known Dirac and Pauli form factors, respectively. One of the most important sources of information about the nucleon structure is the form factors of the electroweak currents. The Pauli form factor F_2 gives the anomalous magnetic moment of the nucleon, $\kappa = F_2(0)$. The charge radius of the nucleon is defined by

$$\langle r^2 \rangle = -6 \frac{dG_E(t)}{dt}\bigg|_{t=0} \tag{29}$$

where $G_E = F_1 - t/(4M^2)F_2$. The axial vector current also defines two form factors,

$$\langle P'|\bar{\psi}\gamma^\mu\gamma_5\psi|P\rangle = G_A(t)\bar{U}(P')\gamma^\mu\gamma_5 U(P) + G_P(t)\bar{U}(P')\frac{\gamma_5\Delta^\mu}{2M_B}U(P) \tag{30}$$

The axial form factor $G_A(0)$ at $t = 0$ is related to the fraction of the nucleon spin carried by the spin of the quarks, $\Delta\Sigma$, and can be measured from polarized DIS and neutrino elastic scattering [4–6]. (Note, however, that $G_A(0) \neq \Delta\Sigma$ with taking into consideration of the axial U(1) anomaly [9].)

A generalization of the vector and axial-vector currents can be made through the following sets of twist-two operators,

$$O_q^{\mu_1,\cdots\mu_n} = \bar{\psi}_q\gamma^{(\mu_1}iD^{\mu_2}\cdots iD^{\mu_n)}\psi,$$

$$\tilde{O}_q^{\mu_1,\cdots\mu_n} = \bar{\psi}_q\gamma^{(\mu_1}\gamma_5 iD^{\mu_2}\cdots iD^{\mu_n)}\psi, \tag{31}$$

9

where all indices $\mu_1 \cdots \mu_n$ are symmetric and traceless, as indicated by (...) in the superscripts. These operators form the totally symmetric representation of the Lorentz group. One can similarly introduce the gluon twist-two operators. For $n > 1$, the above operators are not conserved currents from any global symmetry. Consequently, their matrix elements depend on the momentum-transfer scale μ at which they are probed. For the same reason, there is no low-energy probe that couples to these currents.

One can define the generalized charges $a_n(\mu^2)$ from the forward matrix elements of these currents [34]:

$$\langle P'|O^{\mu_1,\cdots\mu_n}|P\rangle = 2a_n(\mu^2)P^{(\mu_1}P^{\mu_2}\cdots P^{\mu_n)} \tag{32}$$

The moments of the Feynman parton distribution $q(x,\mu^2)$ are related to these charges as

$$\int_{-1}^{1} dx\, x^{n-1}q(x,\mu^2) = \int_{0}^{1} dx\, x^{n-1}\left[q(x,\mu^2) + (-1)^n\bar{q}(x,\mu^2)\right] = a_n(\mu^2) \tag{33}$$

where $\bar{q}(x,\mu^2)$ is defined in the range $-1 < x < 1$. For $x > 0$, $q(x,\mu^2)$ is simply the density of quarks that carry the fraction x of the parent nucleon momentum. The density of antiquarks is customarily denoted by $\bar{q}(x,\mu^2)$, which in the above notation is $-q(-x,\mu^2)$ for $x < 0$.

One can also define the form factors $[A_{qn,m}(t), B_{qn,m}(t)$, and $C_{qn}(t)]$ of these currents using constraints from charge conjugation, parity, time-reversal, and Lorentz symmetries [34]

$$\langle P'|\, O_q^{\mu_1,\cdots\mu_n}|P\rangle$$

$$= \bar{U}(P')\gamma^{(\mu_1}U(P)\sum_{i=0}^{[\frac{n-1}{2}]} A_{qn,2i}(t)\Delta^{\mu_2}\cdots\Delta^{\mu_{2i+1}}\bar{P}^{\mu_{2i+2}}\cdots\bar{P}^{\mu_n)}$$

$$+ \bar{U}(P')\frac{\sigma^{(\mu_1\alpha}i\Delta_\alpha}{2M_B}U(P)\sum_{i=0}^{[\frac{n-1}{2}]} B_{qn,2i}(t)\Delta^{\mu_2}\cdots\Delta^{\mu_{2i+1}}\bar{P}^{\mu_{2i+2}}\cdots\bar{P}^{\mu_n)}$$

$$+ C_{qn}(t)\text{Mod}(n+1,2)\frac{1}{M_B}\bar{U}(P')U(P)\Delta^{(\mu_1}\cdots\Delta^{\mu_n)}\,, \tag{34}$$

where $\text{Mod}(n+1,2)$ is 1 when n is even and 0 when n is odd. Thus, C_{qn} is present only when n is even. Multiplying the light-cone vector n^μ,

$$n_{\mu_1}\cdots n_{\mu_n}\langle P'|O^{\mu_1,\cdots\mu_n}|P\rangle = H_n(\xi,t)\bar{U}\rlap{/}{n}U + E_n(\xi,t)\bar{U}\frac{i\sigma^{\mu\nu}n_\mu\Delta_\nu}{2M_B}U \tag{35}$$

where $H_n(\xi,t)$ and $E_n(\xi,t)$ are polynomials in ξ^2 of degree $n/2$ (n even) or $n-1/2$ (n odd). The coefficients of the polynomials are form factors. It is easy to see that they are the moments of the GPDs $E(x,\xi,t)$ and $H(x,\xi,t)$:

$$\int_{-1}^{1} dx\, x^{n-1}E(x,\xi,t) = E_n(\xi,t)$$

10

$$\int_{-1}^{1} dx\, x^{n-1} H(x, \xi, t) = H_n(\xi, t) \tag{36}$$

Therefore, although GPDs are the functions of three variables, x, ξ and t, their x moment is only a polynomial function of ξ and t. This is called the polynomiality condition.

Using Eqs.(19)-(20), F_1, F_2, G_A and G_P involve the same proton helicity structure as H and E [23, 24],

$$\frac{1}{2\bar{P}+}\langle P', +|\bar{\psi}\gamma^+\psi|P+\rangle \equiv \sqrt{1-\xi^2}F_1(t) - \frac{\xi^2}{\sqrt{1-\xi^2}}F_2(t), \tag{37}$$

$$\frac{1}{2\bar{P}+}\langle P', -|\bar{\psi}\gamma^+\psi|P+\rangle \equiv \eta\frac{\sqrt{t_0-t}}{2M_B}F_2(x, \xi, t), \tag{38}$$

$$\frac{1}{2\bar{P}+}\langle P', +|\bar{\psi}\gamma^+\gamma^5\psi|P+\rangle \equiv \sqrt{1-\xi^2}G_A(t) - \frac{\xi^2}{\sqrt{1-\xi^2}}G_P(t), \tag{39}$$

$$\frac{1}{2\bar{P}+}\langle P', -|\bar{\psi}\gamma^+\gamma^5\psi|P+\rangle \equiv \eta\xi\frac{\sqrt{t_0-t}}{2M_B}G_P(t), \tag{40}$$

More specifically, the first moments of GPDs are constrained by the form factors of the electromagnetic and axial currents. Indeed, by integrating over x, we have

$$\int_{-1}^{1} dx\, H_q(x, \xi, t) = F_1^q(t), \qquad \int_{-1}^{1} dx\, E_q(x, \xi, t) = F_2^q(t),$$

$$\int_{-1}^{1} dx\, \widetilde{H}_q(x, \xi, t) = G_A^q(t), \qquad \int_{-1}^{1} dx\, \widetilde{E}_q(x, \xi, t) = G_P^q(t), \tag{41}$$

where F_1, F_2, G_A and G_P are the Dirac, Pauli, axial, and induced pseudoscalar elastic form factors, respectively.

2. Form factors of energy-momentum tensor and spin structure of the nucleon

The physical significance of GPDs was revealed in studying the spin structure of the nucleon. Let us review this connection. In the constituent quark model, the nucleon is made of three spin 1/2 quarks moving in the s-orbit. The spin of the nucleon is then a vector sum of the quark spins. Although the simple quark model has been very successful in explaining a large body of experimental data, its prediction about the spin structure has been challenged by the polarized DIS data obtained by the European Muon Collaboration (EMC). In polarized DIS, a polarized electron exchanges a polarized photon with a polarized nucleon. The polarized photon is absorbed by a polarized quark whose helicity must have the same sign as that of the photon in the center-of-mass frame, or else angular momentum

11

conservation forbids the absorption. Therefore, polarized DIS allows measurement of the polarized quark distributions in the polarized nucleon. From the data taken in a number of recent experiments, along with the analysis of neutron and hyperon β-decay, the fraction of the nucleon spin carried by the quark spin is determined to be [4–6]

$$\Delta\Sigma = 0.31 \pm 0.07. \text{ (at } Q^2 = 10.7\,\mathrm{GeV}^2) \tag{42}$$

This is significantly below the naive quark model prediction $\Delta\Sigma = 1$.

The fundamental reason for the discrepancy is that the naive quark model quarks are not the same as the QCD quarks. In DIS, the photons interact directly with the QCD current. Applying the predictions of the constituent quark model to the QCD quarks is at best opportunistic. A more interesting approach to understanding the EMC data is to study the spin structure of the nucleon directly in the fundamental theory. Reference clarified the structure of the angular momentum operator in QCD, from which one can write down a decomposition of the nucleon spin:

$$\frac{1}{2} = J_q(\mu) + J_g(\mu), \tag{43}$$

where $J_{q,g}$ are the contributions from the quarks and gluons, respectively. Both contributions are gauge-invariant but renormalization-scale-dependent. $J_{q,g}(\mu)$ can be expressed as the matrix elements of the QCD energy-momentum tensor $T_{q,g}^{\mu\nu}$,

$$J_{q,g}(\mu) = \left\langle P\frac{1}{2} \Big| \int d\boldsymbol{x}\, (\boldsymbol{x} \times \boldsymbol{T}_{q,g})_z \Big| P\frac{1}{2} \right\rangle, \tag{44}$$

which can be extracted from the form factors of the quark and gluon parts of the $T_{q,g}^{\mu\nu}$. Specializing Eq.(34) to $n = 2$, one finds

$$\left\langle P' \big| T_{q,g}^{\mu\nu} \big| P \right\rangle = \bar{U}(P') \Big[A_{q,g}(t)\gamma^{(\mu}\bar{P}^{\nu)} + B_{q,g}(t)\bar{P}^{(\mu}i\sigma^{\nu)\alpha}\Delta_\alpha/2M$$
$$+ C_{q,g}(t)\Delta^{(\mu}\Delta^{\nu)}/M \Big] U(P). \tag{45}$$

Taking the forward limit of the $\mu = 0$ component and integrating over three space, one finds that the $A_{q,g}(0)$ give the momentum fractions of the nucleon carried by quarks and gluons, respectively $[A_q(0) + A_g(0) = 1]$. On the other hand, substituting the above into the nucleon matrix element of Eq.(44), one finds [8]

$$J_{q,g} = \frac{1}{2} \left[A_{q,g}(0) + B_{q,g}(0) \right]. \tag{46}$$

12

Therefore, the matrix elements of the energy-momentum tensor provide the fractions of the nucleon spin carried by quarks and gluons. There is an analogy for this. If one knows the Dirac and Pauli form factors of the electromagnetic current, $F_1(Q^2)$ and $F_2(Q^2)$, then the magnetic moment of the nucleon, defined as the matrix element of $(1/2) \int d^3x \, (\boldsymbol{x} \times \boldsymbol{J})_z$, is $F_1(0) + F_2(0)$.

Because the quark and gluon energy-momentum tensors are examples of twist-two, spin-two, helicity-independent operators, we immediately have the following sum rule for GPDs:

$$\int_{-1}^{1} dx \, x \left[H_q(x, \xi, t) + E_q(x, \xi, t) \right] = A_q(t) + B_q(t), \tag{47}$$

where the ξ dependence, or $C_q(t)$ contamination, drops out. If we extrapolate the sum rule to $t = 0$, the total quark contribution to the nucleon spin is obtained. The total quark contribution J_q can be decomposed gauge-invariantly into the quark spin $\Delta\Sigma/2$ and orbital contribution L_q:

$$J_q = \frac{\Delta\Sigma}{2} + L_q. \tag{48}$$

Knowing J_q and $\Delta\Sigma$, one can extract the quark orbital angular momentum. Thus, a deep understanding of the spin structure of the nucleon can be achieved through the study of GPDs.

3. Transverse momentum dependent (TMD) parton distributions

Parton distributions were introduced by Feynman to describe DIS. They have the simplest interpretation in the infinite momentum frame as the densities of partons in the longitudinal momentum x. In QCD, the quark distribution is defined through the following matrix element:

$$q(x) = \frac{1}{2p^+} \int \frac{d\lambda}{2\pi} e^{i\lambda x} \langle P | \bar\psi(-\lambda n/2) \gamma^+ \psi(\lambda n/2) | P \rangle \tag{49}$$

In the light-cone quantization, it is easy to show

$$q(x)\Big|_{x>0} = \frac{1}{2x} \sum_\lambda \int \frac{d^2 k_\perp}{(2\pi)^3} \frac{\langle P | b_\lambda^\dagger(k^+, k_\perp) b_\lambda(k^+, k_\perp) | P \rangle}{\langle P | P \rangle},$$

$$q(x)\Big|_{x<0} = \frac{-1}{2x} \sum_\lambda \int \frac{d^2 k_\perp}{(2\pi)^3} \frac{\langle P | d_\lambda^\dagger(k^+, k_\perp) d_\lambda(k^+, k_\perp) | P \rangle}{\langle P | P \rangle}, \tag{50}$$

where $b^\dagger$ and $d^\dagger$ are creation operators of a quark and an antiquark, respectively, with longitudinal momentum $k^+ \equiv xp^+$ and transverse momentum $k_\perp$. The interpretation as parton densities is then obvious.

13

The TMD parton distribution functions are defined through the quark density matrix

$$q(x, \mathbf{k}_\perp) + q_T(x, \mathbf{k}_\perp)(\mathbf{k}_\perp \times \mathbf{S}_\perp) \cdot \mathbf{p}$$

$$= \frac{1}{2} \int \frac{d^2\lambda_\perp d\lambda^-}{(2\pi)^3} e^{i(k^+\lambda^- - \mathbf{k}_\perp \cdot \boldsymbol{\lambda}_\perp)} \langle P|\bar{\psi}(0)\gamma^+\psi(\lambda^-, \boldsymbol{\lambda}_\perp)|P\rangle. \tag{51}$$

The new distributions generalize those of Feynman with additional information about partons' transverse momentum. For example, $q(x, \mathbf{k}_\perp)$ is, roughly speaking, the probability of finding a quark with longitudinal momentum xP^+ and transverse momentum $\mathbf{k}_\perp$ in a nucleon (or hadron) with four-momentum $P^\mu = (P^0, 0, P^3)$.

The transverse-polarization $\mathbf{S}_\perp$-dependent term $q_T(x, \mathbf{k}_\perp)$ was first introduced by Sivers and has been called the Sivers function [35]. Physically, it signifies that the parton momentum distribution in a transversely polarized nucleon is not rotationally invariant along the z-direction. It has an azimuthal dependence. At first glance this term appears to violate the naive time-reversal invariance; however, a careful examination indicates that time reversal does not forbid its existence because the quark field contains the gauge link. It has been shown phenomenologically that $q_T(x, \mathbf{k}_\perp)$ can be responsible for the target single-spin asymmetry observed in semi-inclusive deep-inelastic production of pions [35].

When $\Gamma = \gamma^+\gamma_5$, one finds [36, 37]

$$\Delta q(x, \mathbf{k}_\perp)(S \cdot n) + \Delta q_T(x, \mathbf{k}_\perp)(\mathbf{k}_\perp \cdot \mathbf{S}_\perp)$$

$$= \frac{1}{2} \int \frac{d^2\lambda_\perp d\lambda^-}{(2\pi)^3} e^{i(k^+\lambda^- - \mathbf{k}_\perp \cdot \boldsymbol{\lambda}_\perp)} \langle P|\bar{\psi}(0)\gamma^+\gamma_5\psi(\lambda^-, \boldsymbol{\lambda}_\perp)|P\rangle. \tag{52}$$

where $\Delta q(x, \mathbf{k}_\perp)$ is a novel quark helicity distribution in a transversely polarized nucleon. With $\Gamma = \sigma^{+\perp}\gamma_5$, one has four TMD distributions,

$$\delta q_{T'}(x, \mathbf{k}_\perp)\mathbf{S}_\perp + \delta q_T(x, \mathbf{k}_\perp)\mathbf{k}_\perp(\mathbf{k}_\perp \cdot \mathbf{S}_\perp) + \delta q(x, \mathbf{k}_\perp)\mathbf{k}_\perp + \delta q_L(x, \mathbf{k}_\perp)\mathbf{k}_\perp(\mathbf{n} \cdot \mathbf{S})$$

$$= \frac{1}{2} \int \frac{d^2\lambda_\perp d\lambda^-}{(2\pi)^3} e^{i(k^+\lambda^- - \mathbf{k}_\perp \cdot \boldsymbol{\lambda}_\perp)} \langle P|\bar{\psi}(0)\sigma^{+\perp}\gamma_5\psi(\lambda^-, \boldsymbol{\lambda}_\perp)|P\rangle. \tag{53}$$

where $\delta q(x, \mathbf{k}_\perp)$ is a transversity distribution in an unpolarized nucleon and vanishes under naive time-reversal transformation; $\delta q_L(x, \mathbf{k}_\perp)$ is a transversity distribution in a longitudinally polarized nucleon.

TMD distributions have wide-ranging phenomenological applications in semiinclusive DIS, the Drell-Yan process, and back-to-back jet production in e^+e^- annihilation [36–38].

14

4. Partonic interpretation of GPDs

From their definition, it is straightforward to see that in the limit $\xi \to 0$ and $t \to 0$, GPDs reduce to ordinary parton distributions. For instance,

$$H_q(x, 0, 0) = q(x), \quad \widetilde{H}_q(x, 0, 0) = \Delta q(x), \tag{54}$$

where $q(x)$ and $\Delta q(x)$ are the unpolarized and polarized quark distributions. For practical purposes, in the kinematic region where

$$\sqrt{|t|} \ll M_N \quad \text{and} \quad \xi \ll x, \tag{55}$$

an off-forward distribution may be approximated by the corresponding forward one. The first condition, $\sqrt{|t|} \ll M_N$, is crucial - otherwise there is a significant form-factor suppression that cannot be neglected at any x and ξ. For a given t, ξ is restricted to $|\xi| < \sqrt{-t}/M$. Therefore, when $\sqrt{|t|}$ is small, ξ is automatically limited, and there is in fact a large region of x where the forward approximation holds.

The parton content of GPDs is made transparent in light-cone coordinates and light-cone gauge. To see this, let us recall

$$F_{\gamma^+} = \frac{1}{2} \int \frac{d\lambda}{2\pi} e^{i\lambda x} \langle P' | \bar{\psi}_q \left(-\frac{\lambda}{2} n \right) \not{n} \mathcal{P} e^{-ig \int_{\lambda/2}^{-\lambda/2} d\alpha \, n \cdot A(\alpha n)} \psi_q \left(\frac{\lambda}{2} n \right) | P \rangle \tag{56}$$

where the gauge-link operator is explicitly shown. In the light-cone gauge $n \cdot A = 0$, the gauge link between the quark fields can be ignored. Using the light-cone coordinate system (8), we can expand the Dirac field as follows:

$$\psi_+(x^-, \boldsymbol{x}_\perp) = \int \frac{dk^+ d^2 \boldsymbol{k}_\perp}{2k^+ (2\pi)^3} \theta(k^+) \sum_{\lambda = \pm} \left(b_\lambda(k^+, \boldsymbol{k}_\perp) u_\lambda(k) e^{-i(x^- k^+ - \boldsymbol{x}_\perp \cdot \boldsymbol{k}_\perp)} \right.$$
$$\left. + d_\lambda^\dagger(k^+, \boldsymbol{k}_\perp) v_\lambda(k) e^{i(x^- k^+ - \boldsymbol{x}_\perp \cdot \boldsymbol{k}_\perp)} \right) \tag{57}$$

where $\psi_+ = P_+ \psi$ and $P_\pm = \frac{1}{2} \gamma^\mp \gamma^\pm$. The quark (antiquark) creation and annihilation operators, $b_{\lambda k}^\dagger (d_{\lambda k}^\dagger)$ and $b_{\lambda k} (d_{\lambda k})$, obey the usual commutation relation. Substituting the above into Eq.(56), we have [39]

$$F_q(x, \xi) = \frac{1}{2p^+ V} \int \frac{d^2 k_\perp}{2\sqrt{|x^2 - \xi^2/4|}(2\pi)^3} \sum_\lambda$$

$$\times \begin{cases} \langle P' | b_\lambda^\dagger((x - \xi/2)p^+, \vec{k}_\perp + \vec{\Delta}_\perp) b_\lambda((x + \xi/2)p^+, \vec{k}_\perp) | P \rangle, & \text{for } x > \xi/2 \\ \langle P' | d_\lambda^\dagger((-x + \xi/2)p^+, -\vec{k}_\perp - \vec{\Delta}_\perp) b_{-\lambda}((x + \xi/2)p^+, \vec{k}_\perp) | P \rangle, & \text{for } \xi > x > -\xi/2 \\ -\langle P' | d_\lambda^\dagger((-x - \xi/2)p^+, \vec{k}_\perp + \vec{\Delta}_\perp) d_\lambda((-x + \xi/2)p^+, \vec{k}_\perp) | P \rangle, & \text{for } x < -\xi/2 \end{cases} \tag{58}$$

where V is a volume factor. The distribution has different physical interpretations in the three different regions. In the region $x > \xi/2$, it is the amplitude for taking a quark of momentum k out of the nucleon, changing its momentum to $k + \Delta$, and inserting it back to form a recoiled nucleon. In the region $\xi/2 > x > -\xi/2$, it is the amplitude for taking out a quark and antiquark pair with momentum. Finally, in the region $x < -\xi/2$, we have the same situation as in $x > \xi/2$, except the quark is replaced by an antiquark. The first and third regions are similar to those present in ordinary parton distributions, whereas the middle region is similar to that in a meson amplitude.

5. Impact parameter space

A partonic interpretation can also be made by transforming the nucleon states to those in the impact-parameter space [40]. Indeed, the helicity nonflip GPD $H(x, \xi, t)$ for $\xi = 0$ is the Fourier transform of the (unpolarized) impact parameter dependent parton distribution function $q(x, \boldsymbol{b}_\perp)$, i.e.

$$q(x, \boldsymbol{b}_\perp) = \int \frac{d^2 \boldsymbol{\Delta}_\perp}{(2\pi)^2} e^{-i\boldsymbol{\Delta}_\perp \cdot \boldsymbol{b}_\perp} H(x, 0, -\boldsymbol{\Delta}_\perp^2). \tag{59}$$

The important advantages are that $q(x, \boldsymbol{b}_\perp)$ is a real density in the sense that it is the expectation value of a number operator, and its interpretation does not suffer from relativistic effects as explained below. The variables $\boldsymbol{b}_\perp$ and x live in different dimensions, and therefore there is no quantum mechanical uncertainty constraint. Indeed, $q(x, \boldsymbol{b}_\perp)$ is a spatial-and-momentum-density hybrid in that it represents a spatial density in the transverse directions and momentum density in the longitudinal direction. $q(x, \boldsymbol{b}_\perp)$ is also invariant under boost along the z-direction. In particular, if the nucleon has an infinity momentum, its effective mass is also infinity. Therefore, its spatial structure in the transverse directions, just like in nonrelativistic systems, can be obtained directly from the Fourier transformation of the form factors without the relativistic recoil effects [41–43].

B. Double distribution, D-term

One of the non-trivial properties of the generalized parton distributions is the polynomiality of their Mellin moments which follows from the Lorentz invariance of nucleon matrix

16

elements. Indeed the $(N+1)$-th Mellin moment of GPDs corresponds to the nucleon matrix element of the twist-2, spin-$(N+1)$ local operator as shown in Eq.(36). Lorentz invariance then dictates that the Mellin moments of GPDs should be polynomials maximally of the order $N+1$, i.e. the polynomiality property implies that [8]

$$\int_{-1}^{1} x^N H^q(x,\xi) = h_0^{q(N)} + h_2^{q(N)}\xi^2 + \cdots + h_{N+1}^{q(N)}\xi^{N+1}, \tag{60}$$

$$\int_{-1}^{1} x^N H^q(x,\xi) = e_0^{q(N)} + e_2^{q(N)}\xi^2 + \cdots + e_{N+1}^{q(N)}\xi^{N+1}. \tag{61}$$

Note that the corresponding polynomials contain only even powers of the skewedness parameter ξ. This follows from the time reversal invariance [34, 37]. This fact implies that the highest power of ξ is $N+1$ for odd N (singlet GPDs) and N for even N (nonsinglet GPDs). Furthermore due to the fact that the nucleon has spin $1/2$, the coefficients in front of the highest power of ξ for the singlet functions H^q and E^q are related to each other [34, 39]:

$$e_{N+1}^{q(N)} = -h_{N+1}^{q(N)}. \tag{62}$$

The polynomiality conditions (60) and (61) strongly restrict the class of functions of two variables $H^q(x,\xi)$ and $E^q(x,\xi)$. For example the conditions (61) imply that GPDs should satisfy the following integral constrains:

$$\int_{-1}^{1} \frac{dx}{x} [H^q(x,\xi+xz) - H^q(x,\xi)] = -\int_{-1}^{1} \frac{dx}{x} [E^q(x,\xi+xz) - E^q(x,\xi)]$$

$$= z \sum_{n=0}^{\infty} h_{n+1}^{q(n)} z^n \tag{63}$$

Note that the skewedness parameter ξ enters the LHS of this equation, whereas the RHS of the equation is ξ-independent. Therefore this ξ-independence of the above integrals is a criterion of whether the functions $H^q(x,\xi)$, $E^q(x,\xi)$ satisfy the polynomiality conditions (61). Simultaneously these integrals are generating functions for the highest coefficients $h_{N+1}^{(N)}$. In addition, the condition (63) shows that there are nontrivial functional relations between the functions $H^q(x,\xi)$ and $E^q(x,\xi)$.

An elegant possibility to implement the polynomiality conditions (61) for the GPDs is to use the double distributions [48–50]. A detailed discussion of the double distributions has been given in the review of Ref. [51]. In this case the generalized distributions are obtained as a one-dimensional section of the two-variable double distributions $F^q(\beta,\alpha)$, $K^q(\beta,\alpha)$ [52, 53]:

$$H_{DD}^q(x,\xi) = \int_{-1}^{1} d\beta \int_{-1-|\beta|}^{1-|\beta|} d\alpha\, \delta(x-\beta-\alpha\xi)F^q(\beta,\alpha), \tag{64}$$

17

and an analogous for the GPD $E^q(x, \xi)$:

$$E^q_{DD}(x, \xi) = \int_{-1}^{1} d\beta \int_{-1-|\beta|}^{1-|\beta|} d\alpha \, \delta(x - \beta - \alpha\xi) K^q(\beta, \alpha). \qquad (65)$$

Obviously, the double distribution function $F^q(\beta, \alpha)$ should satisfy the condition:

$$\int_{-1-|\beta|}^{1-|\beta|} d\alpha F^q(x, \alpha) = q(x), \qquad (66)$$

in order to reproduce the forward limit (54) for the GPD $H^q(x, \xi)$. It is easy to check that the GPDs obtained by reduction from the double distributions satisfy the polynomiality conditions (61) but always lead to $h_{N+1}^{q(N)} = e_{N+1}^{q(N)} = 0$, i.e. the highest power of ξ for the singlet GPDs is absent. In other words the parameterization of the singlet GPDs in terms of double distributions is not complete. It can be completed by adding the so-called D-term to Eqs.(64) and (65) [54]

$$H^q(x, \xi) = \int_{-1}^{1} d\beta \int_{-1-|\beta|}^{1-|\beta|} d\alpha \, \delta(x - \beta - \alpha\xi) F^q(\beta, \alpha) + \theta \left[1 - \frac{x^2}{\xi^2} \right] D^q \left(\frac{x}{\xi} \right), \qquad (67)$$

$$E^q(x, \xi) = \int_{-1}^{1} d\beta \int_{-1-|\beta|}^{1-|\beta|} d\alpha \, \delta(x - \beta - \alpha\xi) K^q(\beta, \alpha) - \theta \left[1 - \frac{x^2}{\xi^2} \right] D^q \left(\frac{x}{\xi} \right) \qquad (68)$$

Here $D^q(z)$ is an odd function (as it contributes only to the singlet GPDs) having a support $-1 \leq z \leq 1$. In the Mellin moments, the D-term generates the highest power of ξ:

$$h_{N+1}^{q(N)} = -e_{N+1}^{q(N)} = \int_{-1}^{1} dz \, z^N \, D^q(z). \qquad (69)$$

Note that for both GPDs $H^q(x, \xi)$ and $E^q(x, \xi)$ the absolute value of the D-term is the same, it contributes to both functions with opposite sign. The latter feature follows from the relation (62). Goeke, Polyakov and Vanderhaeghen have shown that numerical estimates of the D-term in the chiral quark soliton model gives $D^u(z) \simeq D^d(z)$.

C. GPDs from hard scattering

GPDs are nonperturbative nucleon observables, and apart from the general properties discussed in the previous section, we know little about the dynamical information encoded in them. This section considers several approaches to gain access to them by experimental measurement. It is fortunate that there exists a new class of hard processes in which GPDs can be measured and/or constrained. The simplest is called deeply virtual Compton scattering (DVCS).

In recent years, the search for an experimental measurement of GPDs has open up a new class of QCD hard scattering processes. The simplest, and possibly the most promising, is deep-inelastic exclusive production of photons, mesons, and even lepton pairs. Let us consider briefly two experiments that have been studied extensively in the literature: DVCS, in which a real photon is produced, and diffractive meson production. Both processes have practical advantages and disadvantages. Real photon production is, in a sense, cleaner but the cross section is reduced by an additional power of α_{em}. The Bethe-Heitler contribution can be important but can actually be used to extract the DVCS amplitude through interferences, as in a single-spin asymmetry. Meson production may be easier to detect, but it has a twist suppression of $1/Q^2$. In addition, the theoretical cross section depends on the unknown leading light-cone wave function of the mesons. DVCS was first proposed as a practical way to measure the generalized distributions. Consider virtual photon scattering in which the momenta of the incoming (outgoing) photon and nucleon are $q(q')$ and $P(P')$, respectively. The Compton amplitude is defined as

$$T^{\mu\nu} = i \int d^4z \, e^{i\bar{q}\cdot z} \langle P'|\mathrm{T}\left(J^\mu\left(-\frac{z}{2}\right) J^\nu\left(\frac{z}{2}\right)\right)|P\rangle \,, \tag{70}$$

where $\bar{q} = (q + q')/2$. In the Bjorken limit, $-q^2$ and $P \cdot q \to \infty$ and their ratio remains finite; the scattering is dominated by the single-quark process, in which a quark absorbs the virtual photon, immediately radiates a real one, and falls back to form the recoiling nucleon. In the process, the initial and final photon helicities remain the same. The leading-order Compton amplitude is then

$$T^{\mu\nu} = g_\perp^{\mu\nu} \int_{-1}^{1} dx \left(\frac{1}{x - \xi + i\epsilon} + \frac{1}{x + \xi - i\epsilon}\right) \sum_q e_q^2 F_q(x, \xi, t, Q^2)$$

$$+ i\epsilon^{\mu\nu\alpha\beta} p_\alpha n_\beta \int_{-1}^{1} dx \left(\frac{1}{x - \xi + i\epsilon} - \frac{1}{x + \xi - i\epsilon}\right) \sum_q e_q^2 \tilde{F}_q(x, \xi, t, Q^2) \,, \tag{71}$$

where n and p are the conjugate light-cone vectors defined according to the collinear direction of $\bar{q}$ and $\bar{P}$, and $g_\perp^{\mu\nu}$ is the metric tensor in transverse space. ξ is related to the Bjorken variable $x_B = -q^2/(2P \cdot q)$ by $x_B = 2\xi/(1 + \xi)$.

Development on the experimental front is promising. Recently, both ZEUS and H1 collaborations have announced the first evidence for a DVCS signature, and the HERMES collaboration at DESY and the CLAS collaboration at JLab have made the first measurements of the DVCS single-spin asymmetry [44–47]. More experiments are planned of COMPASS, JLab, and future facilities.

III. LIGHT CONE WAVE FUNCTION IN THE CHIRAL QUARK SOLITON MODEL

A. The effective model

One of the most important features of the QCD lagrangian in the low-energy domain is the chiral symmetry and its spontaneous breakdown (Throughout the thesis, we remain in the chiral limit, i.e. small "current" masses of u ,d and s quarks are ignored). As a consequence of the spontaneous breakdown of this continuous symmetry, there appear massless Nambu-Goldstone bosons (π, K, η), and at the same time, quark acquire the dynamically generated mass (It is sometimes called the "constituent" quark mass). This is the well-known Nambu-Goldstone realization of the chiral symmetry. The simplest effective model that incorporates such basic features of the low-energy QCD may be given by the following functional integral over quarks in the background Goldstone boson field [26–29]:

$$\exp(iS_{eff}[\pi(x)]) = \int D\psi D\bar{\psi} \exp(i \int d^4x \bar{\psi}(i\partial\!\!\!/ - MU^{\gamma_5})\psi)$$

$$U = \exp(i\pi^a(x)\tau^a), \qquad U^{\gamma_5}(x) = \exp(i\pi^a(x)\tau^a\gamma_5) = \frac{1+\gamma_5}{2}U + \frac{1-\gamma_5}{2}U \qquad (72)$$

Here $\psi(x)$ and $\pi^a(x)$ are, respectively, the quark and pion (including K and η) fields, while M is the dynamical quark mass stated above. Note that there is no kinetic term of the pion fields in the above effective action. This means that the $\psi(x)$ and $\pi^a(x)$ are not independent fields, but $\pi^a(x)$ is eventually interpreted as composite fields in the $Q\bar{Q}$ channel. We regard M as an adjustable parameter of the model, and can investigate the effects of its variation on the predictions of various baryon observable.

B. Soliton wave function in field theory at large N_c

In principle, calculation of the wave function of a given state in terms of quarks and antiquarks should be straightforward in the quantum field theory. However, usually this task is too complicated. Hence, the wave functions of baryons in the low normalization point cannot be determined from the first principles of QCD. For this reason, models of baryons become highly desirable, and we attempt to calculate the wave functions at a low normalization point based on the chiral quark soliton model. The most direct way to obtain wave functions of any state is to calculate the evolution operator $S(T)$ for a finite time

T. This operator contains complete information about all physical states. In particular the expansion of $S(T)$ in a series of exponentials $\exp(-iE_nT)$ provides wave functions for physical state "n" according to

$$S(T) = \sum_n |\Psi_n\rangle e^{-iE_nT}\langle\Psi_n|. \tag{73}$$

E_n is the energy of the physical state n, $\langle\Psi_n|$ and $|\Psi_n\rangle$ are its wave functions depending on the coordinates of the system at initial (0) and final (T) time moments. Such approach has been proposed by Feynman for quantum mechanical problems.

In the field theory the operator $S(T)$ can be presented as a functional integral of the type

$$S(T) = \int D\psi(x)D\bar{\psi}(x)D\pi(x)\exp\left\{i\int_0^T dt\int d^3x\,\bar{\psi}\left(i\slashed{\partial} - MU^{\gamma_5}(x)\right)\psi(x)\right\}. \tag{74}$$

The operators $b^\dagger(p), b(p)$ $(d^\dagger(p), d(p))$ are annihilation-creation operators for quarks (antiquarks) which are defined through the expansion of the field $\psi(x)$ into positive- and negative-frequency parts:

$$\psi_\alpha(x) = \int \frac{d^3p}{(2\pi)^3}\sum_\sigma \sqrt{\frac{M}{p_0}}\left(b_\sigma(p)u^\sigma(p)e^{ip\cdot x} + d_\sigma^\dagger(p)v^\sigma(p)e^{-ip\cdot x}\right) \tag{75}$$

(here σ is quark polarization; $u^\sigma(p), v^\sigma(p)$ are free plane wave spinors for $U(x) = 1$).

To calculate the Gaussian integral over the Fermi field, we have to pick out the dependence on boundary conditions. This can be done changing the integration variables in Eq.(74) according to

$$\psi = \psi_0 + \psi', \quad \bar{\psi} = \bar{\psi}_0 + \bar{\psi}' \tag{76}$$

The fixed field ψ_0 ought to be chosen in such a way that it would be the solution of the Dirac equation in the external pion-meson field. The boundary values of the fixed fields ψ_0 are the same ones as for Ψ_n itself: at $t = 0$ positive frequency of Ψ_n and $\bar{\psi}$, or at $t = T$ its negative frequency parts are fixed. Such boundary condition means that in terms of quark operators the expression for $S(T)$ will appear in the form where all quark creation operators $b^\dagger, d^\dagger$ belong to the moment $t = T$, and annihilation operators b, d belong to $t = 0$:

$$S(T) = \int_{\psi(+)=b}^{\psi(-)=d^\dagger} D\psi(x)\int_{\bar{\psi}(+)=d}^{\bar{\psi}(-)=b^\dagger} D\bar{\psi}(x)\int D\pi(x)\exp\left(i\int_0^T dt\mathcal{L}_{eff}\right), \tag{77}$$

where $\mathcal{L}_{eff}$ is the effective Lagrangian of Eq.(74). We do not impose any boundary conditions on the π-meson field. This field appears in the derivation of the effective Lagrangians as a result of bosonization, and it should not be considered as an elementary one.

The required solution ψ_0 leads to the definite Green function of the Dirac equation. The solution of equation

$$(i\slashed{\partial} - MU^{\gamma_5})\psi_0 = 0, \tag{78}$$

with the boundary conditions

$$\psi_0^{(+)}(\boldsymbol{x}, t = 0) = B(\boldsymbol{x}) \equiv \int \frac{d^3\boldsymbol{p}}{(2\pi)^3} e^{i\boldsymbol{p}\cdot\boldsymbol{x}} \sqrt{\frac{p_0}{M}} \sum_\sigma b_\sigma(\boldsymbol{p}) u^\sigma(\boldsymbol{p}),$$

$$\psi_0^{(-)}(\boldsymbol{x}, t = T) = D^\dagger(\boldsymbol{x}) \equiv \int \frac{d^3\boldsymbol{p}}{(2\pi)^3} e^{-i\boldsymbol{p}\cdot\boldsymbol{x}} \sqrt{\frac{p_0}{M}} \sum_\sigma d_\sigma^\dagger(\boldsymbol{p}) v^\sigma(\boldsymbol{p}), \tag{79}$$

can be expressed in terms of the finite time Feynman Green function $G^{(T)}(\boldsymbol{x}, t|\boldsymbol{y}, 0)$

$$\psi_0(\boldsymbol{x}, t) = \int d^3\boldsymbol{y} \int \frac{d^3\boldsymbol{p}}{(2\pi)^3} \sqrt{\frac{p_0}{M}} \sum_\sigma [\; G^{(T)}(\boldsymbol{x}, t|\boldsymbol{y}, 0) u^\sigma(\boldsymbol{p}) b_\sigma(\boldsymbol{p}) e^{i\boldsymbol{p}\cdot\boldsymbol{y}}$$
$$+\; G^{(T)}(\boldsymbol{x}, t|\boldsymbol{y}, T) v^\sigma(\boldsymbol{p}) d_\sigma^\dagger(\boldsymbol{p}) e^{-i\boldsymbol{p}\cdot\boldsymbol{y}}], \tag{80}$$

with an analogous expression for $\bar{\psi}_0(\boldsymbol{x}, t)$. The finite time Green function $G^{(T)}(\boldsymbol{x}, t|\boldsymbol{y}, t')$ is the solution of the Dirac equation in the external field which has vanishing negative-frequency part at $t = 0$ and vanishing positive-frequency part at $t = T$. At $T \to \infty$ finite time Green function reduces to the usual Feynman Green function.

After changing the integration variables according to Eq.(80), we get from Eq.(74) that [55]

$$S(T) = \int D\pi(x) \text{Det}^{(T)}[\pi] S_{ext}[\pi, T], \tag{81}$$

where we used Eq.(77). Here $S_{ext}[\pi, T]$ is the evolution operator in the given external field:

$$S_{ext}[\pi, T] = \exp\{\int d^3\boldsymbol{x} d^3\boldsymbol{y} [D(\boldsymbol{x})\gamma^0 G^{(T)}(\boldsymbol{x}, 0|\boldsymbol{y}, T) D^\dagger(\boldsymbol{y}) + D(\boldsymbol{x})\gamma^0 G^{(T)}(\boldsymbol{x}, \varepsilon|\boldsymbol{y}, 0) B(\boldsymbol{y})$$
$$+ B^\dagger(\boldsymbol{x})\gamma^0 G^{(T)}(\boldsymbol{x}, T|\boldsymbol{y}, 0) B(\boldsymbol{y}) + B^\dagger(\boldsymbol{x})\gamma^0 G^{(T)}(\boldsymbol{x}, T - \varepsilon|\boldsymbol{y}, T) D^\dagger(\boldsymbol{y})]\}, \tag{82}$$

where $\varepsilon \to +0$; the quantity $\text{Det}^{(T)}[\pi]$ is the finite time determinant in the external field. It is the Gaussian functional integral over the fermion field $\psi'(x)$ with zero boundary conditions. For this reason it does not depend on the operators $b, d, b^\dagger$ and $d^\dagger$, being only the functional of pion field $\pi(x)$:

$$\log \text{Det}^{(T)}[\pi] = \int_0^T dt \int d^3\boldsymbol{x} \, \text{Tr} \log[i\slashed{\partial} - MU^{\gamma_5}(x)] \tag{83}$$

Thus the evolution operator in the external field is the coherent exponential of the creation-annihilation operators. The baryon is the lowest possible state in the sector with

22

baryon charge $B = 1$. One can obtain its wave function by applying the evolution operator to any colorless state of N_c quarks and taking the $T \to \infty$ limit. For example, the baryon wave function Φ_B can be obtained from the state of free quarks:

$$c_B \, e^{-iM_BT}\Phi_B(b^\dagger, d^\dagger) = \lim_{T \to \infty} S(T) \prod_{i=1}^{N_c} b^\dagger_{\alpha_i}(\boldsymbol{p}_i)|\Omega_0\rangle$$

$$\sim \int D\pi \mathrm{Det}^{(T)}[\pi] \prod_{i=1}^{N_c} G_i^{(T)}(\boldsymbol{p}_i, 0|\boldsymbol{k}_i, T)b_{\alpha_i}(k) \exp[b^\dagger(p)G^{(T)}(p, T|p', T)d^\dagger(p')] \qquad (84)$$

Here M_B is the baryon mass and c_B is the overlap between the initial state of N_c quarks and baryon wave function. The functional integral of Eq.(83) should be calculated in the saddle-point approximation. One has to find the pion field which extremizes the integrand. At large T, important factors are

$$\mathrm{Det}^{(T)}[\pi] \sim \exp(-iE_{field}[\pi]T), \quad G_i^{(T)}(\boldsymbol{p}_i, 0|\boldsymbol{k}_i, T) \sim \exp(-iE_{level}[\pi]T), \qquad (85)$$

where $E_{field}[\pi]$ is the energy of the Dirac continuum with the given pion field (proportional to N_c) and $E_{level}[\pi]$ is the energy of the (possible) discrete level for the quark in this field. In order to find the saddle-point one has to minimize the sum:

$$\varepsilon[\pi] = E_{field}[\pi] + N_c E_{level}[\pi] \qquad (86)$$

in the presence of the pion field. It is exactly the condition which was used in constructing the nucleon-soliton. Both contributions to the total energy are of the order of N_c. Operator exponential in Eq.(84) does not contribute to the saddle-point Eq.(86) as the Green function $G^{(T)}(p, T|p', T)$ does not contain exponential with the phase proportional to the time T.

The minimum of Eq.(86) is achieved at some stationary pion field and corresponds to the baryon at rest. The value of the energy in the minimum is the baryon mass:

$$M_B = min \, \varepsilon[\pi] \sim O(N_c). \qquad (87)$$

The pion field, which gives this minimum turns out to have the so-called hedgehog symmetry:

$$\bar{\pi}^a(\boldsymbol{x}) = n^a F(r), \quad n^a = \frac{r^a}{r}, \quad U(x) = \begin{pmatrix} \exp{(i\boldsymbol{\tau} \cdot \boldsymbol{n}F(r))} & 0 \\ 0 & 1 \end{pmatrix} \qquad (88)$$

where the profile function $F(r)$ is to be calculated numerically.

We can obtain the wave function of baryon in the leading order of N_c, if we substitute the saddle-point field $\pi(x)$ of Eq.(86) into Eq.(84). In higher orders, one has to express

the general pion field $\pi(\boldsymbol{x}, t) = \bar{\pi} + \pi^{quant}$ and then perform the Gaussian integration in systematic perturbation theory in $1/N_c$. However, in this study, we restrict ourselves to the leading order.

Let us stress that the above procedure for obtaining the baryon wave function is rather general. Indeed, it is a general QCD theorem that at large N_c, the baryon is the soliton of some effective meson Lagrangian. Thus, its wave function can always be presented in the form of Eq.(84), where Green functions should be found in the self-consistent field of all mesons entering this effective Lagrangian. Of course, the exact low-energy meson Lagrangian is unknown. In the present work, we use the instanton vacuum model in order to fix this low-energy Lagrangian. Let us also rewrite baryon wave function in a different form. As explained above, baryon can be described as N_c valence quarks + Dirac continuum in the self-consistent external field. It is clear from Eq.(84) that wave function of the Dirac continuum (i.e. the state with all the negative-energies orbitals occupied) can be expressed as the coherent exponential of the quark-antiquark pairs:

$$
\begin{aligned}
|\Omega\rangle &= \exp\left[\sum_{color} \int d^3x d^3y \, B^\dagger(\boldsymbol{x}) \gamma^0 G^{(T)}(\boldsymbol{x}, T - \epsilon | \boldsymbol{y}, T) D^\dagger(\boldsymbol{y})\right] |0\rangle \\
&\equiv \exp\left[\sum_{color} \int \frac{d^3p_1 d^3p_2}{(2\pi)^3} b^\dagger_{\sigma_1}(\boldsymbol{p}_1) W^{\sigma_1, \sigma_2}(\boldsymbol{p}_1, \boldsymbol{p}_2) d^\dagger_{\sigma_2}(\boldsymbol{p}_2)\right] |0\rangle
\end{aligned}
\tag{89}
$$

where $|0\rangle$ is the vacuum of quarks and antiquarks. The function $W^{\sigma_1, \sigma_2}(\boldsymbol{p}_1, \boldsymbol{p}_2)$ can be called the wave function of the quark-antiquark pair. We shall specify the pair wave function bellow.

It is assumed that the self-consistent chiral field creates a bound-state level for quarks, whose wave function ψ_{level} satisfies the static Dirac equation with eigenenergy E_{level}:

$$
\psi_{lev}(\boldsymbol{x}) = \begin{pmatrix} \epsilon^{ji} h(r) \\ -i\epsilon^{jk}(\sigma \cdot \mathbf{n})^i_k j(r) \end{pmatrix}
$$

$$
\begin{cases} h' + hM \sin F - j(M \cos F + E_{lev}) = 0, \\ j' + 2j/r - jM \sin F - h(M \cos F - E_{lev}) = 0. \end{cases}
\tag{90}
$$

Here i is a spin index and j is flavor index. In the non-relativistic limit ($E_{lev} \approx M$) the $L = 0$ upper component of the Dirac spinor $h(r)$ is large while the $L = 1$ lower component $j(r)$ is small.

The valence quark part of the baryon wave function is given by the product of N_c quark creation operators that fill in the discrete level [30–32]:

$$\text{valence} = \prod_{color=1}^{N_c} \int d^3p \, F(p) \, b^\dagger(p),$$ (91)

$$F(p) = \int (d^3p') \sqrt{\frac{M}{P_0}} \left[\bar{u}(p)\gamma_0\psi_{lev}(p)(2\pi)^3\delta(p-p') - W(p,p')\bar{v}(p')\gamma_0\psi_{lev}(-p') \right],$$ (92)

where $\psi_{lev}(p)$ is the Fourier transform of Eq.(90). The second term in Eq.(92) is the contribution of the distorted Dirac sea to the one-quark wave function. $u_\sigma(p)$ and $v_\sigma(p)$ are the plane-wave Dirac spinors projecting to the positive and negative frequencies, respectively. In the standard basis they have the form

$$u_\sigma(p) = \begin{pmatrix} \sqrt{\frac{\epsilon+M}{2M}} s_\sigma \\ \sqrt{\frac{\epsilon-M}{2M}} \frac{p\cdot\sigma}{|p|} s_\sigma \end{pmatrix}, \quad v_{-\sigma}(-p) = C\bar{u}_\sigma^T(p), \quad \bar{u}u = 1 = -\bar{v}v,$$ (93)

where $\epsilon = +\sqrt{p^2 + M^2}$ and s_σ are two 2-component spinors normalized to unity, for example,

$$s_1 = \begin{pmatrix} 1 \\ 0 \end{pmatrix}, \quad s_2 = \begin{pmatrix} 0 \\ 1 \end{pmatrix}, \quad \sigma = 1, 2.$$ (94)

The charge conjugation matrix in this representation take the form

$$C = \begin{pmatrix} -i\sigma_2 & 0 \\ 0 & i\sigma_2 \end{pmatrix}$$ (95)

The full baryon wave function is given by the product of the valence part (92) and the coherent exponent (89) describing the distorted Dirac sea. Symbolically, one writes the baryon wave function in terms of the quark-antiquark creation operators

$$B[b^\dagger, d^\dagger] = \prod_{color=1}^{N_c} \int dp \, F(p) \, b^\dagger(p) \exp\left(\int dp \, dp' \, b^\dagger(p) \, W(p,p') \, d^\dagger(p') \right) |0\rangle.$$ (96)

At this point one has to recall that the saddle-point at the self-consistent chiral field is degenerate in global translations and global SU(3) flavor rotations. Integrating over translations leads to the momentum conservation: the sum of all quarks and antiquarks momenta have to be equal to the baryon momentum. Integration over rotations R leads to the projection of the flavor state of all quarks and antiquarks onto the spin-flavor state $B(R)$ describing a particular baryon from the $(\mathbf{8}, \frac{1}{2}^+)$, $(\mathbf{10}, \frac{3}{2}^+)$ or $(\overline{\mathbf{10}}, \frac{1}{2}^+)$ multiplet.

Restoring color ($\alpha = 1, 2, 3$), flavor ($f = 1, 2, 3$), isospin ($j = 1, 2$) and spin ($\sigma = 1, 2$) indices, the quark wave function inside a particular baryon B with spin projection k is given,

25

in full glory, by

$$\Psi_k^B = \int dR\, B_k^*(R)\, \epsilon^{\alpha_1\alpha_2\alpha_3} \prod_{n=1}^{3} \int d\boldsymbol{p_n}\, R_{j_n}^{f_n}\, F^{j_n\sigma_n}(\boldsymbol{p_n})\, b_{\alpha_n f_n\sigma_n}(\boldsymbol{p_n})$$

$$\cdot \exp\left(\int d\boldsymbol{p}\, d\boldsymbol{p'}\, b_{\alpha f\sigma}(\boldsymbol{p})\, R_j^f\, W_{j'\sigma'}^{j\sigma}(\boldsymbol{p},\boldsymbol{p'})\, R_{f'}^{\dagger j'}\, d^{\dagger f'\sigma'}(\boldsymbol{p'})\right) |0\rangle \tag{97}$$

Expanding the coherent exponent to the 0th, 1st, 2nd order one reads off the 3-,5-,7-...quark wave functions of particular baryon from the octet, decuplet or antidecuplet.

To make this powerful formula fully workable, we need to give explicit expressions for the baryon rotational state $B(R)$, the valence wave function $F^{j\sigma}(\boldsymbol{p})$ and the $Q\bar{Q}$ wave function in a baryon $W_{j'\sigma'}^{j\sigma}(\boldsymbol{p},\boldsymbol{p'})$.

C. Baryon rotational wave functions

In general, baryon rotational states $B(R)$ are given by the SU(3) Wigner finite rotational matrices, and any particular projection can be obtained by a routine SU(3) Clebsch-Gordan technique. However, in order to see the symmetries of the quark wave functions, it is helpful to use explicit expressions for $B(R)$, and integrate over the Haar measure in Eq.(96).

1. $(8,\frac{1}{2})$

From the SU(3) group point of view, the octet of baryons transforms exactly as an octet of mesons; therefore, its rotational wave function can be composed of quark (transforming as R) and an antiquark (transforming as $R^\dagger$). Accordingly, the rotational wave function of an octet baryon labeled by $a = 1...8$ and having a spin index $k = 1, 2$ is

$$\left[D^{(8,\frac{1}{2})*}(R)\right]_k^a \sim \epsilon_{kl}\, R_f^{\dagger l}\, (t^a)_g^f\, R_3^g \tag{98}$$

where ϵ_{kl} is the antisymmetric 2×2 tensor and t^a are the SU(3) generators. In particular, the proton ($a = 6 + i7$) and neutron ($a = 4 + i5$) rotational wave functions with spin $k = 1, 2$ are

$$p_k(r)^* = \sqrt{8}\, \epsilon_{kl} R_1^{\dagger l}\, R_3^3, \qquad n_k(R)^* = \sqrt{8} \epsilon_{kl}\, R_2^{\dagger l}\, R_3^3 \tag{99}$$

26

2. $(\mathbf{10}, \frac{3}{2})$

The decuplet states can be composed of three quarks; they are labeled by a triple flavor index $\{f_1 f_2 f_3\}$ symmetrized in flavor and by a triple spin index $\{k_1 k_2 k_3\}$ symmetrized in spin:

$$\left[D^{(10,\frac{3}{2})*}(R) \right]_{\{f_1 f_2 f_3\},\{k_1 k_2 k_3\}} \sim \epsilon_{k'_1 k_1} \epsilon_{k'_2 k_2} \epsilon_{k'_3 k_3} R_{f_1}^{\dagger k'_1} R_{f_2}^{\dagger k'_2} R_{f_3}^{\dagger k'_3} |_{\text{sym in } \{f_1 f_2 f_3\}} \tag{100}$$

For example, the Δ-resonance rotational wave functions are

$$\Delta^{++}, \text{spin projection} + \frac{3}{2} \qquad \Delta^{++}_{\uparrow\uparrow}(R)^* = \sqrt{10} \, R_1^{\dagger 2} R_1^{\dagger 2} R_1^{\dagger 2} \,, \tag{101}$$

$$\Delta^{0}, \text{spin projection} + \frac{1}{2} \qquad \Delta^{0}_{\uparrow}(R)^* = \sqrt{10} \, R_2^{\dagger 2} (2 \, R_2^{\dagger 1} R_1^{\dagger 2} + R_2^{\dagger 2} R_1^{\dagger 1})) \,. \tag{102}$$

3. $(\overline{\mathbf{10}}, \frac{1}{2})$

From the SU(3) group point of view, the antidecuplet can be composed of three antiquarks and its conjugate rotational wave function is

$$\left[D^{(\overline{10},\frac{3}{2})*}(R) \right]_k^{\{f_1 f_2 f_3\}} \sim R_3^{f_1} R_3^{f_2} R_k^{f_3} |_{\text{sym in } \{f_1 f_2 f_3\}} \tag{103}$$

In particular, the Θ^+ rotational wave function which is one of the member of the antidecuplet with strangeness $+1$, is

$$\Theta^+, \text{spin projection} \, k \qquad \Theta^+_k(R)^* = \sqrt{30} \, R_3^3 R_3^3 R_3^k \tag{104}$$

They are normalized in such a way that for any spin projection

$$\int dR \, B^*_{spin}(R) \, B^{spin}(R) = 1 \tag{105}$$

4. The $Q\bar{Q}$ pair wave function

The pair wave function $W^{j\sigma}_{j'\sigma'}(\boldsymbol{p}, \boldsymbol{p}')$ is expressed in terms of the finite-time quark Green function at equal times in the external chiral field. We define the Green function as the solution of the equation

$$[i\slashed{\partial} - M(\Sigma + i\Pi\gamma_5)]_{\boldsymbol{x}_1,t_1} \, G(\boldsymbol{x}_1, t_1 | \boldsymbol{x}_2, t_2) = \delta(t_1 - t_2)\delta^{(3)}(\boldsymbol{x}_1 - \boldsymbol{x}_2). \tag{106}$$

27

On the chiral circle $\Pi(r) = \boldsymbol{n} \cdot \boldsymbol{\tau} \sin P(r)$, $\Sigma(r) = \cos P(r)$. The quantity $V = M(-1 + \Sigma + i\Pi\gamma_5)$ will be called the perturbation by the non-zero mean field. In what follows we shall rename $\Sigma - 1 \to \Sigma$. For the static hedgehog mean field lying on the chiral circle

$$\Sigma_{j'}^j(\boldsymbol{x}) = (\cos P(r) - 1)\delta_{j'}^j, \quad \Pi_{j'}^j(\boldsymbol{x}) = (\boldsymbol{n} \cdot \boldsymbol{\tau})_{j'}^j \sin P(r). \tag{107}$$

We shall need their Fourier transforms,

$$\Sigma(\boldsymbol{q}) = \int d\boldsymbol{x} e^{-i\boldsymbol{q} \cdot \boldsymbol{x}} \Sigma(\boldsymbol{x}), \quad \Pi(\boldsymbol{q}) = \int d\boldsymbol{x} e^{-i\boldsymbol{q} \cdot \boldsymbol{x}} \Pi(\boldsymbol{x}). \tag{108}$$

In the frame where a baryon has a constant velocity v along the z axis both fields get the arguments $(x, y, z) \to \left(x, y, \frac{z - vt}{\sqrt{1 - v^2}}\right)$. Both fields can be written through the Fourier transforms in the rest frame:

$$\Sigma, \Pi\left(x, y, \frac{z - vt}{\sqrt{1 - v^2}}\right) = \int d\boldsymbol{q} \exp\left(iq_x x + iq_y y + iq_z \frac{z - vt}{\sqrt{1 - v^2}}\right) \Sigma, \Pi(\boldsymbol{q}). \tag{109}$$

One can present the Green function as a perturbation expansion in $V = \Sigma + i\Pi\gamma_5$

$$\frac{1}{i\not{\partial} - M - V} = \frac{1}{i\not{\partial} - M} + \frac{1}{i\not{\partial} - M}V\frac{1}{i\not{\partial} - M} + \frac{1}{i\not{\partial} - M}V\frac{1}{i\not{\partial} - M}V\frac{1}{i\not{\partial} - M} + \tag{110}$$

The important point is that all free Green functions in this equation should be understood with the Feynman $-\epsilon$ prescription in the momentum space, meaning the shift $M - i0$ in the free propagators [25].

The perturbation (107) is in fact very specific: its modulus is always less than unity. If the pion field is much less than unity, the perturbation is small. If the chiral field is not small but has either low ($q \ll M$) or large ($q \gg M$) momenta, the perturbation is, effectively, also small as will become clear from the final expression for the pair wave function. Therefore, it is not a bad idea to restrict oneself to the first order in the perturbation in V which we are going to do here. Keeping higher orders in V has no principle difficulties but in our experience the first order result is usually within $10-15\%$ from exact (all orders) calculations. In the first order in the external field V the Green function is, according to Eq. (110),

$$G^{(1)}(\boldsymbol{x}_1, t_1|\boldsymbol{x}_2, t_2) = \int_0^T dt \int d^3\boldsymbol{z}\, G^{(0)}(\boldsymbol{x}_1, t_1|\boldsymbol{z}, t)\, V(\boldsymbol{z}, t)\, G^{(0)}(\boldsymbol{z}, t|\boldsymbol{x}_2, t_2). \tag{111}$$

Here T is the "observation time" during which the external chiral field exists; it should be put to infinity to obtain the ground-state baryon with given quantum numbers. We can

write it further in the momentum representation:

$$G^{(1)}(\boldsymbol{x}_1, t_1 | \boldsymbol{x}_2, t_2) = \int d\boldsymbol{q}_1 d\boldsymbol{q}_2 \exp\left(-i\boldsymbol{q}_1 \cdot \boldsymbol{x}_1 - i\boldsymbol{q}_2 \cdot \boldsymbol{x}_2\right) G^{(1)}(\boldsymbol{q}_1, t_1 | \boldsymbol{q}_2, t_2),$$

$$G^{(1)}(\boldsymbol{q}_1, t_1 | \boldsymbol{q}_2, t_2) = \int \frac{d\omega_1 d\omega_2}{(2\pi)^2} \int_0^T dt' \int d^3 z \int d\boldsymbol{q} \exp\left[iq_x x + iq_y y + iq_z \frac{z - vt'}{\sqrt{1 - v^2}}\right]$$

$$\cdot \exp\left[-i\omega_1(t' - t_1) + i\boldsymbol{q}_1 \cdot \boldsymbol{z} - i\omega_2(t_2 - t') + i\boldsymbol{q}_2 \cdot \boldsymbol{z}\right] \frac{1}{\not{q}_1 - M + i0} V(\boldsymbol{q}) \frac{1}{\not{q}_2 - M + i0}$$

$$\tag{112}$$

where $q_{1,2\mu} = (\omega_{1,2}, \boldsymbol{q}_{1,2})$, $\not{q}_{1,2} = \omega_{1,2}\gamma_0 - \boldsymbol{q}_{1,2} \cdot \boldsymbol{\gamma}$.

The definition of the (conjugate) pair wave function is

$$W^{j'\sigma'}_{cj\sigma}(\boldsymbol{p}, \boldsymbol{p}') = -i\sqrt{\frac{\epsilon\epsilon'}{M^2}} \left[\bar{v}^{\sigma'}(\boldsymbol{p}')G(\boldsymbol{p}, 0 | \boldsymbol{p}', 0)^{j'}_j u_\sigma(\boldsymbol{p})\right] \tag{113}$$

with the plane-wave spinors u, v defined in Eq. (93). One has to integrate Eq. (113) over $\omega_{1,2}$ and the intermediate point $(\boldsymbol{z}, t')$ where the perturbation V acts. Because of the Feynman "$M - i0$" rule, one closes the integration contour in ω_1 in the lower semiplane and finds the contribution of the pole $\omega_1 = \epsilon = \sqrt{\boldsymbol{p}^2 + M^2}$. Integration over ω_2 is closed in the upper semiplane with $\omega_2 = -\epsilon' = -\sqrt{\boldsymbol{p}'^2 + M^2}$. This is an important (although natural) result: the $Q\bar{Q}$ pair has a positive-energy antiquark and necessarily a negative-energy quark. The physical interpretation, in terms of the level density of the Dirac sea, is given in the following. If the mean field makes the Dirac sea less dense than in the vacuum at certain momenta, it means a hole or the presence of an antiquark with positive energy. If the Dirac sea is more dense in some partial wave and at some momenta, it means the presence of an additional negative-energy quark with the corresponding quantum numbers. Since the total number of levels in the sea is its baryon number and is conserved whatever the background field, it implies that any distortion of the Dirac sea by the mean field creates an equal number of quarks and antiquarks or, else, quark-antiquark $(Q\bar{Q})$ pairs inside a baryon.

Integration over d^3z leads to the 3-momentum conservation, $\boldsymbol{q}_\perp = -(\boldsymbol{p} + \boldsymbol{p}')_\perp$, $q_z = -(p_z + p'_z)/\sqrt{1 - v^2}$. Integration over the intermediated time t' gives the energy denominator $-i/[\epsilon + \epsilon' - i0 - (p_z + p'_z)v]$. Finally, one has to use the Dirac equation for the plane-wave spinors: $(M - \not{p})u_\sigma(\boldsymbol{p}) = 0, \bar{v}^{\sigma'}(\boldsymbol{p}')(M + \not{p}') = 0$. As a result one obtains

$$W^{j'\sigma'}_{cj\sigma}(\boldsymbol{p}, \boldsymbol{p}') = \sqrt{\frac{M^2}{\epsilon\epsilon'}} \frac{\sqrt{1 - v^2}}{\epsilon + \epsilon' - (p_z + p'_z)v} \left[\bar{v}^{\sigma'}(\boldsymbol{p}')V(-\boldsymbol{p} - \boldsymbol{p}')^{j'}_j u_\sigma(\boldsymbol{p})\right] \tag{114}$$

29

In the infinite momentum frame, one has to take the limit $v \to 1$. The momentum of the baryon with mass M_B is

$$P = \frac{M_B v}{\sqrt{1-v^2}}, \quad \text{hence} \, v = \frac{P}{\sqrt{P^2 + M_B^2}} \simeq 1 - \frac{M_B^2}{2P^2}. \tag{115}$$

The quark and the anti-quark of the $Q\bar{Q}$ pair have the 4-momenta

$$p = \left(zP + \frac{p_\perp^2 + M^2}{2zP}, \boldsymbol{p}_\perp, zP\right), \quad p' = \left(z'P + \frac{p_\perp'^2 + M^2}{2z'P}, \boldsymbol{p}'_\perp, z'P\right), \tag{116}$$

hence the energy denominator is

$$\frac{\sqrt{1-v^2}}{\epsilon + \epsilon' - (p_z + p_z')v} = \frac{M_B}{P} \frac{2zz'P}{Z}, \quad Z \equiv M_B^2 zz'(z + z') + z(p_\perp'^2 + M^2) + z'(p_\perp^2 + M^2). \tag{117}$$

In the infinite momentum frame, it is convenient to rescale the annihilation-creation operators, $b_\sigma^{IMF}(z, \boldsymbol{p}_\perp) = \sqrt{P/2\pi} b_\sigma(\boldsymbol{p})$ and similarly for $b^\dagger, d, d^\dagger$, where the subscript $\sigma = 1, 2$ refers now to helicity states. The new operators satisfy the anticommutation relations

$$\left\{ b^{\alpha_1 f_1 \sigma_1}(z_1, \boldsymbol{p}_{1\perp}), b^\dagger_{\alpha_2 f_2 \sigma_2}(z_2, \boldsymbol{p}_{2\perp}) \right\} = \delta^{\alpha_1}_{\alpha_2} \delta^{f_1}_{f_2} \delta^{\sigma_1}_{\sigma_2} \delta(z_1 - z_2)(2\pi)^2 \delta^{(2)}(\boldsymbol{p}_{1\perp} - \boldsymbol{p}_{2\perp}) \tag{118}$$

and similarly for the new $d, d^\dagger$. The use of the rescaled operators requires rescaling $W_{cj\sigma}^{j'\sigma'}$ by a factor of $P/(2\pi)$. Taking the $v \to 1$ limit in the spinors (93) one gets finally

$$W_{cj\sigma}^{j'\sigma'}(z, \boldsymbol{p}_\perp; z', \boldsymbol{p}'_\perp) = \frac{M M_B}{2\pi Z} \left\{ \Sigma_j^{j'}(\boldsymbol{q}) \left[M(z' - z)\sigma_3 + \boldsymbol{Q}_\perp \cdot \boldsymbol{\sigma}_\perp \right]_\sigma^{\sigma'} \right.$$
$$\left. + i\Pi_j^{j'}(\boldsymbol{q}) \left[-M(z' + z)\mathbf{1} - i\epsilon_{\alpha\beta} Q_{\perp\alpha}\sigma_{\perp\beta} \right]_\sigma^{\sigma'} \right\} \tag{119}$$

$$\boldsymbol{q} = ((\boldsymbol{p} + \boldsymbol{p}')_\perp, (z + z')M_B), \quad Q_{\perp\alpha} = z p'_{\perp\alpha} - z' p_{\perp\alpha}, \quad \alpha, \beta = 1, 2 \tag{120}$$

The non-primed indices refers here to the quark and the primed ones to the antiquark.

Eq.(119) gives the wave function of the additional $Q\bar{Q}$ pairs in a baryon in the infinite momentum frame. The indices $j, j' = 1, 2$ are the isospin indices (to be rotated by the SU(3) flavor matrices R in Eq. (97)) and $\sigma, \sigma' = 1, 2$ are the quark and antiquark helicity states. The annihilation-creation operators in Eq. (97) are now understood to be normalized by the condition (118), and the integrals over momenta there are understood as $\int dz \int d^2 p_\perp/(2\pi)^2$.

5. Discrete-level wave function

As seen from Eq.(92), the discrete-level wave function $F^{j\sigma}(\boldsymbol{p}) = F_{lev}^{j\sigma}(\boldsymbol{p}) + F_{sea}^{j\sigma}(\boldsymbol{p})$ consists of two pieces: one is directly the wave function of the valence level, the other is related to

30

the change of the number of quarks at the discrete level due to the presence of the distorted Dirac sea, it is a relativistic effect and can be ignored in the non-relativistic limit, together with the lower $L = 1$ component $j(p)$ of the level wave function.

In the infinite momentum frame the evaluation of the spinors $\bar{u}, \bar{v}$ from Eq.(93) produces

$$F_{lev}^{j\sigma}(z, \boldsymbol{p}_\perp) = \sqrt{\frac{M_B}{2\pi}} \left[\epsilon^{j\sigma} h(p) + (p_z \mathbf{1} + i\epsilon_{\alpha\beta} p_{\perp\alpha} \sigma_{\perp\beta})_{\sigma'}^{\sigma} \epsilon^{j\sigma'} \frac{j(p)}{|p|} \right]_{p_z = zM_B - \epsilon} \tag{121}$$

where $h, j(p)$ are the Fourier transforms of the valence wave functions

$$h(p) = \int d^3 x \, e^{-i\boldsymbol{p}\cdot\boldsymbol{x}} h(r) = 4\pi \int dr \, r^2 \frac{\sin pr}{pr} h(r), \tag{122}$$

$$j^a(p) = \int d^3 x \, e^{-i\boldsymbol{p}\cdot\boldsymbol{x}} (-in^a) j(r) = \frac{p^a}{|p|} j(p), \quad j(p) = \frac{4\pi}{p^2} \int dr \, (pr \cos pr - \sin pr) j(r). \tag{123}$$

Similarly, the evaluation of the "sea" part of the discrete-level wave function gives

$$F_{sea}^{j\sigma}(z, \boldsymbol{p}_\perp) = -\sqrt{\frac{M_B}{2\pi}} \int dz' \frac{d^2 \boldsymbol{p}_\perp'}{(2\pi)^2} W_{j'\sigma'}^{j\sigma}(p, p') \epsilon^{j'\sigma''} \left[(\sigma_3)_{\sigma''}^{\sigma'} h(p') - (\boldsymbol{\sigma} \cdot \boldsymbol{p}')_{\sigma''}^{\sigma'} \frac{j(p')}{|p'|} \right]_{p_z = zM_B - \epsilon} \tag{124}$$

where the pair wave function (119) has to be used. The conjugate functions are hermitian conjugate.

We have thus all quantities entering the master Eq.(97) for the $3, 5, 7, \dots$ Fock components of baryons' wave functions.

IV. LIGHT-CONE WAVE FUNCTION REPRESENTATION OF THE GENERALIZED PARTON DISTRIBUTIONS IN THE CHIRAL QUARK SOLITON MODEL

Recently, Diakonov and Petrov showed the way to calculate the various physical observable in terms of the light-cone wave function based on the CQSM [30–32]. It is straightforward to extend it to the structure functions including the GPDs, and we will show how these functions can be represented in the CQSM.

In the second quantization, the normalization constant can be represented in principle as the superposition of those of each Fock components:

$$\mathcal{N}(B) = \frac{1}{2}\delta_l^k \langle \Psi^{\dagger l} \Psi_k \rangle = \mathcal{N}^{(3Q)}(B) + \mathcal{N}^{(5Q)}(B) + \mathcal{N}^{(7Q)}(B) + \qquad (125)$$

As we explained in the previous section, the expansion of the coherent exponent of the $Q\bar{Q}$ pair wave function is well converged series in terms of their Fock components, so we will take up to the $5Q$ component in the wave function.

A. 3 quark components

We first consider the three quark components in baryon. Each of three valence quarks are rotated in the SU(3) flavor space by the matrix R_j^f where $f = 1, 2, 3$ is the flavor and $j = 1, 2$ is the isospin index. To obtain the color-flavor-spin-space $3Q$ wave function of a particular baryon, one has to integrate over all 8-parameter SU(3) rotations R with the rotational wave function $B_k^*(R)$ corresponding to the chosen baryon with spin projection k. Then the wave function of the three quark components of baryon can be represented as

$$\Psi^{(3Q)}(B) = T(B)_{j_1 j_2 j_2, k}^{f_1 f_2 f_3} \times F^{j_1 \sigma_1}(p_1) F^{j_2 \sigma_2}(p_2) F^{j_3 \sigma_3}(p_3) \qquad (126)$$

where $T(B)_{j_1 j_2 j_2, k}^{f_1 f_2 f_3}$ means the SU(3) group integral as

$$T(B)_{j_1 j_2 j_2, k}^{f_1 f_2 f_3} \equiv \int dR \, B_k^*(R) R_{j_1}^{f_1} R_{j_2}^{f_2} R_{j_3}^{f_3}. \qquad (127)$$

Hence the normalization of the three quark component is

$$\mathcal{N}^{(3Q)}(B) = \frac{(6 \cdot 6)}{2} \delta_l^k T(B)_{j_1 j_2 j_2, k}^{f_1 f_2 f_3} T(B)_{f_1 f_2 f_3}^{l_1 l_2 l_2, l} \int d\, z_{1,2,3} \int \frac{d^2\, p_{1,2,3}}{(2\pi)^6} \delta(z_1 + z_2 + z_3 - 1) \qquad (128)$$

$$\cdot (2\pi)^2 \delta(p_1 + p_2 + p_3) F^{j_1 \sigma_1}(p_1) F^{j_2 \sigma_2}(p_2) F^{j_3 \sigma_3}(p_3) F_{l_1 \sigma_1}^\dagger(p_1) F_{l_2 \sigma_2}^\dagger(p_2) F_{l_3 \sigma_3}^\dagger(p_3),$$

the factor $(6 \cdot 6)$ comes from the fact that there are 3! possible contractions, and ensuing contraction in color indices gives another factor of $3! = \epsilon^{\alpha_1 \alpha_2 \alpha_3} \epsilon_{\alpha_1 \alpha_2 \alpha_3}$.

A typical physical observable is the matrix element of some operator sandwiched between the initial and final baryon wave functions. These operators can be written in terms of the creation or annihilation operators $a, a^\dagger, b, b^\dagger$ as Eq.(118), and in the $3Q$ components only the $a^\dagger a$ term survives because there is no antiquark. First, we consider the quark operators of the vector charge type $\bar{q}\gamma^+ q$ in the forward limit $t \to 0$. This charge gives the quark number in the baryon. We obtain the following expression for the vector charge

$$
V^{(3Q)} = \frac{(6 \cdot 6 \cdot 3)}{2} \delta_l^k T(B)_{j_1 j_2 j_2, k}^{f_1 f_2 f_3} T(B)_{f_1 f_2 g_3}^{l_1 l_2 l_2, l} \int (dp_{1,2,3}) \tag{129}
$$
$$
\cdot \left[F^{j_1 \sigma_1}(p_1) F^{j_2 \sigma_2}(p_2) F^{j_3 \sigma_3}(p_3) \right] \left[F^\dagger_{l_1 \sigma_1}(p_1) F^\dagger_{l_2 \sigma_2}(p_2) F^\dagger_{l_3 \tau_3}(p_3) \right] \left[\delta^{\tau_3}_{\sigma_3} J^{g_3}_{f_3} \right] ,
$$

where we use the abbreviation $\int (dp_{1,2,3})$ for the integral over momenta with the conservation δ-functions as in Eq.(129). Although we assume that the third quark is struck, there is a factor of 3 by considering which quark of the three quarks can be struck. $J^{g_3}_{f_3}$ is the flavor content of the charge, and $\tau, \sigma = 1, 2$ are helicity states. For example, if we consider up quark charge, $J^{g_3}_{f_3} = \delta^{g_3}_1 \delta^1_{f_3}$. One can easily check that in the proton case the above quark number gives exactly 2 for the up quark and 1 for the down quark after dividing the 3 quark normalization $\mathcal{N}^{(3Q)}(p)$ [32].

From the above representation, we can easily develop formulas for many other structure functions. For the off-forward matrix element, one has to change the momentum of one of the quarks on which the operator acts, by the corresponding momentum transfer, and leave the rest quarks momenta unaltered. As shown in Eqs.(23) and (25), the light-cone helicity non-flip form factors are linear combination of the Dirac and Pauli form factor. Hence the matrix element corresponding to the helicity non-flip form factor in the 3 quark approximation is

$$
\sqrt{1 - \xi^2} F_1^{(3Q)}(t) - \frac{\xi^2}{\sqrt{1 - \xi^2}} F_2^{(3Q)}(t) = \frac{(6 \cdot 6 \cdot 3)}{2} \delta_l^k T(B)_{j_1 j_2 j_2, k}^{f_1 f_2 f_3} T(B)_{f_1 f_2 f_3}^{l_1 l_2 l_2, l} \int (dp_{1,2,3}) \tag{130}
$$
$$
\cdot \left[F^{j_1 \sigma_1}(p_1) F^{j_2 \sigma_2}(p_2) F^{j_3 \sigma_3} \left(p_3 - \frac{\Delta}{2} \right) \right]
$$
$$
\cdot \left[F^\dagger_{l_1 \sigma_1}(p_1) F^\dagger_{l_2 \sigma_2}(p_2) F^\dagger_{l_3 \tau_3} \left(p_3 + \frac{\Delta}{2} \right) \right] \left[\delta^{\tau_3}_{\sigma_3} \delta^{g_3}_{f_3} \right]
$$

We next consider the matrix elements of the GPD which have an additional argument of the light-cone momentum fraction x_B. In our expression, the Bjorken variable x_B corresponds to z_3 which is the longitudinal momentum fraction of the third quark with respect

to the total baryon momentum $P_B = M_B V/\sqrt{1 - V^2}$. Therefore, for the spin non-flip GPD $\mathcal{H}_{++} = \sqrt{1 - \xi^2}H(x, \xi, t) - \frac{\xi^2}{\sqrt{1-\xi^2}}E(x, \xi, t)$, one should leave the z_3 unintegrated in the above expression of the light-cone helicity non-flip form factor Eq.(130):

$$\mathcal{H}_{++}(x_B, \xi, t) = \sqrt{1 - \xi^2}H^{(3Q)}(x_B = z_3, \xi, t) - \frac{\xi^2}{\sqrt{1 - \xi^2}}E^{(3Q)}(x_B = z_3, \xi, t) \qquad (131)$$

$$= \frac{(6 \cdot 6 \cdot 3)}{2}\delta_l^k T(B)_{j_1 j_2 j_2, k}^{f_1 f_2 f_3} T(B)_{f_1 f_2 f_3}^{l_1 l_2 l_2, l}$$

$$\int \frac{d^2 p_{1,2,3\perp}}{(2\pi)^6}dz_{1,2}\delta(z_1 + z_2 + z_3 - 1)(2\pi)^2\delta(p_{1\perp} + p_{2\perp} + p_{3\perp})$$

$$\cdot \left[F^{j_1\sigma_1}(p_1)F^{j_2\sigma_2}(p_2)F^{j_3\sigma_3}\left(p_3 - \frac{\Delta}{2}\right)\right]$$

$$\cdot \left[F_{l_1\sigma_1}^\dagger(p_1)F_{l_2\sigma_2}^\dagger(p_2)F_{l_3\tau_3}^\dagger\left(p_3 + \frac{\Delta}{2}\right)\right]\left[\delta_{\sigma_3}^{\tau_3}\delta_{f_3}^{g_3}\right]$$

The impact parameter space parton distribution functions $q(x, \boldsymbol{b}_\perp)$ is the Fourier transform of this expression with $\xi = 0$

$$q(x, \boldsymbol{b}_\perp) = \int \frac{d^2\boldsymbol{b}_\perp}{(2\pi)^2}e^{-i\boldsymbol{b}_\perp \cdot \boldsymbol{\Delta}_\perp}\mathcal{H}_{++}(x, 0, t = -\boldsymbol{\Delta}_\perp^2) = \int \frac{d^2\boldsymbol{b}_\perp}{(2\pi)^2}e^{-i\boldsymbol{b}_\perp \cdot \boldsymbol{\Delta}_\perp}H(x, 0, -\boldsymbol{\Delta}_\perp^2). \qquad (132)$$

From this expression Eq.(131), one can obtain the Feynman parton distribution functions $q(x)$ by taking the forward limit $t \to 0$. Similarly the Transverse Momentum Dependent (TMD) parton distributions $q(x, \boldsymbol{p}_\perp)$ can also be obtained by leaving the unintegrated transverse momentum $p_{3\perp}$ in the forward limit in Eq.(131):

$$q^{(3Q)}(x, \boldsymbol{p}_\perp) = \frac{(6 \cdot 6 \cdot 3)}{2}\delta_l^k T(B)_{j_1 j_2 j_2, k}^{f_1 f_2 f_3}T(B)_{f_1 f_2 f_3}^{l_1 l_2 l_2, l} \qquad (133)$$

$$\int \frac{d^2 p_{1,2\perp}}{(2\pi)^4}dz_{1,2}\delta(z_1 + z_2 + z_3 - 1)(2\pi)^2\delta(p_{1\perp} + p_{2\perp} + p_{3\perp})$$

$$\cdot \left[F^{j_1\sigma_1}(p_1)F^{j_2\sigma_2}(p_2)F^{j_3\sigma_3}(p_3)\right]\left[F_{l_1\sigma_1}^\dagger(p_1)F_{l_2\sigma_2}^\dagger(p_2)F_{l_3\tau_3}^\dagger(p_3)\right]\left[\delta_{\sigma_3}^{\tau_3}\delta_{f_3}^{g_3}\right]$$

For the spin polarized case, one replaces averaging over baryon spin by $\frac{1}{2}(\sigma_3)_l^k$, and the axial charge operator is now $(\sigma_3)_{\sigma_3}^{\tau_3}$ instead of $\delta_{\sigma_3}^{\tau_3}$. For example, if we consider the polarized parton distribution function $\Delta q(x)$, one gets

$$\Delta q^{(3Q)}(x) = \frac{(6 \cdot 6 \cdot 3)}{2}(\sigma_3)_l^k T(B)_{j_1 j_2 j_2, k}^{f_1 f_2 f_3}T(B)_{f_1 f_2 f_3}^{l_1 l_2 l_2, l} \qquad (134)$$

$$\int \frac{d^2 p_{1,2,3\perp}}{(2\pi)^6}dz_{1,2}\delta(z_1 + z_2 + z_3 - 1)(2\pi)^2\delta(p_{1\perp} + p_{2\perp} + p_{3\perp})$$

$$\cdot \left[F^{j_1\sigma_1}(p_1)F^{j_2\sigma_2}(p_2)F^{j_3\sigma_3}(p_3)\right]\left[F_{l_1\sigma_1}^\dagger(p_1)F_{l_2\sigma_2}^\dagger(p_2)F_{l_3\tau_3}^\dagger(p_3)\right]\left[(\sigma_3)_{\sigma_3}^{\tau_3}\delta_{f_3}^{g_3}\right]$$

34

Formulas of the polarized functions $\widetilde{\mathcal{H}}_{++} = \sqrt{1 - \xi^2}\widetilde{H}(x, \xi, t) - \frac{\xi^2}{\sqrt{1-\xi^2}}\widetilde{E}(x, \xi, t)$, $\Delta q(x, \boldsymbol{p}_\perp)$, $\Delta q(x, \boldsymbol{b}_\perp)$ can be obtained from those of the non-polarized case by changing the operators $\delta_l^k \to (\sigma_3)_l^k$, $\delta_{\sigma_3}^{\tau_3} \to (\sigma_3)_{\sigma_3}^{\tau_3}$.

B. 5 quark components

Next, we consider the 5 quark components in the baryons. Convoluting the linear order $Q\bar{Q}$ wave function in the expansion of the coherent exponent with the three valence quark wave functions, we can get the 5 quark wave function in the baryons as

$$\Psi^{(5Q)} = T(B)^{f_1 f_2 f_3 f_4, j_5}_{j_1 j_2 j_3 j_4, f_5, k} \times F^{j_1 \sigma_1}(p_1) F^{j_2 \sigma_2}(p_2) F^{j_3 \sigma_3}(p_3) W^{j_4 \sigma_4}_{j_5 \sigma_5}(p_4, p_5), \tag{135}$$

where the $T(B)^{f_1 f_2 f_3 f_4, j_5}_{j_1 j_2 j_3 j_4, f_5, k}$ represents the SU(3) group integral involving now three R's from the valence level and R, $R^\dagger$ from the pair, times the rotational wave function $B_k^*(R)$ of the baryon in question

$$T(B)^{f_1 f_2 f_3 f_4, j_5}_{j_1 j_2 j_3 j_4, f_5, k} \equiv \int dR\, B_k^*(R) R_{j_1}^{f_1} R_{j_2}^{f_2} R_{j_3}^{f_3} R_{j_4}^{f_4} R_{f_5}^{\dagger j_5}, \tag{136}$$

where we systematically attribute the indices 1,2,3 to the valence quarks, index 4 to the extra quark of the $Q\bar{Q}$ pair, and index 5 to the antiquark. The normalization factor of the 5 quark component is

$$\mathcal{N}^{(5Q)}(B) = \frac{108}{2}\delta_l^k T(B)^{f_1 f_2 f_3 f_4, j_5}_{j_1 j_2 j_3 j_4, f_5, k} T(B)^{l_1 l_2 l_3 l_4, f_5, l}_{f_1 f_2 g_3 g_4, l_5} \int (dp_{1-5}) \tag{137}$$

$$F^{j_1 \sigma_1}(p_1) F^{j_2 \sigma_2}(p_2) F^{j_3 \sigma_3}(p_3) W^{j_4 \sigma_4}_{j_5 \sigma_5}(p_4, p_5)$$

$$F^\dagger_{l_1 \sigma_1}(p_1) F^\dagger_{l_2 \sigma_2}(p_2) F^\dagger_{l_3 \sigma_3}(p_3) W^{l_5 \sigma_5}_{c l_4 \sigma_4}(p_4, p_5) \delta_{f_3}^{g_3} \delta_{f_4}^{g_4}$$

where we have denoted

$$\int (dp_{1-5}) = \int dz_{1-5} \int \frac{d^2 p_{1-5\perp}}{(2\pi)^{10}} (2\pi)^2 \delta(\boldsymbol{p}_{1\perp} + \ldots + \boldsymbol{p}_{5\perp}) \delta(z_1 + \ldots + z_5 - 1). \tag{138}$$

The factor of 108 arises from the following consideration: one contracts $a^\dagger$ from the pair wave function with a in the conjugate pair, and all the valence operators are contracted with each other. There are 6 such possibilities, and the contraction in color gives a factor $3 \cdot 6$, all in all 108.

The ratio of the normalization factors $\mathcal{N}^{(5Q)}(B)/\mathcal{N}^{(3Q)}(B)$ gives the probability to find a 5 quark component in a mainly 3 quark baryon. In the case of the nucleon, Diakonov and Petrov indicated its value is $0.535 \simeq 50\%$.

For the matrix elements of a typical physical observable, there are three contributions: one when the charge operator acts on the antiquark, the second when it acts on the quark from the pair, third when it acts on one of the three valence quarks. At first, we write down the expression for the 5 quark component of the vector charge in the forward limit.

$$V^{(5Q)} = \frac{108}{2}\delta_l^k T(B)_{j_1 j_2 j_3 j_4, f_5, k}^{f_1 f_2 f_3 f_4, j_5} T(B)_{f_1 f_2 g_3 g_4, l_5}^{l_1 l_2 l_3 l_4, g_5, l}$$ \tag{139}

$$\times \int \frac{d^2 p_{1-5\perp}}{(2\pi)^{10}} \int dz_{1-5}(2\pi)^2 \delta(p_{1\perp} + ... + p_{5\perp})\delta(z_1 + ... + z_5 - 1)$$

$$\times F^{j_1\sigma_1}(p_1)F^{j_2\sigma_2}(p_2)F^{j_3\sigma_3}(p_3) W_{j_5\sigma_5}^{j_4\sigma_4}(p_4, p_5)$$

$$\times F_{l_1\sigma_1}^\dagger(p_1)F_{l_2\sigma_2}^\dagger(p_2)F_{l_3\sigma_3}^\dagger(p_3) W_{cl_4\sigma_4}^{l_5\sigma_5}(p_4, p_5)$$

$$\times \left[3J_{f_3}^{g_3}\delta_{f_4}^{g_4}\delta_{g_5}^{f_5}\delta_{\sigma_3}^{\tau_3}\delta_{\sigma_4}^{\tau_4}\delta_{\tau_5}^{\sigma_5} + \delta_{f_3}^{g_3} J_{f_4}^{g_4}\delta_{g_5}^{f_5}\delta_{\sigma_3}^{\tau_3}\delta_{\sigma_4}^{\tau_4}\delta_{\tau_5}^{\sigma_5} - \delta_{f_3}^{g_3}\delta_{f_4}^{g_4} J_{g_5}^{f_5}\delta_{\sigma_3}^{\tau_3}\delta_{\sigma_4}^{\tau_4}\delta_{\tau_5}^{\sigma_5}\right]$$

In order to express the GPD $H(x,\xi,t)$ and $E(x,\xi,t)$, one has to change the momentum of one of the quarks on which the operator acts, by the corresponding momentum transfer as in the process of the 3Q component case, thereby extracting three separate contributions from the valence contribution, the quark from the $Q\bar{Q}$ pair, and the antiquarks respectively. The valence contribution in the 5 quark component is

$$\mathcal{H}_{++,val}^{(5Q)}(x,\xi,t) = \frac{108}{2}\delta_l^k T(B)_{j_1 j_2 j_3 j_4, f_5, k}^{f_1 f_2 f_3 f_4, j_5} T(B)_{f_1 f_2 g_3 g_4, l_5}^{l_1 l_2 l_3 l_4, g_5, l}$$ \tag{140}

$$\times \int \frac{d^2 p_{1-5\perp}}{(2\pi)^{10}} \int dz_1 dz_2 dz_4 dz_5(2\pi)^2 \delta(p_{1\perp} + ... + p_{5\perp})\delta(z_1 + ... + z_5 - 1)$$

$$\times F^{j_1\sigma_1}(p_1)F^{j_2\sigma_2}(p_2)F^{j_3\sigma_3}\left(\bar{p}_3 + \frac{\Delta}{2}\right) W_{j_5\sigma_5}^{j_4\sigma_4}(p_4, p_5)$$

$$\times F_{l_1\sigma_1}^\dagger(p_1)F_{l_2\sigma_2}^\dagger(p_2)F_{l_3\sigma_3}^\dagger\left(\bar{p}_3 - \frac{\Delta}{2}\right) W_{cl_4\sigma_4}^{l_5\sigma_5}(p_4, p_5)$$

$$\times \left[3J_{f_3}^{g_3}\delta_{f_4}^{g_4}\delta_{g_5}^{f_5}\delta_{\sigma_3}^{\tau_3}\delta_{\sigma_4}^{\tau_4}\delta_{\tau_5}^{\sigma_5}\right] ,$$

the quark contribution from the $q\bar{q}$ pair is

$$\mathcal{H}_{++,q-sea}^{(5Q)}(x,\xi,t) = \frac{108}{2}\delta_l^k T(B)_{j_1 j_2 j_3 j_4, f_5, k}^{f_1 f_2 f_3 f_4, j_5} T(B)_{f_1 f_2 g_3 g_4, l_5}^{l_1 l_2 l_3 l_4, g_5, l}$$ \tag{141}

$$\times \int \frac{d^2 p_{1-5\perp}}{(2\pi)^{10}} \int dz_1 dz_2 dz_3 dz_5(2\pi)^2 \delta(p_{1\perp} + ... + p_{5\perp})\delta(z_1 + ... + z_5 - 1)$$

$$\times F^{j_1\sigma_1}(p_1)F^{j_2\sigma_2}(p_2)F^{j_3\sigma_3}(p_3)W_{j_5\sigma_5}^{j_4\sigma_4}\left(\bar{p}_4 + \frac{\Delta}{2}, p_5\right)$$

$$\times F_{l_1\sigma_1}^\dagger(p_1)F_{l_2\sigma_2}^\dagger(p_2)F_{l_3\sigma_3}^\dagger(p_3)W_{cl_4\sigma_4}^{l_5\sigma_5}\left(\bar{p}_4 - \frac{\Delta}{2}, p_5\right)$$

$$\times \left[\delta_{f_3}^{g_3} J_{f_4}^{g_4}\delta_{g_5}^{f_5}\delta_{\sigma_3}^{\tau_3}\delta_{\sigma_4}^{\tau_4}\delta_{\tau_5}^{\sigma_5}\right] ,$$

36

and the antiquark contribution is

$$\mathcal{H}_{\bar{q}-sea}^{(5Q)}(x,\xi,t) = \frac{108}{2}\delta_l^k T(B)_{j_1 j_2 j_3 j_4, j_5, k}^{f_1 f_2 f_3 f_4, j_5} T(B)_{f_1 f_2 g_3 g_4, l_5}^{l_1 l_2 l_3 l_4, g_5, l}$$

$$\times \int \frac{d^2 \boldsymbol{p}_{1-5\perp}}{(2\pi)^{10}} \int dz_1 dz_2 dz_3 dz_4 (2\pi)^2 \delta(\boldsymbol{p}_{1\perp} + ... + \bar{\boldsymbol{p}}_{5\perp})\delta(z_1 + ... + \bar{z}_5 - 1)$$

$$\times F^{j_1\sigma_1}(p_1)F^{j_2\sigma_2}(p_2)F^{j_3\sigma_3}(p_3)W_{j_5\sigma_5}^{j_4\sigma_4}\left(p_4, \bar{p}_5 + \frac{\Delta}{2}\right)$$

$$\times F_{l_1\sigma_1}^{\dagger}(p_1)F_{l_2\sigma_2}^{\dagger}(p_2)F_{l_3\sigma_3}^{\dagger}(p_3)W_{cl_4\sigma_4}^{l_5\sigma_5}\left(p_4, \bar{p}_5 - \frac{\Delta}{2}\right)$$

$$\times \left[-\delta_{f_3}^{g_3}\delta_{f_4}^{g_4}J_{g_5}^{f_5}\delta_{\sigma_3}^{\tau_3}\delta_{\sigma_4}^{\tau_4}\delta_{\tau_5}^{\sigma_5}\right] \tag{142}$$

As in the 3 quark components, the matrix elements of the spin polarized case can be obtained by the replacement of the helicity operators $\delta_l^k \to (\sigma_3)_l^k$, $\delta_{\sigma_{3,4,5}}^{\tau_{3,4,5}} \to (\sigma_3)_{\sigma_{3,4,5}}^{\tau_{3,4,5}}$.

One can also get other structure functions by the same procedure as the 3 quark components. The impact parameter space distributions are the Fourier transform of the $\mathcal{H}_{++}^{(5Q)}(x,0,t)$ or $\widetilde{\mathcal{H}}_{++}^{(5Q)}(x,0,t)$ as Eq.(214), the parton distributions are the forward limit of $\mathcal{H}_{++}^{(5Q)}(x,\xi,t)$ or $\widetilde{\mathcal{H}}_{++}^{(5Q)}(x,\xi,t)$

$$q(x) = \lim_{t \to 0}\mathcal{H}_{++}(x,\xi,t) = H(x,0,0),$$
$$\Delta q(x) = \lim_{t \to 0}\widetilde{\mathcal{H}}_{++}(x,\xi,t) = \widetilde{H}(x,0,0), \tag{143}$$

and TMD parton distributions are the unintegrated versions of Eq(143) over the transverse momenta of the struck quark

$$q(x,\boldsymbol{b}_\perp) = \lim_{t \to 0}\mathcal{H}_{++}(x;\boldsymbol{b}_\perp,\xi,t) = H(x;\boldsymbol{b}_\perp,0,0),$$
$$\Delta q(x;\boldsymbol{b}_\perp) = \lim_{t \to 0}\widetilde{\mathcal{H}}_{++}(x;\boldsymbol{b}_\perp,\xi,t) = \widetilde{H}(x;\boldsymbol{b}_\perp,0,0). \tag{144}$$

C. $|x| < \xi/2$ region

As we have explained in the sec.II, in the $|x| < \xi/2$ region, baryon emits a quark-antiquark pair, and the GPDs has the physical meaning as the meson distribution amplitude not as the partonic densities. The matrix elements in this region should be the overlap between the initial $N + 1$ component and the final $N - 1$ component [23, 24]. There are two cases according to the momenta of the quark and antiquark in the pair, one when the quark with + component momentum $(x + \xi/2)M_B$ and the antiquark with $-(x - \xi/2)M_B$ are emitted, the second when the quark with $-(x - \xi/2)M_B$ and antiquark with $(x + \xi/2)M_B$ are emitted.

We assign the quark with $(x + \xi/2)M_B$ case to the distribution amplitude in the $0 < x < \xi/2$ region, and the antiquark with $(x + \xi/2)M_B$ case to the one in the $-\xi/2 < x < 0$ region, following the case with $|x| > \xi/2$ where the quark or antiquark with $(x + \xi/2)M_B$ is struck. Its representation is

$$
\mathcal{H}_{++}^{(5Q \to 3Q)}(x, \xi, t) = \pm \frac{108}{2} \delta_l^k T(B)_{j_1 j_2 j_3 j_4, f_5, k}^{f_1 f_2 f_3 f_4, j_5} T(B)_{f_1 f_2 f_3}^{l_1 l_2 l_3, l} \int \frac{d^2 p_{1-5\perp}}{(2\pi)^{10}} \int dz_1 dz_2 dz_3 \quad (145)
$$

$$
\times \ (2\pi)^2 \delta(p_{1\perp} + p_{2\perp} + p_{3\perp}) \delta(z_1 + z_2 + z_3 - 1)
$$

$$
\times \ (2\pi)^2 \delta(p_{4\perp} + p_{5\perp})
$$

$$
\times \ F^{j_1 \sigma_1}(p_1) F^{j_2 \sigma_2}(p_2) F^{j_3 \sigma_3}(p_3) W_{l_4 \sigma_4}^{l_5 \sigma_5} (p_4 \mp \Delta/2, p_5 \pm \Delta/2)
$$

$$
\times \ F_{l_1 \sigma_1}^\dagger(p_1) F_{l_2 \sigma_2}^\dagger(p_2) F_{l_3 \sigma_3}^\dagger(p_3) \left[\delta_{-\sigma_5}^{\sigma_4} J_{f_4}^{f_5} \right],
$$

where the $+$ sign in front of RHS represents the distribution amplitude in the $0 < x < \xi/2$ case, on the other hand, the $-$ sign represents the one in the $-\xi/2 < x < 0$ case. In the above representation, we take the quark in the emitted quark -antiquark as the one of the $Q\bar{Q}$ pair arisen from the coherent exponent. Hence, the three valence quarks in the $5Q$ component are contracted with the $3Q$ component with equal momenta respectively. Then the total $Q\bar{Q}$ pair momentum turns into the emitted meson momentum as $q = (\xi M_B, \Delta_\perp)$. The spin polarized GPDs $\widetilde{\mathcal{H}}_{++}(x, \xi, t)$ can be also obtained by replacing $\delta_l^k \to \sigma_l^k$, and $\delta_{-\sigma_5}^{\sigma_4} \to \sigma_{-\sigma_5}^{\sigma_4}$.

D. Overlap integrals in the infinite momentum frame

After all contractions in Eqs.(140)-(145) over flavor (f, g), isospin (j, i) and spin (σ, τ) indices, one is left with scalar integrals over longitudinal (z) and transverse $(p_\perp)$ momenta of five quarks. The integrals over the relative transverse momenta in the $Q\bar{Q}$ pair are generally UV divergent, reflecting the divergence of the negative energy Dirac sea of quarks. In this study, we cut this divergence by the Pauli-Villars cutoff method at $M_{PV} = 562\text{MeV}$. This value is chosen from the requirement that the constant $F_\pi = 93\text{MeV}$ is reproduced with $M = 375\text{MeV}$.

The pair wave function W is determined by the Fourier transforms of the mean field $\Pi(q)$ and $\Sigma(q)$. In the matrix elements of the initial $5Q$ and final $5Q$ components with zero momentum transfer, the following seven scalar integrals arise from squaring Eq.(119), corresponding to i) the full square of $\Pi(q)$ for the spin polarized and non-polarized cases ii) the square of $\Sigma(q)$ for the spin polarized and non-polarized cases, iii) the square of the

third component $\Pi_3(q)$ for the spin polarized and non-polarized cases, and iv) the mixed $\Pi(q)\Sigma(q)$ term. We name these terms,

$$K_{\pi\pi} = \frac{M^2}{2\pi} \int \frac{d^3q}{(2\pi)^3} \Phi\left(\frac{q_z}{M_B}, q_\perp\right) \theta(q_z) q_z \Pi^2(q) \tag{146}$$

$$\int_0^1 dy \int \frac{d^2 Q_\perp^2}{(2\pi)^2} \left[\frac{Q_\perp^2 + M^2}{(Q_\perp^2 + M^2 + y(1-y)q^2)^2} - (M \to M_{PV}) \right],$$

$$\Delta K_{\pi\pi} = \frac{M^2}{2\pi} \int \frac{d^3q}{(2\pi)^3} \Delta\Phi\left(\frac{q_z}{M_B}, q_\perp\right) \theta(q_z) q_z \Pi^2(q) \tag{147}$$

$$\int_0^1 dy \int \frac{d^2 Q_\perp^2}{(2\pi)^2} \left[\frac{Q_\perp^2 + M^2}{(Q_\perp^2 + M^2 + y(1-y)q^2)^2} - (M \to M_{PV}) \right],$$

$$K_{\sigma\sigma} = \frac{M^2}{2\pi} \int \frac{d^3q}{(2\pi)^3} \Phi\left(\frac{q_z}{M_B}, q_\perp\right) \theta(q_z) q_z \Sigma^2(q) \tag{148}$$

$$\int_0^1 dy \int \frac{d^2 Q_\perp^2}{(2\pi)^2} \left[\frac{Q_\perp^2 + M^2(2y-1)^2}{(Q_\perp^2 + M^2 + y(1-y)q^2)^2} - (M \to M_{PV}) \right],$$

$$\Delta K_{\sigma\sigma} = \frac{M^2}{2\pi} \int \frac{d^3q}{(2\pi)^3} \Delta\Phi\left(\frac{q_z}{M_B}, q_\perp\right) \theta(q_z) q_z \Sigma^2(q) \tag{149}$$

$$\int_0^1 dy \int \frac{d^2 Q_\perp^2}{(2\pi)^2} \left[\frac{Q_\perp^2 + M^2(2y-1)^2}{(Q_\perp^2 + M^2 + y(1-y)q^2)^2} - (M \to M_{PV}) \right],$$

$$K_{33} = \frac{M^2}{2\pi} \int \frac{d^3q}{(2\pi)^3} \Phi\left(\frac{q_z}{M_B}, q_\perp\right) \theta(q_z) \frac{q_z^3}{q^2} \Pi^2(q) \tag{150}$$

$$\int_0^1 dy \int \frac{d^2 Q_\perp^2}{(2\pi)^2} \left[\frac{Q_\perp^2 + M^2}{(Q_\perp^2 + M^2 + y(1-y)q^2)^2} - (M \to M_{PV}) \right],$$

$$\Delta K_{33} = \frac{M^2}{2\pi} \int \frac{d^3q}{(2\pi)^3} \Delta\Phi\left(\frac{q_z}{M_B}, q_\perp\right) \theta(q_z) \frac{q_z^3}{q^2} \Pi^2(q) \tag{151}$$

$$\int_0^1 dy \int \frac{d^2 Q_\perp^2}{(2\pi)^2} \left[\frac{Q_\perp^2 + M^2}{(Q_\perp^2 + M^2 + y(1-y)q^2)^2} - (M \to M_{PV}) \right],$$

$$K_{3\sigma} = \frac{M^2}{2\pi} \int \frac{d^3q}{(2\pi)^3} \Phi\left(\frac{q_z}{M_B}, q_\perp\right) \theta(q_z) \frac{q_z^2}{|q|} \Pi(q)\Sigma(q) \tag{152}$$

$$\int_0^1 dy \int \frac{d^2 Q_\perp^2}{(2\pi)^2} \left[\frac{Q_\perp^2 + M^2(2y-1)}{(Q_\perp^2 + M^2 + y(1-y)q^2)^2} - (M \to M_{PV}) \right]$$

In this representation, the integrals dp_{1-5} have been rearranged such that one first integrate over the relative momentum inside the $Q\bar{Q}$ pair $y, Q_\perp$ and then over the 3-momentum q of the pair as a whole. The step function $\theta(q_z)$ ensures that in the infinite momentum frame the longitudinal momentum carried by the pair is the positive. By $\Phi(z, q_\perp)$ we denote the probability that the three valence quarks leave the longitudinal fraction $z = z_4 + z_5 = q_z/M_B$ and the transverse momentum $q_\perp = p_{4\perp} + p_{5\perp}$ to the $Q\bar{Q}$ pair:

$$\Phi(z, q_\perp) = \int \frac{d^2 p_{1,2,3\perp}}{(2\pi)^6} dz_{1,2,3} (2\pi)^2 \delta(p_{1\perp} + p_{2\perp} + p_{3\perp} + q_\perp) \delta(z_1 + z_2 + z_3 + z - 1)$$

$$\cdot |F(p_1)|^2 \cdot |F(p_2)|^2 \cdot |F(p_3)|^2 \tag{153}$$

In the $3Q$ components of the baryons, there are no additional $Q\bar{Q}$ pair, and all quantities are proportional to $\Phi(0,0)$. Since the normalization of the valence level wave function is arbitrary, we choose it such that $\Phi(0,0) = 1$. On the other hand, $\Delta\Phi(z, \mathbf{q}_\perp)$ means the probability that the three valence quarks leave the momentum q_z and $\mathbf{q}_\perp$ to the $Q\bar{Q}$ pair when the spin polarization operator acts on the three valence quarks:

$$\Delta\Phi(z, \mathbf{q}_\perp) = \int \frac{d^2 p_{1,2,3\perp}}{(2\pi)^6} dz_{1,2,3} (2\pi)^2 \delta(\mathbf{p}_{1\perp} + \mathbf{p}_{2\perp} + \mathbf{p}_{3\perp} + \mathbf{q}_\perp) \delta(z_1 + z_2 + z_3 + z - 1)$$
$$\cdot |F(p_1)|^2 \cdot |F(p_2)|^2 \cdot |\Delta F(p_3)|^2, \tag{154}$$

As seen from Eq.(92), the discrete-level wave function $F(p) = F_{lev}(p) + F_{sea}(p)$ consist of two pieces: one is directly the wave function of the valence level, the other is related to the change of the number of quarks at the discrete level due to the presence of the Dirac sea. Hence, the square of the valence wave function can be denoted as

$$|F(p)|^2 = |F_{lev}(p)|^2 + F_{lev}^\dagger(p) \cdot F_{sea}(p) + F_{lev}(p) \cdot F_{sea}^\dagger(p) + |F_{sea}(p)|^2, \tag{155}$$

and we write down explicitly the square of the valence part $|F_{lev}(p)|^2$:

$$|F_{lev}(p)|^2 = \frac{M_B}{2\pi} \left[(h(p) + \frac{p_z}{|p|} j(p))^2 + \frac{p_\perp^2}{p^2} j^2(p) \right] \tag{156}$$

and the square of the level part in the spin-polarized case

$$|\Delta F_{lev}(p)|^2 = \frac{M_B}{2\pi} \left[(h(p) + \frac{p_z}{|p|} j(p))^2 - \frac{p_\perp^2}{p^2} j^2(p) \right] \tag{157}$$

The complete expressions for the $|F(p)|^2$ and $|\Delta F(p)|^2$ including the sea part contribution $F(p)_{sea}$ are given in Appendix C.

Let us give examples how the normalization, vector and axial charge of the baryon up to the $5Q$ components are expressed through the integrals after all contractions in Eqs.(146)-(152) are performed.

Nucleon normalization:

$$\mathcal{N}(N) = 9\Phi(0,0) + \frac{18}{5}(11K_{\pi\pi} + 23K_{\sigma\sigma}). \tag{158}$$

For the proton case, the vector charge of the u, d, s quark contributions in the $3q$ component:

$$V_u^{(3Q)} = 18\Phi(0,0), \quad V_d^{(3Q)} = 9\Phi(0,0), \quad V_s^{(3Q)} = 0, \tag{159}$$

40

and the axial charge of the u, d, s quark contributions in the $3q$ component:

$$A_u^{(3Q)} = 12\Delta\Phi(0,0), \quad A_d^{(3Q)} = -9\Delta\Phi(0,0), \quad A_s^{(3Q)} = 0. \tag{160}$$

The vector and axial charge of the valence contribution in the $5Q$ components:

$$V_u^{(val\,in\,5Q)} = 3(54K_{\sigma\sigma} + 21.36K_{\pi\pi}),$$

$$V_d^{(val\,in\,5Q)} = 3(26.4K_{\sigma\sigma} + 14.88K_{\pi\pi}),$$

$$V_s^{(val\,in\,5Q)} = 3(2.4K_{\sigma\sigma} + 3.36K_{\pi\pi}),$$

$$A_u^{(val\,in\,5Q)} = 3(36.24\Delta K_{\sigma\sigma} + 9.84\Delta K_{\pi\pi} + 3.36\Delta K_{33}),$$

$$A_d^{(val\,in\,5Q)} = 3(-8.48\Delta K_{\sigma\sigma} - 6.88\Delta K_{\pi\pi} + 6.08\Delta K_{33}),$$

$$A_s^{(val\,in\,5Q)} = 3(-0.11\Delta K_{\sigma\sigma} - 1.76\Delta K_{\pi\pi} + 2.56\Delta K_{33}), \tag{161}$$

the quark contribution from the $Q\bar{Q}$:

$$V_u^{(sea)} = 38.16K_{\sigma\sigma} + 26.64K_{\pi\pi},$$

$$V_d^{(sea)} = 32.88K_{\sigma\sigma} + 12.72K_{\pi\pi},$$

$$V_s^{(sea)} = 11.76K_{\sigma\sigma} + 0.24K_{\pi\pi},$$

$$A_u^{(sea)} = -30.24K_{3\sigma},$$

$$A_d^{(sea)} = 19.68K_{3\sigma},$$

$$A_s^{(sea)} = 3.36K_{3\sigma}, \tag{162}$$

and the antiquark contributions

$$V_{\bar{u}}^{(sea)} = -34.56K_{\sigma\sigma} - 11.52K_{\pi\pi},$$

$$V_{\bar{d}}^{(sea)} = -29.28K_{\sigma\sigma} - 17.76K_{\pi\pi},$$

$$V_{\bar{s}}^{(sea)} = -18.96K_{\sigma\sigma} - 10.32K_{\pi\pi},$$

$$A_{\bar{u}}^{(sea)} = -23.04K_{3\sigma},$$

$$A_{\bar{d}}^{(sea)} = +12.48K_{3\sigma},$$

$$A_{\bar{s}}^{(sea)} = +3.36K_{3\sigma}, \tag{163}$$

The physical observables are given by adding these contribution and then dividing the normalization, for example, the vector charge of the u quark is

$$V_u = \frac{V^{(3Q)} + V_u^{(val\,in\,5Q)} + V_u^{(sea)} + V_{\bar{u}}^{(sea)}}{\mathcal{N}} = 2, \tag{164}$$

41

which gives exactly the u quark number in the proton as expected.

Another quantity in which we are interested is the spin content of the proton. From the above expressions of the axial charge, the representations of spin components of each flavor are

$$\Delta u = \frac{12\Delta\Phi(0,0) + 108.72\Delta K_{\sigma\sigma} + 29.52\Delta K_{\pi\pi} + 10.08\Delta K_{33} - 53.28K_{3\sigma}}{9\Phi(0,0) + 39.6K_{\pi\pi} + 82.8K_{\sigma\sigma}},$$

$$\Delta d = \frac{-3\Delta\Phi(0,0) - 25.44\Delta K_{\sigma\sigma} - 20.64\Delta K_{\pi\pi} + 18.24\Delta K_{33} + 32.16K_{3\sigma}}{9\Phi(0,0) + 39.6K_{\pi\pi} + 82.8K_{\sigma\sigma}},$$

$$\Delta s = \frac{-0.48\Delta K_{\sigma\sigma} - 5.28\Delta K_{\pi\pi} + 7.68\Delta K_{33} + 6.72K_{3\sigma}}{9\Phi(0,0) + 39.6K_{\pi\pi} + 82.8K_{\sigma\sigma}}, \tag{165}$$

hence the proton spin content is

$$\Delta\Sigma = \Delta u + \Delta d + \Delta s = \frac{9\Delta\Phi(0,0) + 82.88\Delta K_{\sigma\sigma} + 3.6\Delta K_{\pi\pi} + 36\Delta K_{33} - 14.4K_{3\sigma}}{9\Phi(0,0) + 39.6K_{\pi\pi} + 82.8K_{\sigma\sigma}}, \tag{166}$$

and the isovector axial charge is

$$g_A^{(3)} = \Delta u - \Delta d = \frac{15\Delta\Phi(0,0) + 134.16\Delta K_{\sigma\sigma} + 50.16\Delta K_{\pi\pi} - 8.16\Delta K_{33} - 85.44K_{3\sigma}}{9\Phi(0,0) + 39.6K_{\pi\pi} + 82.8K_{\sigma\sigma}}. \tag{167}$$

Recently Diakonov and Petrov evaluated the isovector axial charge $g_A^{(3)}$ in the nonrelativistic limit where they neglected the $L = 1$ lower component $j(p)$ and the sea quark contribution. In the non-relativistic limit, the integrals of $5Q$ components are set to be zero, and the probability $\Delta\Phi(z, \boldsymbol{p}_\perp)$ for the spin polarized case becomes equal the $\Phi(z, \boldsymbol{p}_\perp)$ for the spin non-polarized one because there is no effect the lower components and the sea contribution $F_{sea}(p)$ to the one quark wave function. Therefore in the non-relativistic approximation the nucleon axial charge is

$$g_A^{(3)} = \frac{15\Phi(0,0)}{9\Phi(0,0)} = \frac{5}{3} \simeq 1.67 \tag{168}$$

which is well known result of the nonrelativistic quark model. The account for any number of pairs and for the relativistic corrections is expected to bring $g_A^{(3)}$ very close to the experimental value $g_A^{(3)} = 1.27$. For the same reason, in the nonrelativistic $3Q$ approximation, the proton spin content is

$$\Delta\Sigma = \frac{9\Phi(0,0)}{9\Phi(0,0)} = 1, \tag{169}$$

which is also the value expected in the nonrelativistic quark model. Again, this value may be expected to be close to the experimental value 0.31 ± 0.07 measured by the EMC collaboration by taking account of the relativistic effects and higher Fock components [4, 5].

Although the overlap integrals of the structure functions including the GPDs can also be expressed in terms of the chiral mean field as in the static observable for the vector and axial charges, a little caution are required. For example, the full square integral of the scalar field $K_{\sigma\sigma}$ has to be classified further into the three contributions: one when the charge operator acts on the quark in the $Q\bar{Q}$, second when it acts on the antiquark, third when it acts on one of the three valence quarks. When one of the three valence quark is measured, the overlap integral of the square of $\Sigma(p)$ is

$$K_{\sigma\sigma}^{(val\,in\,5Q)}(x = \bar{z}_3, \xi, t) = \frac{M^2}{2\pi} \int \frac{d^3 q}{(2\pi)^3} \Phi\left(q_z, \boldsymbol{q}_\perp; z_3, \xi, t\right) \theta(q_z) q_z \Pi^2(\boldsymbol{q}) \tag{170}$$

$$\int_0^1 dy \int \frac{d^2 \boldsymbol{Q}_\perp^2}{(2\pi)^2} \left[\frac{\boldsymbol{Q}_\perp^2 + M^2}{(\boldsymbol{Q}_\perp^2 + M^2 + y(1-y)\boldsymbol{q}^2)^2} - (M \to M_{PV}) \right],$$

where we interpret $\Phi\left(q_z, \boldsymbol{q}_\perp; z_3, \xi, t\right)$ as the probability that the three valence quarks leave the momentum $q_z, \boldsymbol{q}_\perp$ to the $Q\bar{Q}$ pair when the third quark has the longitudinal momentum at rest frame $p_{3z} = z_3 M_B - \varepsilon_{lev}$ and with the momentum transfer Δ as

$$\Phi(z, \boldsymbol{q}_\perp; z_3, \xi, t) = \int \frac{d^2 \boldsymbol{p}_{1,2,3\perp}}{(2\pi)^6} dz_1 dz_2 (2\pi)^2 \delta(\boldsymbol{p}_{1\perp} + \boldsymbol{p}_{2\perp} + \boldsymbol{p}_{3\perp} + \boldsymbol{q}_\perp) \delta(z_1 + z_2 + z_3 + z - 1)$$

$$\cdot |F(p_1)|^2 \cdot |F(p_2)|^2 \cdot (F^\dagger \left(p_3 - \frac{\Delta}{2}\right) \cdot F \left(p_3 + \frac{\Delta}{2}\right))\Big|_{p_{1,2,3z}=z_{1,2,3}M_B - \varepsilon_{lev}} \tag{171}$$

When the quark or the antiquark is struck, the overlap integrals are:

$$K_{\sigma\sigma}^{(q\,in\,sea)}(x = z_4, \xi, t) = \frac{M^2}{2\pi} \int \frac{d^2 \boldsymbol{p}_{4,5\perp} dz_5}{(2\pi)^5} \Phi\left(z, \boldsymbol{p}_\perp\right) \theta(\bar{z}) \Pi(\boldsymbol{q}^I) \Pi(\boldsymbol{q}^F) \tag{172}$$

$$\left[\frac{\boldsymbol{Q}_\perp^I \cdot \boldsymbol{Q}_\perp^F + M^2}{(\boldsymbol{Q}_\perp^2 + M^2 + y(1-y)\boldsymbol{q}^2)^I \cdot (\boldsymbol{Q}_\perp^2 + M^2 + y(1-y)\boldsymbol{q}^2)^F} \right.$$

$$\left. -(M \to M_{PV}) \right],$$

$$K_{\sigma\sigma}^{(\bar{q}\,in\,sea)}(x = z_5, \xi, t) = \frac{M^2}{2\pi} \int \frac{d^2 \boldsymbol{p}_{4,5\perp} dz_4}{(2\pi)^5} \Phi\left(z, \boldsymbol{p}_\perp\right) \theta(\bar{z}) \Pi(\boldsymbol{q}^I) \Pi(\boldsymbol{q}^F) \tag{173}$$

$$\left[\frac{\boldsymbol{Q}_\perp^I \cdot \boldsymbol{Q}_\perp^F + M^2}{(\boldsymbol{Q}_\perp^2 + M^2 + y(1-y)\boldsymbol{q}^2)^I \cdot (\boldsymbol{Q}_\perp^2 + M^2 + y(1-y)\boldsymbol{q}^2)^F} \right.$$

$$\left. -(M \to M_{PV}) \right],$$

where we denote the momentum with the indices I (F) as the one before (after) the charge operator acts on the quark. For the case that the quark in the $Q\bar{Q}$ pair is struck,

$$\begin{cases} \boldsymbol{Q}_\perp^I = \left(z_4 + \frac{\xi}{2}\right) \boldsymbol{p}_{5\perp} - z_5 \left(\boldsymbol{p}_{4\perp} - \frac{\boldsymbol{\Delta}_\perp}{2}\right), & \boldsymbol{q}^I = \left(\boldsymbol{p}_4 - \frac{\boldsymbol{\Delta}}{2}\right) + \boldsymbol{p}_5, & y^I = \frac{z_5}{(z_4 + \xi/2) + z_5} \\ \boldsymbol{Q}_\perp^F = \left(z_4 - \frac{\xi}{2}\right) \boldsymbol{p}_{5\perp} - z_5 \left(\boldsymbol{p}_{4\perp} + \frac{\boldsymbol{\Delta}_\perp}{2}\right), & \boldsymbol{q}^F = \left(\boldsymbol{p}_4 + \frac{\boldsymbol{\Delta}}{2}\right) + \boldsymbol{p}_5, & y^F = \frac{z_5}{(z_4 - \xi/2) + z_5} \end{cases} \tag{174}$$

43

and the antiquark struck case,

$$\begin{cases} \boldsymbol{Q}_\perp^{\mathrm{I}} = z_4 \left(\boldsymbol{p}_{5\perp} - \frac{\boldsymbol{\Delta}_\perp}{2}\right) - \left(z_5 + \frac{\xi}{2}\right)\boldsymbol{p}_{4\perp}, & \boldsymbol{q}^{\mathrm{I}} = \boldsymbol{p}_4 + \left(\boldsymbol{p}_5 - \frac{\boldsymbol{\Delta}}{2}\right), & y^{\mathrm{I}} = \frac{z_5}{z_4+(z_5+\xi/2)} \\ \boldsymbol{Q}_\perp^{\mathrm{F}} = z_4 \left(\boldsymbol{p}_{5\perp} + \frac{\boldsymbol{\Delta}_\perp}{2}\right) - \left(z_5 - \frac{\xi}{2}\right)\boldsymbol{p}_{4\perp}, & \boldsymbol{q}^{\mathrm{F}} = \boldsymbol{p}_4 + \left(\boldsymbol{p}_5 + \frac{\boldsymbol{\Delta}}{2}\right), & y^{\mathrm{F}} = \frac{z_5}{z_4+(z_5-\xi/2)} \end{cases}$$
(175)

After all, in the $|x| > \xi/2$ region, the light-cone helicity non-flip, spin non-polarized GPDs $\mathcal{H}_{++}^q(x,\xi,t)$ and spin polarized $\widetilde{\mathcal{H}}_{++}^q(x,\xi,t)$ of each flavor are represented as

$$\mathcal{H}_{++}^u(x,\xi,t) = \begin{cases} \frac{1}{\mathcal{N}(p)}\left(6\Phi(0,0;x,\xi,t) + 162 K_{\sigma\sigma}^{\mathrm{val\ in5}Q}(x,\xi,t)\right. \\ \qquad \left. +64.08 K_{\pi\pi}^{\mathrm{val\ in5}Q}(x,\xi,t)\right) & \text{valence} \\ \frac{1}{\mathcal{N}(p)}\left(38.16 K_{\sigma\sigma}^{q\,\mathrm{in\ sea}}(x,\xi,t) + 26.24 K_{\pi\pi}^{q\,\mathrm{in\ sea}}(x,\xi,t)\right) & \text{Dirac sea, quark} \\ \frac{1}{\mathcal{N}(p)}\left(34.56 K_{\sigma\sigma}^{q\,\mathrm{in\ sea}}(x,\xi,t) + 11.52 K_{\pi\pi}^{q\,\mathrm{in\ sea}}(x,\xi,t)\right) & \text{Dirac sea, antiquark} \end{cases}$$
(176)

$$\mathcal{H}_{++}^d(x,\xi,t) = \begin{cases} \frac{1}{\mathcal{N}(p)}\left(3\Phi(0,0;x,\xi,t) + 79.2 K_{\sigma\sigma}^{\mathrm{val\ in5}Q}(x,\xi,t)\right. \\ \qquad \left. +34.64 K_{\pi\pi}^{\mathrm{val\ in5}Q}(x,\xi,t)\right) & \text{valence} \\ \frac{1}{\mathcal{N}(p)}\left(32.88 K_{\sigma\sigma}^{q\,\mathrm{in\ sea}}(x,\xi,t) + 12.72 K_{\pi\pi}^{q\,\mathrm{in\ sea}}(x,\xi,t)\right) & \text{Dirac sea, quark} \\ \frac{1}{\mathcal{N}(p)}\left(29.28 K_{\sigma\sigma}^{q\,\mathrm{in\ sea}}(x,\xi,t) + 17.76 K_{\pi\pi}^{q\,\mathrm{in\ sea}}(x,\xi,t)\right) & \text{Dirac sea, antiquark} \end{cases}$$
(177)

$$\mathcal{H}_{++}^s(x,\xi,t) = \begin{cases} \frac{1}{\mathcal{N}(p)}\left(7.2 K_{\sigma\sigma}^{\mathrm{val\ in5}Q}(x,\xi,t) + 10.08 K_{\pi\pi}^{\mathrm{val\ in5}Q}(x,\xi,t)\right) & \text{valence} \\ \frac{1}{\mathcal{N}(p)}\left(11.76 K_{\sigma\sigma}^{q\,\mathrm{in\ sea}}(x,\xi,t) + 0.24 K_{\pi\pi}^{q\,\mathrm{in\ sea}}(x,\xi,t)\right) & \text{Dirac sea, quark} \\ \frac{1}{\mathcal{N}(p)}\left(18.96 K_{\sigma\sigma}^{q\,\mathrm{in\ sea}}(x,\xi,t) + 10.32 K_{\pi\pi}^{q\,\mathrm{in\ sea}}(x,\xi,t)\right) & \text{Dirac sea, antiquark} \end{cases}$$
(178)

$$\widetilde{\mathcal{H}}_{++}^u(x,\xi,t) = \begin{cases} \frac{1}{\mathcal{N}(p)}\left(12\Delta\Phi(0,0;x,\xi,t) + 108.72\Delta K_{\sigma\sigma}^{\mathrm{val\ in5}Q}(x,\xi,t)\right. \\ \qquad \left. +29.52\Delta K_{\pi\pi}^{\mathrm{val\ in5}Q}(x,\xi,t) + 10.08\Delta K_{33}(x,\xi,t)\right) & \text{valence} \\ \frac{1}{\mathcal{N}(p)}\left(-30.24 K_{3\sigma}^{q\,\mathrm{in\ sea}}(x,\xi,t)\right) & \text{Dirac sea, quark} \\ \frac{1}{\mathcal{N}(p)}\left(-23.04 K_{3\sigma}^{q\,\mathrm{in\ sea}}(x,\xi,t)\right) & \text{Dirac sea, antiquark} \end{cases}$$
(179)

$$\widetilde{\mathcal{H}}_{++}^d(x,\xi,t) = \begin{cases} \frac{1}{\mathcal{N}(p)}\left(-3\Delta\Phi(0,0;x,\xi,t) - 25.44\Delta K_{\sigma\sigma}^{\mathrm{val\ in5}Q}(x,\xi,t)\right. \\ \qquad \left. -20.64\Delta K_{\pi\pi}^{\mathrm{val\ in5}Q}(x,\xi,t) + 18.24\Delta K_{33}(x,\xi,t)\right) & \text{valence} \\ \frac{1}{\mathcal{N}(p)}\left(19.68 K_{\sigma\sigma}^{q\,\mathrm{in\ sea}}(x,\xi,t)\right) & \text{Dirac sea, quark} \\ \frac{1}{\mathcal{N}(p)}\left(12.48 K_{\sigma\sigma}^{q\,\mathrm{in\ sea}}(x,\xi,t)\right) & \text{Dirac sea, antiquark} \end{cases}$$
(180)

44

$$
\widetilde{\mathcal{H}}^s_{++}(x,\xi,t) = \begin{cases} \frac{1}{\mathcal{N}(p)}\left(-0.48\Delta K^{\text{val in}5Q}_{\sigma\sigma}(x,\xi,t)\right. \\ \left. -5.28\Delta K^{\text{val in}5Q}_{\pi\pi}(x,\xi,t) + 7.68\Delta K_{33}(x,\xi,t)\right) & \text{valence} \\ \frac{1}{\mathcal{N}(p)}\left(3.36 K^{q\text{ in sea}}_{\sigma\sigma}(x,\xi,t)\right) & \text{Dirac sea, quark} \\ \frac{1}{\mathcal{N}(p)}\left(3.36 K^{\bar{q}\text{ in sea}}_{\sigma\sigma}(x,\xi,t)\right) & \text{Dirac sea, antiquark.} \end{cases} \tag{181}
$$

Next we show the results in the center region $|x| < \xi/2$ which can be represented in terms of the non-diagonal matrix element in the Fock state components. After all contraction over the spin, flavor, and isospin indices, the spin non-polarized GPDs $\mathcal{H}_{++}(x,\xi,t)$ have only the scalar components of the mean chiral field,

$$
\mathcal{H}^{(5Q\to 3Q)}_{++}(x,\xi,t) \sim -\delta^{\sigma_4}_{-\sigma_5}S(x,\xi,t) \equiv -\delta^{\sigma_4}_{-\sigma_5}\int \frac{d^3 \boldsymbol{p}_\perp}{(2\pi)^5}\frac{\Sigma(\boldsymbol{q})}{Z}\frac{x}{\xi}, \tag{182}
$$

where

$$
\boldsymbol{q} = \left(\frac{\xi}{(1+\xi/2)}M_B, -\frac{\boldsymbol{\Delta}_\perp}{(1+\xi/2)}\right),
$$

$$
Z = \left(\frac{1}{(1+\xi/2)^2}(\xi^2 M_B^2 - \boldsymbol{\Delta}^2_\perp) + M_B^2 - \frac{(x^2-\xi^2/4)}{\xi^2(1+\xi/2)^2}(-\xi\boldsymbol{p}_\perp - x\boldsymbol{\Delta}_\perp)^2\right) \tag{183}
$$

The operator acting on the quark antiquark helicities $\delta^{\sigma_4}_{-\sigma_5}$ means that the quark antiquark in the $Q\bar{Q}$ pair has to appear in the total helicity state

$$
(|\uparrow\downarrow\rangle + |\downarrow\uparrow\rangle). \tag{184}
$$

One should recall that the function $\mathcal{H}^{(3Q\to 5Q)}_{++}$ in this region corresponds to the D-term introduced in Sec.II. It is important to argue the relation between the spontaneous chiral symmetry breaking and the D-term [56]. In particular, this is seen clearly in the case of the pion GPD. To see this, it is useful to decompose the D-term in the Gegenbauer polynomials

$$
D(z) = (1-z^2)\left(d_1 C_1^{3/2}(z) + d_3 C_3^{3/2}(z) + d_5 C_5^{3/2}(z) + \cdots\right) \tag{185}
$$

In the case of pion D-term , the value of the coefficient d_1 in the parameterization (185) can be computed in a model independent way and it is strictly nonzero [57–60]. To compute the pion D-term, Polyakov used the soft-pion theorem for the singlet GPD in the pion [56]. This soft-pion theorem has been derived using the fact that the pion is a (pseudo)Goldstone boson of the spontaneously broken chiral symmetry. They obtained the expression for pion D-term

$$
D(z) = -\frac{5M^\pi}{4}(1-z^2)\left(C_1^{3/2}(z) + \cdots\right), \tag{186}
$$

where M^π is the momentum fraction carried by the quarks in the pion. One see therefore that the first Gegenbauer coefficient of the pion D-term is negative and strictly nonzero [57].

The nucleon D-term is not fixed by general principles. However, Petrov et.al. expect that the contribution of the pion cloud of the nucleon can be significant [57]. Quantitatively for the coefficients d_1, d_3, d_5, the numerical estimate which is based on the calculation of GPDs in the chiral quark soliton model gives

$$d_1 \simeq -4.0, \quad d_3 \simeq -1.2, \quad d_5 \simeq -0.5. \tag{187}$$

They argued that the coincidence of the signs in the nucleon and pion D-terms hints that the D-term in the nucleon is intimately related to the spontaneous breaking of the chiral symmetry. On the other hand, Eq.(182) which is obtained by the overlap integral of the light-cone wave function indicates more directly that the physics of the spontaneously chiral symmetry breaking plays an important role in determining the size and the sign of the D-term. As one can see from Eq.(182), the nontrivial structure in terms of $z = x/\xi$ is determined mainly by the scalar part of the mean chiral field $\Sigma(q)$. As we will show in Sec.V, the sign of the function $\mathcal{H}_{++}^{3Q \to 5Q}$ gives same sign as that of the pion D-term.

On the other hand, the spin polarized GPDs $\widetilde{\mathcal{H}}_{++}(x, \xi, t)$ in this region have zero amplitude since the SU(3) flavor group integration gives zero value. This is because we have taken only the 1st order $Q\bar{Q}$ pair in the wave function, so if we include higher Fock contribution the $\widetilde{\mathcal{H}}_{++}(x, \xi, t)$ in the central region may have non-zero value. The spin non-polarized GPDs $\mathcal{H}_{++}^q(x, \xi, t)$ of each flavor can be represented as

$$\mathcal{H}_{++}^u(x, \xi, t) = \begin{cases} 21.6 S(x, \xi, t)/\mathcal{N}(B) & \text{for } 0 < x < \xi/2 \\ -21.6 S(x, \xi, t)/\mathcal{N}(B) & \text{for } -\xi/2 < x < 0 \end{cases} \tag{188}$$

$$\mathcal{H}_{++}^d(x, \xi, t) = \begin{cases} 19.8 S(x, \xi, t)/\mathcal{N}(B) & \text{for } 0 < x < \xi/2 \\ -19.8 S(x, \xi, t)/\mathcal{N}(B) & \text{for } -\xi/2 < x < 0 \end{cases} \tag{189}$$

$$\mathcal{H}_{++}^s(x, \xi, t) = \begin{cases} 12.6 S(x, \xi, t)/\mathcal{N}(B) & \text{for } 0 < x \leqslant \xi/2 \\ -12.6 S(x, \xi, t)/\mathcal{N}(B) & \text{for } -\xi/2 < x < 0 \end{cases} \tag{190}$$

These Eqs.(176)-(181) (188)-(190) are the our final representation for the GPDs, and in a sense "*master*" formulae from which the impact parameter space PDF, TMD PDF, and form factor, all structure functions we want, can be obtained with appropriate operation.

V. NUMERICAL RESULTS AND DISCUSSION

For the numerical evaluation of the integrals contained in the overlap representations of the matrix elements, we need first of all the self consistent profile function. This function can be evaluated self-consistently with the following variational principle

$$\frac{\delta}{\delta F(r)} E[F(r)] = 0. \tag{191}$$

The resultant shape of the self-consistent profile function are dependent also on the dynamical quark mass M. In this study, we will perform the numerical estimate of the all physical quantities with the quark mass $M = 375\text{MeV}$, and with the Pauli-Villars mass $M_{PV} = 562\text{MeV}$ reproducing the pion decay constant 93MeV. Our profile function self-consistently obtained with the mass $M = 375\text{MeV}$ is shown in Fig.2.
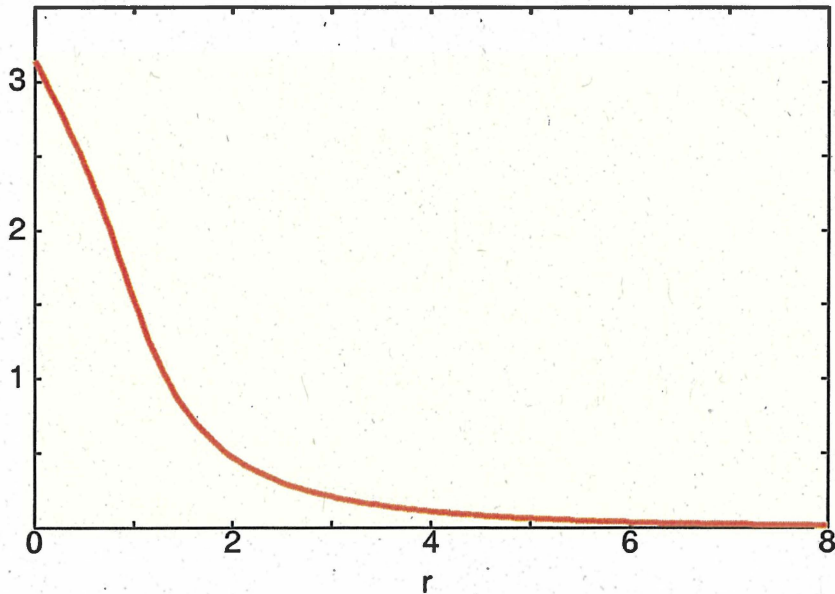

FIG. 2: Self-consistent profile function $F(r)$: the horizontal axis is plotted in units of $1/M$ with M=375MeV.

With this profile function, the baryon mass M_B becomes 1017.5MeV, the classical mass (without quantum correction) in the mean field approximation. The self-consistent pseudoscalar $\Pi(\boldsymbol{p})$ and scalar $\Sigma(\boldsymbol{p})$ field is plotted in Fig.4.

We first evaluate the probability distribution $\Phi(z, \boldsymbol{q}_\perp)$ for the three valence quarks spin unpolarized case and also $\Delta\Phi(z, \boldsymbol{q}_\perp)$ for the one of the three valence quarks spin polarized case. These probabilities have the physical meaning as that the $Q\bar{Q}$ pair carry the fraction
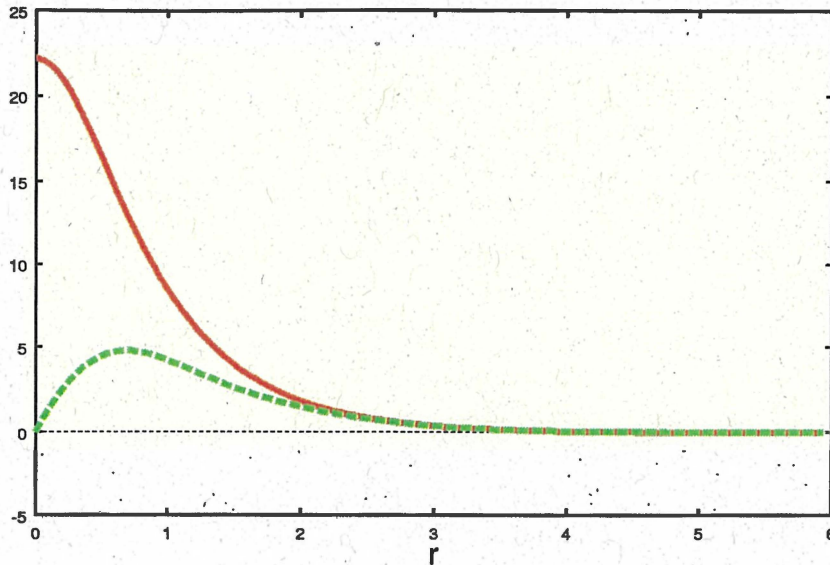
FIG. 3: Upper s-wave component $h(r)$ (solid) and the lower p-wave component $j(r)$ (dashed) of the bound state quark wave function. All the three valence quarks have the energy $E_{lev} = 150\text{MeV}$.
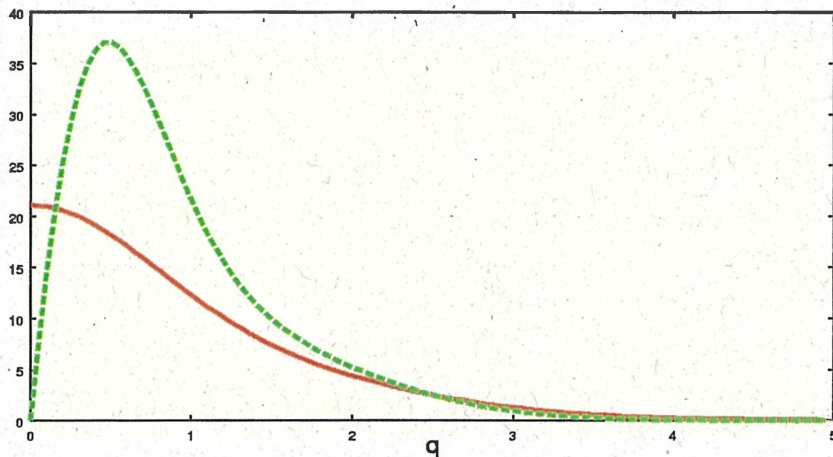

FIG. 4: The self-consistent pseudoscalar $|\Pi(q)|$ (dashed) and scalar $|\Sigma(q)|$ (solid) fields in baryons in the momentum space. The horizontal axis is in units of $M = 375\text{MeV}$

z of the baryon momentum and the transverse momentum $\boldsymbol{q}_\perp$. We show the numerically evaluated probability in the two cases, one with the non-relativistic approximation where we set the discrete wave function involved in Eq.(121) as $F(\boldsymbol{p}) \simeq \sqrt{\mathcal{M}_B/2\pi}\, h(\boldsymbol{p})$, second with the lower $L = 1$ component $j(\boldsymbol{p})$.

For the spin polarized case, the probability $\Delta\Phi(z, \boldsymbol{q}_\perp)$ is equal to the spin unpolarized probability $\Phi(z, \boldsymbol{q}_\perp)$ in the non-relativistic approximation. When we include the $L = 1$ lower component $j(\boldsymbol{p})$ in the discrete wave function, both probability densities are drasti-
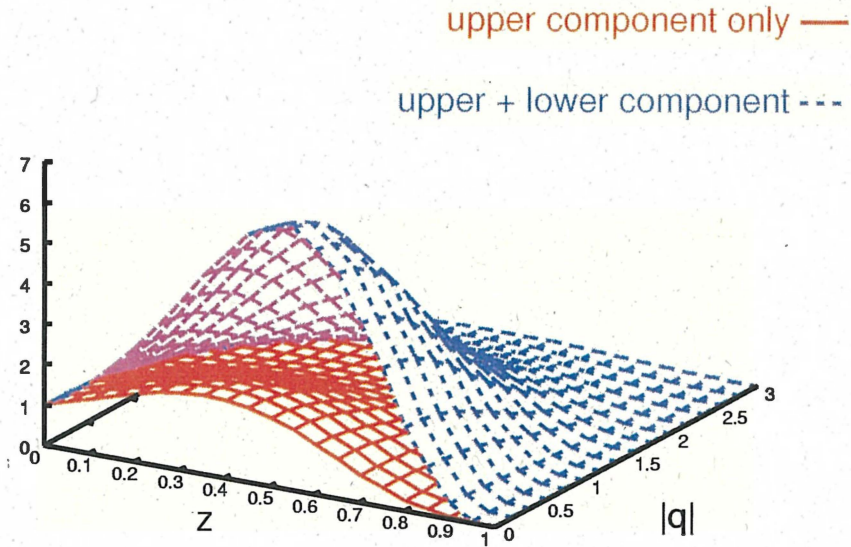
48

FIG. 5: The probability distributions $\Phi(z, \boldsymbol{q}_\perp)$ that the $Q\bar{Q}$ pair carries the fraction z of the baryon momentum and the transverse momentum $\boldsymbol{q}_\perp$ plotted in units of $M = 375\text{MeV}$. The solid curved surface shows the probability with the s-wave upper component $h(r)$ only, the dashed curved surface is that also the p-wave lower component $j(r)$ included.
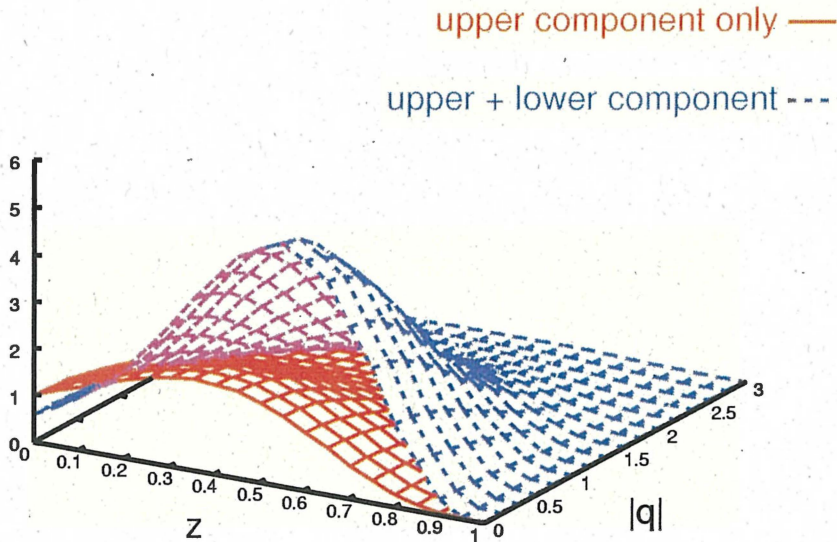
FIG. 6: The spin polarized probability distribution $\Delta\Phi(x, \boldsymbol{q}_\perp)$.

cally changed. From Figs.5,6, one sees that the $\Delta\Phi(z, \boldsymbol{q}_\perp)$ is reduced compared with the unpolarized one $\Phi(z, \boldsymbol{q}_\perp)$. Since the numerical calculation of the probability distribution with sea-quark effects $F_{sea}(\boldsymbol{p})$ by our computer takes too much time, it is not evaluated except the value at the zero momentum point $\Phi(0,0)$ and $\Delta\Phi(0,0)$. The nucleon $3Q$ nor-

malization is denoted with the value at the zero momentum carried by the $Q\bar{Q}$ pair $\Phi(0,0)$

$$\mathcal{N}^{(3Q)}(N) = 9\Phi(0,0) \tag{192}$$

and flavor decomposition of the nucleon $3Q$ axial charge are

$$A_u^{(3)} = 12\Delta\Phi(0,0) = \begin{cases} 12 & \text{(upper component only)} \\ 7.56 & \text{(upper + lower component)} \\ 6.12 & \text{(upper + lower component + Dirac sea effect)} \end{cases} \tag{193}$$

$$A_d^{(3Q)} = -3\Delta\Phi(0,0) = \begin{cases} -3 & \text{(upper component only)} \\ -1.89 & \text{(upper + lower component)} \\ -1.53 & \text{(upper + lower component + Dirac sea effect)} \end{cases} \tag{194}$$

$$A_s^{(3Q)} = 0 \tag{195}$$

From Eq.(167), $g_A^{(3)}$ and the nucleon spin contents in the $3Q$ component approximation are

$$g_A^{(3)} = \frac{5\Delta\Phi(0,0)}{3\Phi(0,0)} = \begin{cases} 1.67 & \text{(upper component only)} \\ 1.05 & \text{(upper + lower component)} \\ 0.85 & \text{(upper + lower component + Dirac sea effect)} \end{cases} \tag{196}$$

$$\Delta\Sigma = \frac{\Delta\Phi(0,0)}{\Phi(0,0)} = \begin{cases} 1 & \text{(upper component only)} \\ 0.63 & \text{(upper + lower component)} \\ 0.51 & \text{(upper + lower component + Dirac sea effect)} \end{cases} \tag{197}$$

With the above probability distributions $\Delta\Phi(z,\boldsymbol{q})$ and $\Phi(z,\boldsymbol{q})$, the numerical evaluation of the integrals (146)-(152) yields

$$K_{\pi\pi} = 0.07478, \quad K_{\sigma\sigma} = 0.03693, \quad K_{3\sigma} = 0.05750, \quad K_{33} = 0.05655,$$

$$\Delta K_{\pi\pi} = 0.05160, \quad \Delta K_{\sigma\sigma} = 0.02666, \quad \Delta K_{3\sigma} = 0.04134. \tag{198}$$

Putting these value into Eq.(158), we obtain nucleon $5Q$ normalization:

$$\mathcal{N}^{(5Q)} = 15.019 \tag{199}$$

and flavor decomposition of the nucleon $5Q$ axial charge:

$$A_u^{(5Q)} = 1.775, \quad A_d^{(5Q)} = 0.860, \quad A_s^{(5Q)} = 0.419. \tag{200}$$

50

In the 5Q approximation, the flavor decomposed nucleon spin content are

$$\Delta u = \frac{A_u^{(3Q)} + A_u^{(5Q)}}{\mathcal{N}^{(3Q)} + \mathcal{N}^{(5Q)}} = 0.53,$$

$$\Delta d = -0.04,$$

$$\Delta s = 0.02, \tag{201}$$

from which the isovector axial coupling constant and nucleon spin contents are

$$g_A^{(3)} = 0.57, \quad \Delta \Sigma = 0.51. \tag{202}$$

With the relativistic effects, the nucleon axial coupling constant $g_A^{(3)}$ has been underestimated compared with the experimental value 1.27, even in the 3Q component approximation. The 5Q component effect works to reduce $g_A^{(3)}$ to smaller value. This value may be further modified by taking account of more higher Fock component in the baryon wave function. This is well known as $g_A^{(3)}$ problem in the chiral soliton model, and is caused by the fact that we are working in the relativistic mean field approximation without quantum corrections. Indeed, the isovector axial coupling constant has a sizable $1/N_c$ correction which is a quantum quark loop effect. Wakamatsu and Watabe indicated that the model can give the reasonable value of g_A if we include the subleading order in the $1/N_c$ expansion [61]. On the other hand, the spin content of the nucleon $\Delta\Sigma$, as the isoscalar axial charge, has only subleading correction in the Ω expansion. Again, the spin content $\Delta\Sigma$ may be also more reduced if we include the higher Fock components, and can be expected to be more close to its experimental value 0.31 [29]. Now, we find that the ratio of the 5Q to the main 3Q normalization in the nucleon with lower component is fairly large, i.e.

$$\frac{\mathcal{N}^{(5Q)}}{\mathcal{N}^{(3Q)}} = 0.668 \simeq 67\%. \tag{203}$$

A. Quark distribution function $q(x)$ and $\Delta q(x)$

Next, we will show the predictions for the distribution functions. First, we compute unpolarized and polarized spin non-flip GPD $H_q(x,\xi,t)$ and $\widetilde{H}_q(x,\xi,t)$ of each flavor q in the forward limit, $t \to 0$, where it coincides with the usual quark and antiquark distributions. These results are shown in Figs.7,8, and 9 for unpolarized distributions and in Figs.10,11, and 12 for polarized distributions, where we plot separately the contributions of the discrete
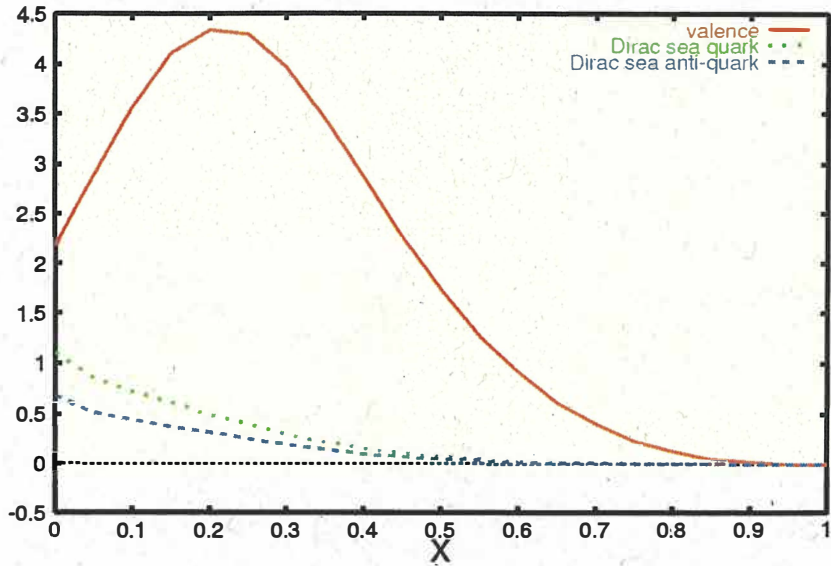
51

FIG. 7: Theoretical prediction for the unpolarized u quark distribution $u(x)$. solid curve: the discrete level contribution. dashed curve: Dirac sea quark contribution. dashed dotted curve: Dirac sea antiquark contribution
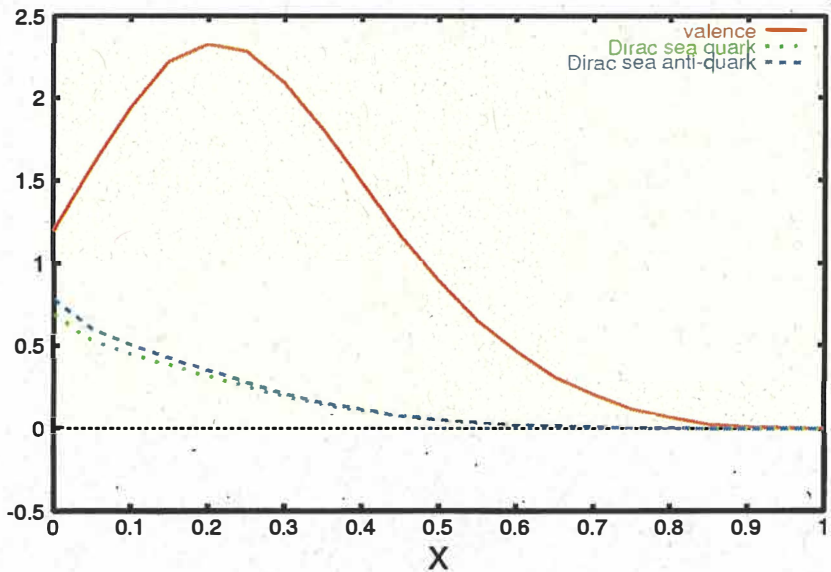

FIG. 8: Theoretical prediction for the unpolarized d quark distribution $d(x)$. The curves have the same meanings as in Fig.7.

level and that of the Dirac sea quarks. Note that the contribution of the discrete level is the sum of all contribution of $3q$ component and valence quarks contribution of the $5Q$ component. The discrete level distribution functions have peaked around at $x = 1/3$. On the other hand, the contribution of the Dirac sea quarks arise from the additional $Q\bar{Q}$ pair
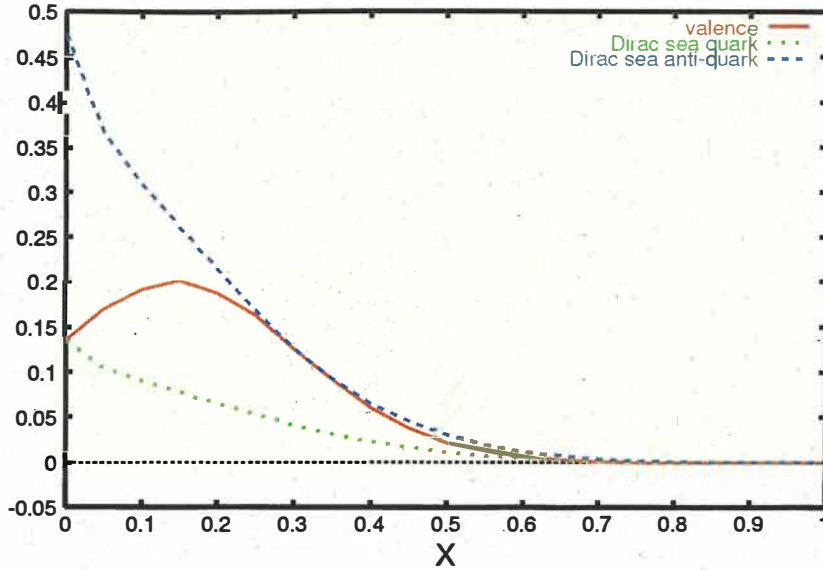
FIG. 9: Theoretical prediction for the unpolarized s quark distribution $s(x)$. The curves have the same meanings as in Fig.7.
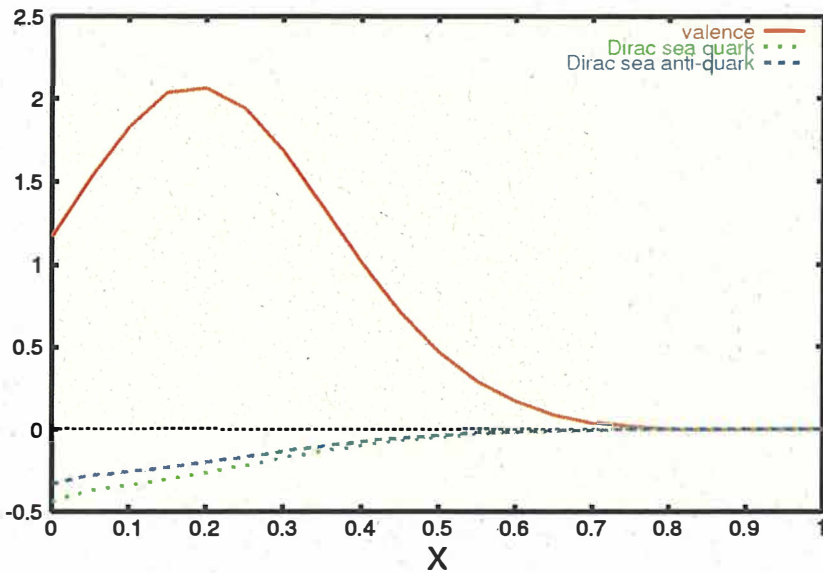

FIG. 10: Theoretical prediction for the polarized u quark distribution $\Delta u(x)$. solid curve: the discrete level contribution. dashed curve: Dirac sea quark contribution. dashed dotted curve: Dirac sea antiquark contribution

in the $5Q$ component. It has peaked at the $x = 0$. The behavior of the $Q\bar{Q}$ pair distribution qualitatively reproduces well the predictions obtained by the cranking formula based on the same model [62–71]. As character of this model, Dirac sea contributions are closely related to the effect of the pion clouds. It is interesting, in the present formalism, that only one
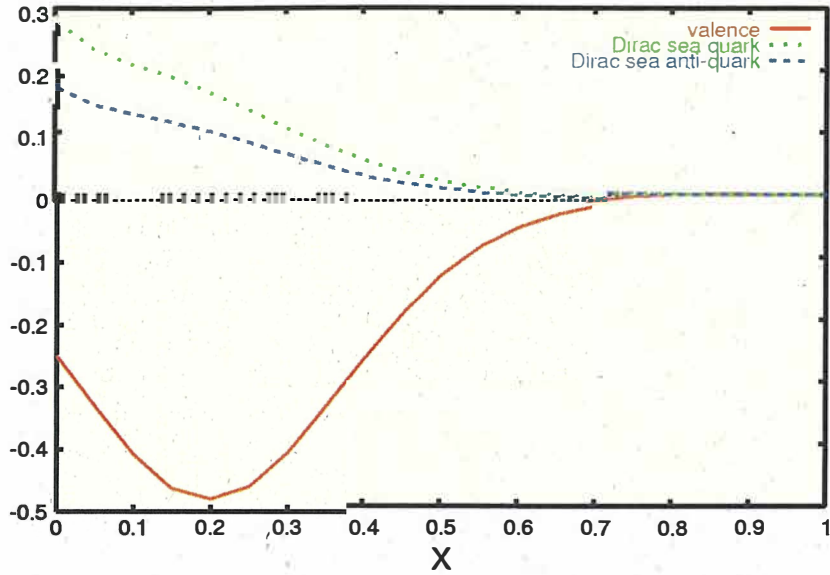
FIG. 11: Theoretical prediction for the polarized d quark distribution $\Delta d(x)$. The curves have the same meanings as in Fig.7.
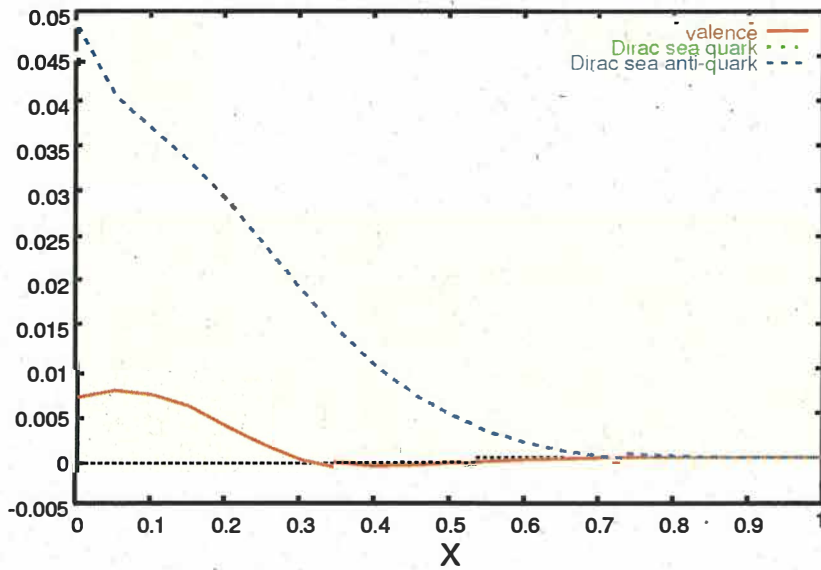

FIG. 12: Theoretical prediction for the polarized s quark distribution $\Delta s(x)$. The curves have the same meanings as in Fig.7.

quark-antiquark pair reproduce the Dirac continuum effects. The absolute value of the Dirac sea contribution in the present estimate, however, is about one third compared with the one based on the perturbation in the soliton angular velocity Ω. This is because only the 1st order $Q\bar{Q}$ pair has been included in the present calculation. If higher Fock components are included, we would expect comparable absolute value as the result obtained based on the

cranking treatment [68–71]. We emphasize that our results obtained based on the light-cone wave function satisfy the positivity of the unpolarized parton distributions.

It may sound peculiar that the strange quark has valence contribution in the $x > 0$ region. However, because of the SU(3) flavor rotation in the $5Q$ Fock components, valence quarks are mixed state in the SU(3) flavor space. It is important to realize that, as far as total numbers of s and $\bar{s}$ quarks are precisely equal in the nucleon, valence quarks can have the strangeness component. There are two types of contributions to $s(x)$, one the valence contribution having the peak around $x = 1/3$, second Dirac sea contribution having the peak rapidly growing at $x = 0$, while there is only Dirac sea contribution for $\bar{s}(x)$. From this reason, the shape of the strange quark and antiquark distributions have significant asymmetry. In Fig.13, we show the CQSM prediction for $x\left[s(x) - \bar{s}(x)\right]$. This asymmetry
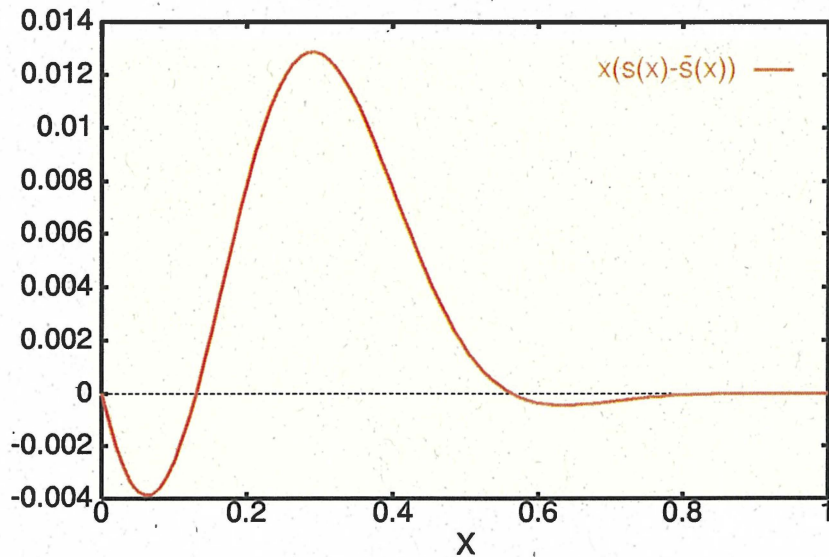

FIG. 13: The theoretical prediction for $x\left[s(x) - \bar{s}(x)\right]$ at the energy scale 16 GeV^2.

of $s(x)$ and $\bar{s}(x)$ distributions would be the origin of the NuTeV anomaly. The NuTeV Collaboration extracted the value of the weak mixing angle, $\sin^2 \theta_W$, by measuring the ratio of neutrino neutral-current and charged-current cross sections on iron [72, 73]. Their value, $\sin^2 \theta_W = 0.2277 \pm 0.0013(\text{stat}) \pm 0.0009(\text{syst})$, is 3 standard deviations above the standard model prediction. The measured ratio R^- is related to the Weinberg angle θ_W by

$$
R^- \equiv \frac{\sigma_{NC}^\nu - \sigma_{NC}^{\bar{\nu}}}{\sigma_{CC}^\nu - \sigma_{CC}^{\bar{\nu}}}
$$

$$
= \frac{1}{2} - \sin^2 \theta_W + \delta R_A^- + \delta R_{QCD}^- + \delta R_{EW}^-, \tag{204}
$$

55

where the three correction terms, respectively, stand for the target nonisoscalarity correction (δR_A^-), QCD corrections $(\delta R_{\rm QCD}^-)$, and higher-order electroweak corrections $(\delta R_{\rm EW}^-)$. The QCD corrections come from three main sources as

$$\delta R_{\rm QCD}^- = \delta R_s^- + \delta R_I^- + \delta R_{\rm NLO}^-, \tag{205}$$

where δR_s^-, δR_I^- and $\delta R_{\rm NLO}^-$, respectively, stand for possible strange-sea asymmetry $(S^- \equiv s - \bar{s} \neq 0)$, isospin violation $(u_{p,n} \neq d_{n,p})$ effects in the parton density of the nucleon, and the NLO corrections. If we focus on the first correction due to the possible asymmetry of the strange sea in the nucleon, the QCD correction is given as

$$\delta R_s^- \simeq -\left(\frac{1}{2} - \frac{7}{6}\sin^2\theta_W\right)\frac{[S^-]}{[Q^-]}, \tag{206}$$

where

$$[S^-] \equiv \int_0^1 x\,[s(x) - \bar{s}(x)]\,dx, \tag{207}$$

$$[Q^-] \equiv \int_0^1 x\,\left[u(x) - \bar{u}(x) + d(x) - \bar{d}(x)\right]dx. \tag{208}$$

Recently, the CTEQ group performed a global PDF fit including the NuTeV "dimuon events" on the neutrino and antineutrino production of charm [74, 75]. Their analysis leads to a central value $[S^-]_{\rm CTEQ} \simeq 0.002$. Note that the positive $[S^-]$, which means that the momentum distribution of s quark is harder than that of the $\bar{s}$ quark in the nucleon, works to reduce the discrepancy between the NuTeV determination of $\sin^2\theta_W$ and the world average of other measurements. As shown in Fig.13, the CQSM predicts the s quarks carry more momentum fraction than the $\bar{s}$ quarks, and the moment of the $x\,[s(x) - \bar{s}(x)]$ is given as $[S^-]_{\rm CQSM} \simeq 0.0016$ at the energy scale $Q^2 = 16$ GeV^2 evolved from the model energy scale 0.3GeV^2 in order to compare with the NuTeV measurement. Inserting this value with $[Q^-] = 0.226$ obtained by the same model into Eq.(206), we obtain the correction due to the strange sea asymmetry

$$\delta R_s^- = -0.0034, \tag{209}$$

which explains nearly 70% of the NuTeV anomaly. This estimate are performed without the SU(3) symmetry breaking term, arising from the effective mass difference Δm_s between the strange and non-strange quarks. It was also shown that $[S^-]$ is sensitive to the Δm_s. With the SU(3) breaking term Δm_s, it was confirmed in this model that the momentum carried

by s quarks becomes more large compared with that of the $\bar{s}$ quarks, then the asymmetry of the s quarks and $\bar{s}$ quarks distribution may resolved the NuTeV anomaly [76].

Also very interesting are the isovector antiquark distributions $\bar{u}(x) - \bar{d}(x)$ and $\Delta\bar{u}(x) - \Delta\bar{d}(x)$. An interesting quantity related to the isovector antiquark distribution is the Gottfried sum , which is defined as

$$S_G = \frac{1}{3} + \frac{2}{3}\int_0^1 dx\left[\bar{u}(x) - \bar{d}(x)\right], \tag{210}$$

The integral on the RHS is scale-dependent only at the two loop level; its scale dependence is negligible over the entire perturbative region. If the sea quark distribution were isospin symmetric, $\bar{u}(x) = \bar{d}(x)$, which would be the case if, for example, one assumed the sea quark distribution to be generated entirely radiatively, this quantity would be equal to 1/3 "Gottfried sum rule". However, the NMC experiment finds a significant deviation from this value,

$$S_G = 0.2356 \pm 0.0026 \quad \text{at} \quad Q^2 = 4\text{GeV}^2, \tag{211}$$

indicating that the sea quark distribution is rather far from flavor-symmetric [77]. Note that the Gottfried sum rule does not follow from any fundamental principles of QCD. In fact, the large-N_c picture of the nucleon as a chiral soliton naturally explains the presence of a flavor-antisymmetric antiquark distribution. In Fig.14, one can see that the antiquark distribution $\bar{u} - \bar{d}$ indicates the isospin asymmetry. Note, however, that the present prediction
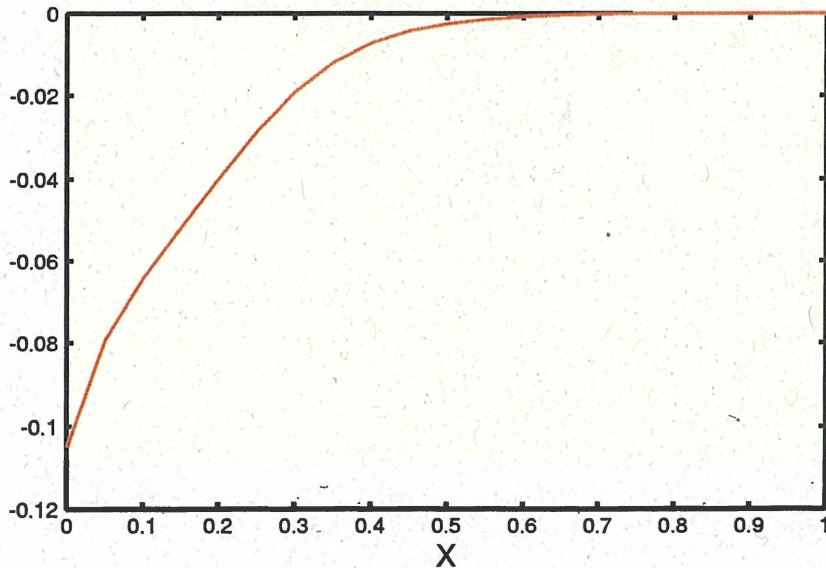

FIG. 14: The theoretical prediction for the unpolarized antiquark asymmetry $\bar{u}(x) - \bar{d}(x)$.

for the asymmetry $\bar{u}(x) - \bar{d}(x)$ is not enough to reproduce the value extracted by the NMC collaboration, although the model predicts excess of the $\bar{d}$ quark than the $\bar{u}$ quark in the proton. Our model gives

$$S_G = 0.29 \quad \text{at} \quad Q^2 = 0.3\text{GeV}^2. \tag{212}$$

In fact, in the model calculation based on the cranking formalism, the unpolarized isovector distribution arise in the next to leading order in the $1/N_c$ expansion. Therefore, if we include subleading $1/N_c$ quantum corrections in this formalism, we would expect more large asymmetry of $\bar{u}(x) - \bar{d}(x)$ distribution [70, 71]. It has been suggested by several authors that this isospin asymmetric sea is due to the pionic contribution to the sea quark distribution. Henley and Miller argued that the pionic contribution to the difference between the number of $d\bar{d}$ pairs and $u\bar{u}$ ones in the proton is equal to the difference between the number of π^+ and π^- in the proton [78]. In the CQSM, the difference of the $\bar{d}$ quarks and $\bar{u}$ ones arise from the SU(3) flavor rotating chiral mean field. In fact, the hedgehog ansatz Eq.(88) breaks the flavor SU(3) and spatial rotational symmetry [70, 71]. We have to rotate chiral mean field in the flavor and ordinary space in order to restore the symmetry. The nucleon in this model is obtained as the collective rotational state.

Next we show the model prediction for the polarized antiquark distribution. As shown in Fig.15, our model predictions also indicate the breakdown of the SU(2) symmetric sea quark polarization, $\Delta\bar{u}(x) = \Delta\bar{d}(x)$, which is frequently used in semiphenomenological analysis of parton distributions. In the present mean field approximation, $\bar{u}$ is weakly polarized in the opposite direction to the proton spin, while $\bar{d}$ is polarized along the proton spin. However, these spin polarization direction of each flavor may be reversed if we include the $1/N_c$ quantum correction. Indeed, the same model prediction including the subleading $1/N_c$ correction based on the perturbative expansion of the soliton rotational angular velocity Ω shows the sizable breakdown of polarized antiquark distribution $\Delta\bar{u}(x) - \Delta\bar{d}(x)$ with positive sign, which indicates that the polarizations of $\bar{u}$ and $\bar{d}$ prefer parallel and anti-parallel to the proton spin respectively [62–65]. Although strange quark and antiquark only appear from the sea quark polarization, the polarized strange distributions also have asymmetry between quark and antiquark contributions. The origin of this asymmetry is the same as those of the unpolarized strange quark distribution. The polarized sea quark asymmetry is the one of the prominent prediction based on the chiral quark soliton model.
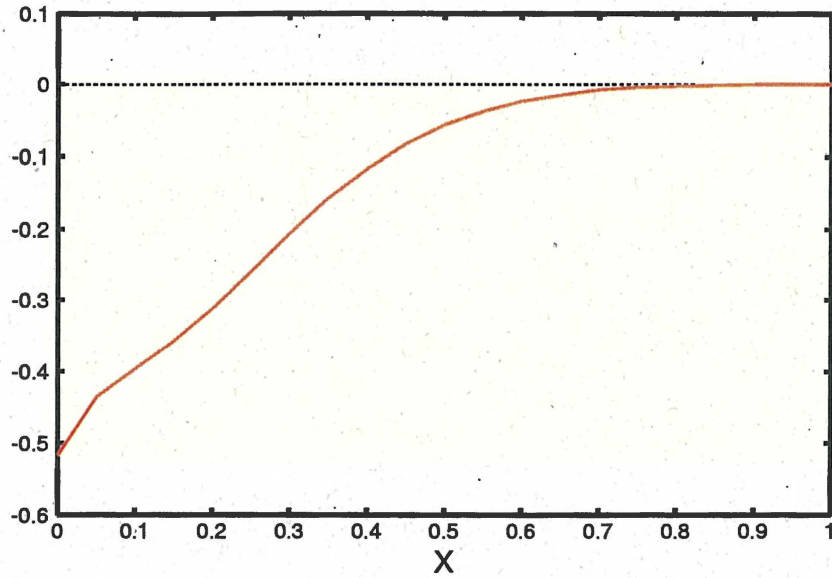
58

FIG. 15: The theoretical prediction for the polarized antiquark asymmetry $\Delta\bar{u}(x) - \Delta\bar{d}(x)$.

B. TMD parton distribution $q(x, \boldsymbol{p}_\perp)$ and $\Delta q(x, \boldsymbol{p}_\perp)$

The TMD parton distributions can be easily evaluated by leaving the transverse momentum of the struck quark unintegrated. Figs.16-21 show the model predictions of the flavor decomposed TMD parton distributions.
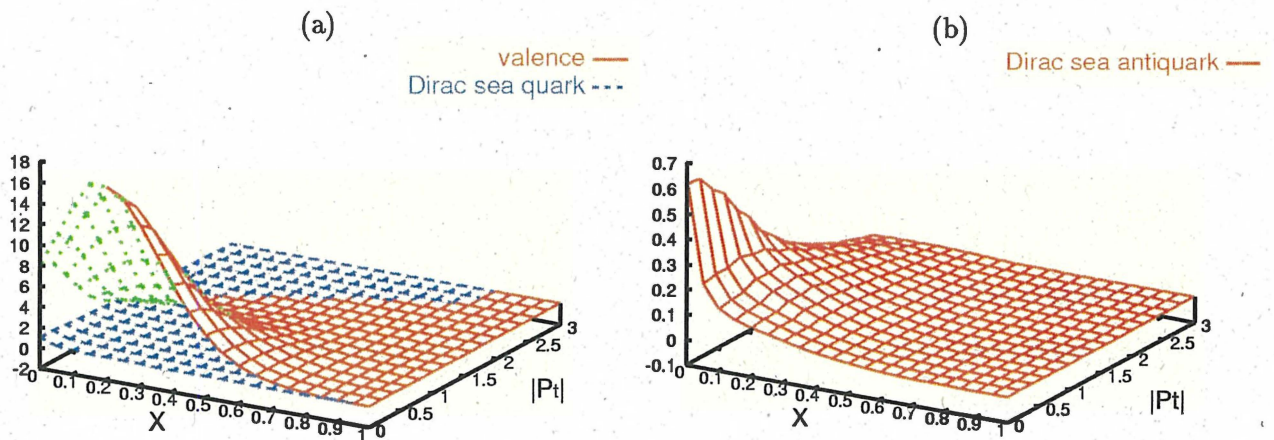
FIG. 16: The theoretical predictions for the unpolarized TMD distribution $u(x, \boldsymbol{p}_\perp)$ with the fraction x of the baryon momentum and the transverse momentum $\boldsymbol{p}_\perp$ plotted in units of $M = 375$MeV. (a)The red curved surface is the discrete valence contribution, while the blue curved surface is the Dirac sea quark contribution. (b)The theoretical prediction for the antiquark TMD distribution $\bar{u}(x, \boldsymbol{p}_\perp)$.

59

FIG. 17: The theoretical predictions for the unpolarized TMD distribution $d(x, \boldsymbol{p}_\perp)$ and $\bar{d}(x, \boldsymbol{p}_\perp)$. The curved surfaces have the same meaning as in Fig.16

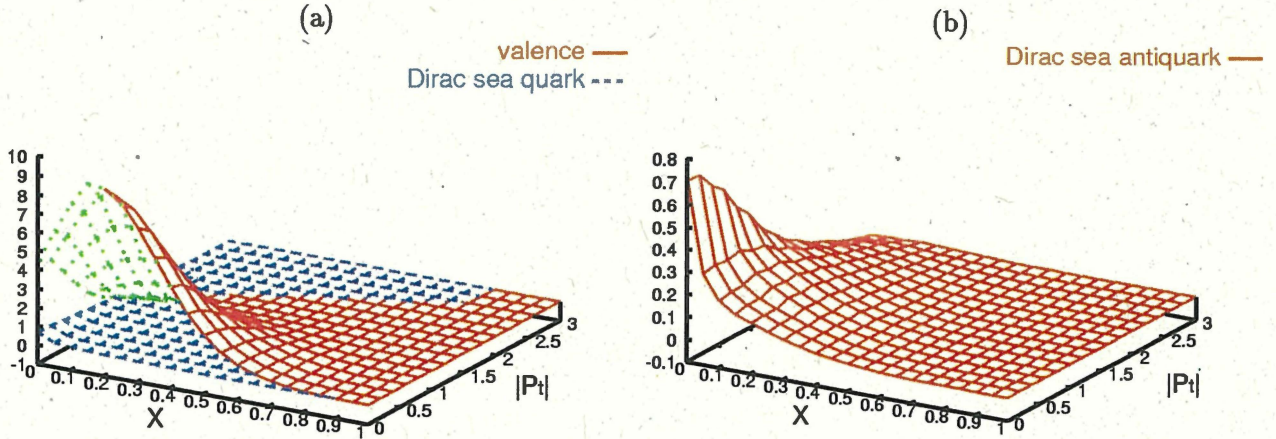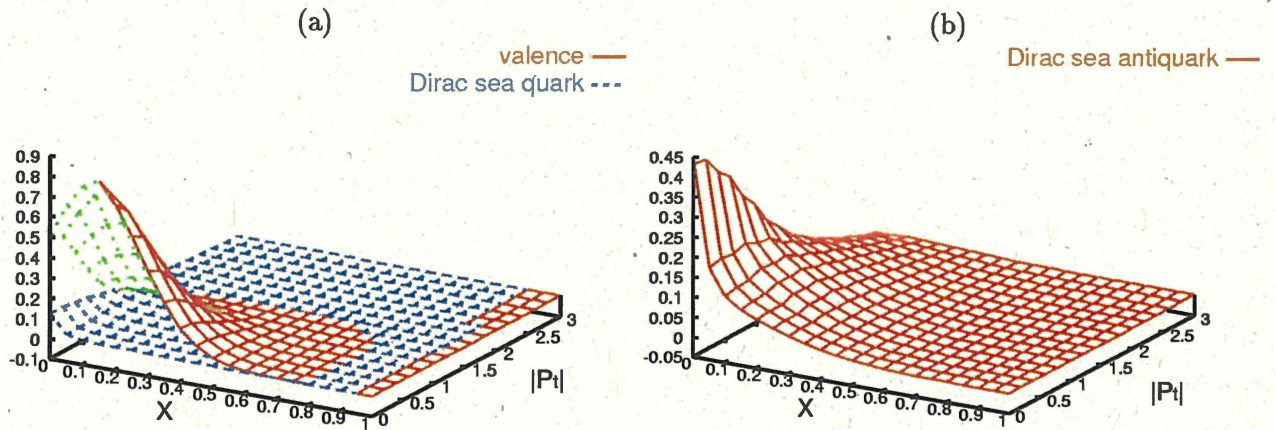FIG. 18: The theoretical predictions for the unpolarized TMD distribution $s(x, \boldsymbol{p}_\perp)$ and $\bar{s}(x, \boldsymbol{p}_\perp)$. The curved surfaces have the same meaning as in Fig.16

For the distributions in the transverse direction, we show its dependence on the absolute value $|\boldsymbol{p}_\perp|$. All the discrete level distributions have Gaussian shape in the transverse direction, and are fully suppressed in the region $|\boldsymbol{p}_\perp| > 0.5\text{GeV}$. On the other hand, the Dirac sea quark distribution has a long tail contribution in the transverse direction, although its absolute value is very small in the low $|\boldsymbol{p}_\perp|$ region compared with that of the discrete level distribution. In Fig.22, we show the unpolarized u quark distribution in the transverse direction with the fixed Bjorken variable $x = 0.3$. This long tail contribution comes from the deep negative-energy Dirac sea continuum distorted by the presence of the chiral mean field.

Recently, the transverse momentum dependent PDF have attracted much attention in the relation with the single spin asymmetry (SSA) measured in the semi-inclusive deep inelastic
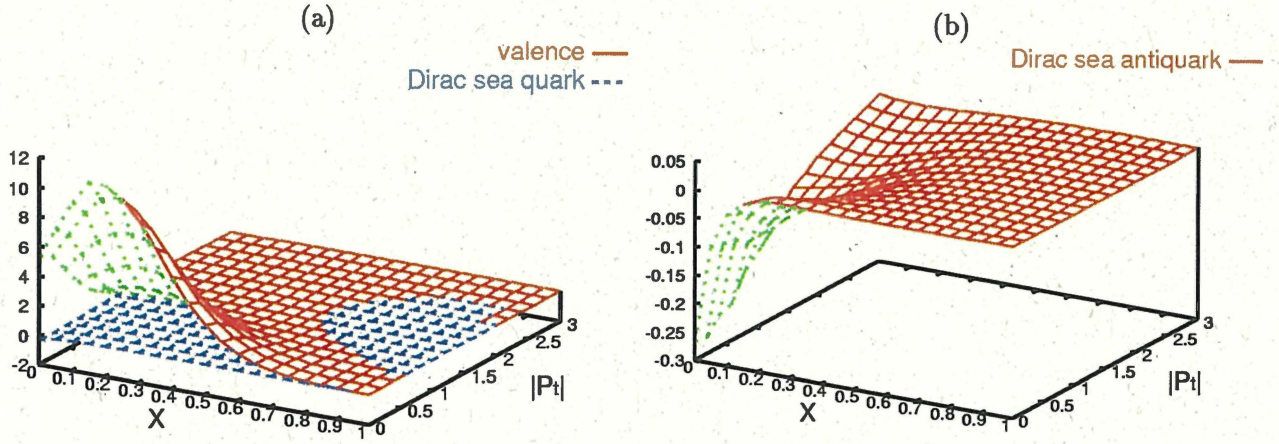
FIG. 19: The theoretical predictions for the polarized TMD distribution $\Delta u(x, \boldsymbol{p}_\perp)$ and $\Delta \bar{u}(x, \boldsymbol{p}_\perp)$. The curved surfaces have the same meanings as in Fig.16

FIG. 20: The theoretical predictions for the polarized TMD distribution $\Delta d(x, \boldsymbol{p}_\perp)$ and $\Delta \bar{d}(x, \boldsymbol{p}_\perp)$. The curved surfaces have the same meaning as in Fig.16

scatterings [79, 80]. Interestingly, these SSA phenomena can be explained by taking account of the "Sivers function" $f_{1T}^\perp(x, \boldsymbol{p}_\perp)$ [35]. Recently, Collins et.al. tried to extract information for the Sivers function from the HERMES data [81, 82]. They assumed the Gaussian function in the transverse direction as

$$f(x, \boldsymbol{p}_\perp) \equiv f(x)\frac{\exp(-\boldsymbol{p}_\perp^2/p_{unp}^2)}{\pi p_{unp}^2},$$

$$f_{1T}^\perp(x, \boldsymbol{p}_\perp) \equiv f_{1T}^\perp(x)\frac{\exp(-\boldsymbol{p}_\perp^2/p_{siv}^2)}{\pi p_{siv}^2}, \tag{213}$$

and use the mean square, and mean transverse momentum in their analysis of the HERMES data

$$\langle \boldsymbol{p}_\perp^2 \rangle = \frac{\int d^2\boldsymbol{p}_\perp \boldsymbol{p}_\perp^2 f(x, \boldsymbol{p}_\perp)}{\int d^2\boldsymbol{p}_\perp f(x, \boldsymbol{p}_\perp)} = p_{unp}^2,$$
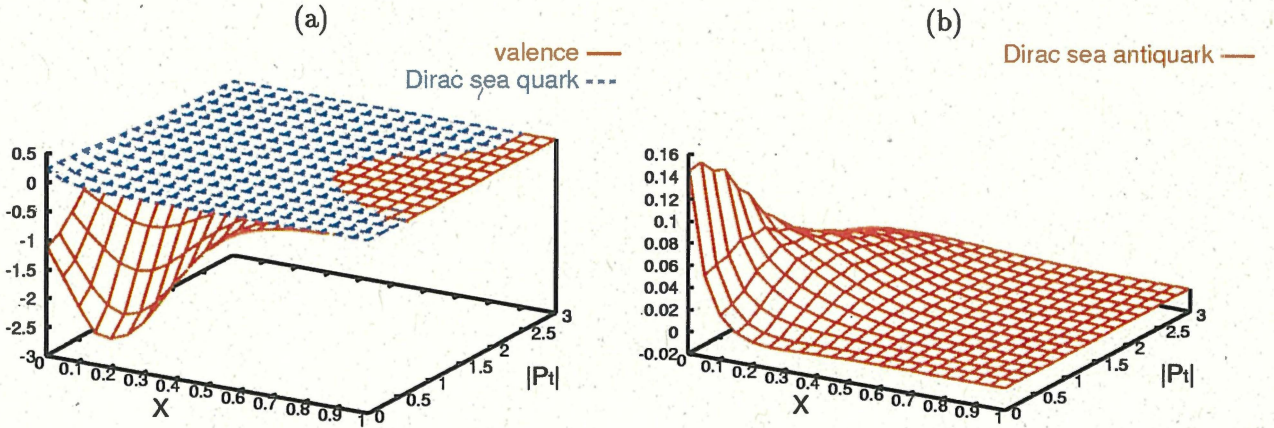
61
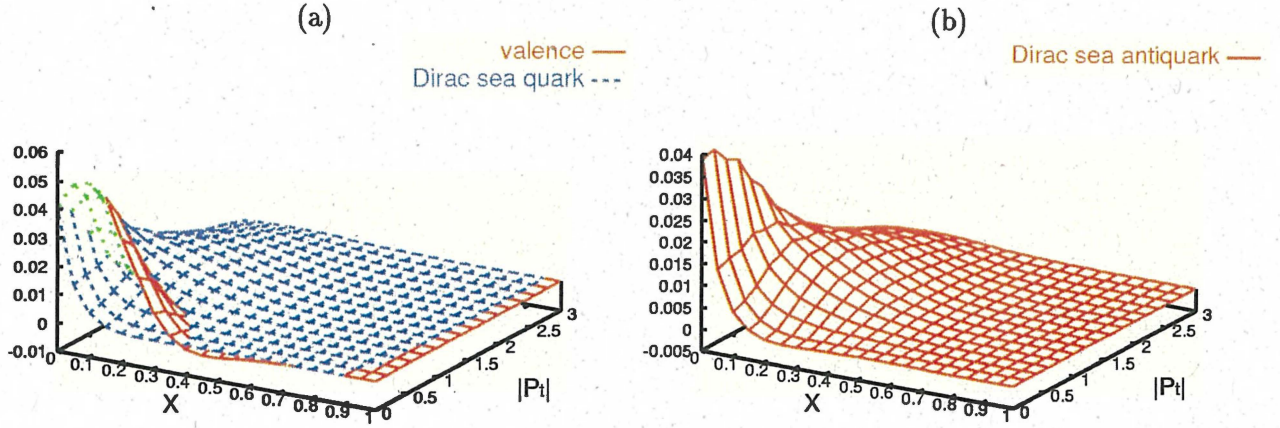
FIG. 21: The theoretical predictions for the polarized TMD distribution $\Delta s(x, \boldsymbol{p}_\perp)$ and $\Delta \bar{s}(x, \boldsymbol{p}_\perp)$. The curved surfaces have the same meaning in as Fig.16
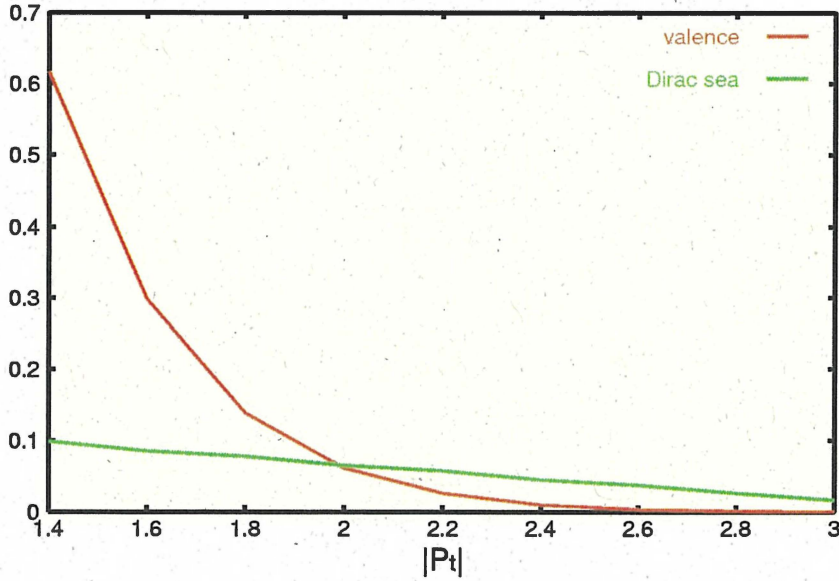
FIG. 22: The theoretical prediction for $u(x, \boldsymbol{p}_\perp)$ at $x = 0.3$. The transverse momentum is plotted in units of $M = 375\text{MeV}$.

$$\langle \boldsymbol{p}_\perp \rangle = \frac{\int d^2 \boldsymbol{p}_\perp |\boldsymbol{p}_\perp| f(x, \boldsymbol{p}_\perp)}{\int d^2 \boldsymbol{p}_\perp f(x, \boldsymbol{p}_\perp)} = \frac{\sqrt{\pi}}{2} p_{unp}. \tag{214}$$

However, our analysis here shows that it is not the good assumption when the Dirac sea distribution has a long tail contribution in the transverse direction. If we include higher Fock components in this formalism, the Dirac sea contribution predicted in the CQSM may be more enhanced. Then, the mean square and mean transverse momentum are strongly influenced by the large $\boldsymbol{p}_\perp$ region, and would be drastically different from the ones obtained by the Gaussian ansatz Eq.(214). The Sivers function "$f_{1T}^\perp(x, \boldsymbol{p}_\perp)$" itself is a time reversal

odd function. Whether one can calculate such a T-odd functions using a chiral model is still examined by many people [83, 84]. Nonetheless, the important fact the CQSM suggests is that one have to take into consideration the Dirac sea contribution more seriously in the investigation of the SSA phenomena.

C. GPDs: $\mathcal{H}_{++}(x,\xi,\Delta_\perp^2 = 0)$ **and** $\tilde{\mathcal{H}}_{++}(x,\xi,\Delta_\perp^2 = 0)$ **with zero transverse momentum transfer**

Now, we will start to show the GPDs in the case $t \neq 0$. As we have reviewed in sec.II, this structure function defined by the off-forward matrix element have information of quark spatial distribution as well as those of momentum distribution. The electromagnetic form factors calculated in the chiral quark soliton model agree rather well with the experimentally measured ones up to transferred momenta of the order $-t \sim 1\text{GeV}^2$ [85, 86]. First, we will give the model predictions with zero transverse momentum transfer $\Delta_\perp^2 = 0$, where

$$t = -4M_B^2 \frac{\xi^2}{(1 - \xi^2)}. \tag{215}$$

In the overlap representation, the GPDs are parameterized in terms of the longitudinal momentum transfer ξ:

$$\mathcal{H}_{++}(x,\xi) = \theta\left(x - \frac{\xi}{2}\right)\mathcal{H}_{++}^{(N \to N)}(x,\xi) + \theta\left(\frac{\xi}{2} - x\right)\mathcal{H}_{++}^{(N+1 \to N-1)}(x,\xi). \tag{216}$$

In the $|x| > \xi/2$ region, superscript $(N \to N)$ means that the structure function is denoted by the diagonal matrix element in the Fock components. On the other hand, the function in the center region $|x| < \xi/2$ is represented by $N + 1 \to N - 1$ non-diagonal Fock component transition. In Fig.23, a typical shape of the flavor decomposed GPD $\mathcal{H}_{++}^q(x,\xi,t)$ as a function of the variable x is shown at $\xi/2 = 0.3$. For $\xi/2 = 0.3$ one has $t = 0.35\text{GeV}^2$. In this figure, we show separately the contributions of the valence level and of the Dirac continuum. We see that the Dirac continuum contribution is essential especially in the region $-\xi/2 < x < \xi/2$, and also in the region $x < -\xi/2$, corresponding to (minus) antiquark distributions, the Dirac continuum contribution ensures the positivity of antiquarks. Let us also note that the points $|x| = \xi/2$ divide the interval of the variable $x(-1 < x < 1)$ in three regions:$x < -\xi/2$, where the function $\mathcal{H}_{++}(x,\xi,t)$ describes the antiquark distribution; $x > \xi/2$, where it corresponds to the quark distribution, and $-\xi/2 < x < \xi/2$, where $H(x,\xi,t)$
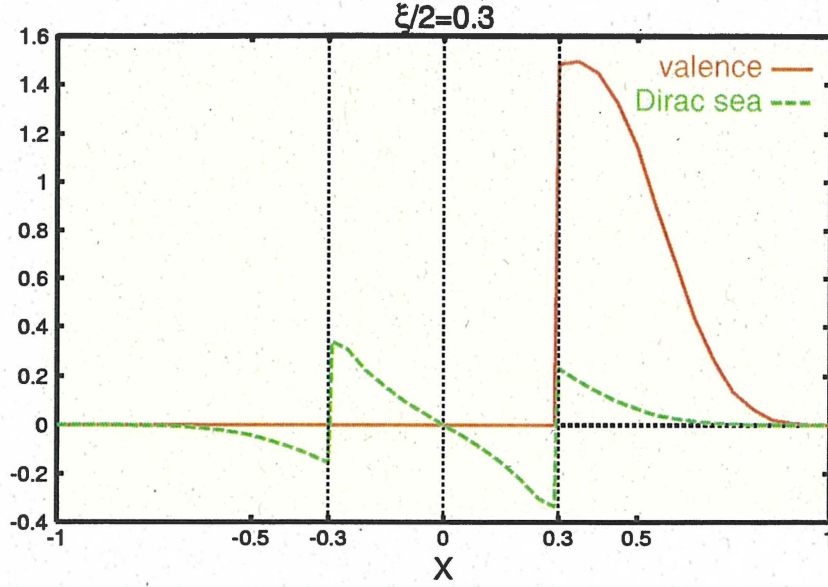
FIG. 23: The u quark distribution $H(x, \xi, \Delta^2)$ for $\Delta_\perp^2 \equiv -\Delta^2 - \xi^2 M_N^2 = 0$ and $\xi/2 = 0.3$. Solid curve: contribution from the valence level. Dashed curve: contribution from the Dirac sea continuum.

resembles a meson wave function. It is therefore natural that the function $\mathcal{H}_{++}(x, \xi, t)$ has discontinuity at $|x| = \xi/2$. Actually, we divide artificially the division of the x integrals into separate domains:

$$\int_{-1}^{-\xi/2-\epsilon} dx \, \mathcal{H}_{++}^{(N \to N)}(x, \xi) + \int_{-\xi/2+\epsilon}^{\xi/2-\epsilon} dx \, \mathcal{H}_{++}^{(N+1 \to N-1)}(x, \xi) + \int_{\xi/2+\epsilon}^{1} dx \, \mathcal{H}_{++}^{(N \to N)}(x, \xi). \quad (217)$$

In the present approximation, i.e. the absence of the higher Fock components, the GPD of the center region $|x| < \xi/2$ is odd function of x, so that the integration from this region is zero. The form factor integrated over x contains a $N \to N$ diagonal transition in Fock space. However, such discontinuity would lead immediately to a violation of the factorization theorems for DVCS processes, since the expression for the DVCS amplitude (71) contains a factor

$$\int_{-1}^{1} dx \left(\frac{1}{x - \xi/2 + i\epsilon} + \frac{1}{x + \xi/2 - i\epsilon} \right) H(x, \xi, t), \quad (218)$$

which would be logarithmically divergent if $H(x, \xi, t)$ was discontinuous at $|x| = \xi/2$. On the other hand, Petrov, et al. have indicated that the discontinuities are artifacts of neglecting the momentum dependence of the constituent quark mass [57]. They show that if

64

FIG. 24: The theoretical predictions for (a) the valence distribution $\mathcal{H}_{++}^{u-val.}(x,\xi,\Delta_\perp^2=0)$ and (b) the Dirac sea quark distribution $\mathcal{H}_{++}^{u-sea}(x,\xi,\Delta_\perp^2=0)$.

FIG. 25: The theoretical predictions for (a) the valence distribution $\mathcal{H}_{++}^{d-val.}(x,\xi,\Delta_\perp^2=0)$ and (b) the Dirac sea quark distribution $\mathcal{H}_{++}^{d-sea}(x,\xi,\Delta_\perp^2=0)$.

one include the momentum dependence of the quark mass, the discontinuities are smeared, and the model predicts the characteristic crossovers at $|x| = \xi/2$. Hence, the integrals is finite but enhanced by the contribution near $|x| = \xi/2$. In the present light cone wave function formalism, it is very complicated to include the momentum dependence of the quark mass. We emphasize that the active quark antiquark pair in the center region $|x| < \xi/2$ are correlated in the scalar isoscalar (or σ channel Eq.(182)). Such a contribution is supported by the recent preliminary HERMES data on beam-charge asymmetry in DVCS [87]. As explained in the Sec.IV, the function in this region corresponds to the so-called D-term. As is shown in Fig.(23), we can see that the amplitude in the region $0 < x < |\xi/2|$ has
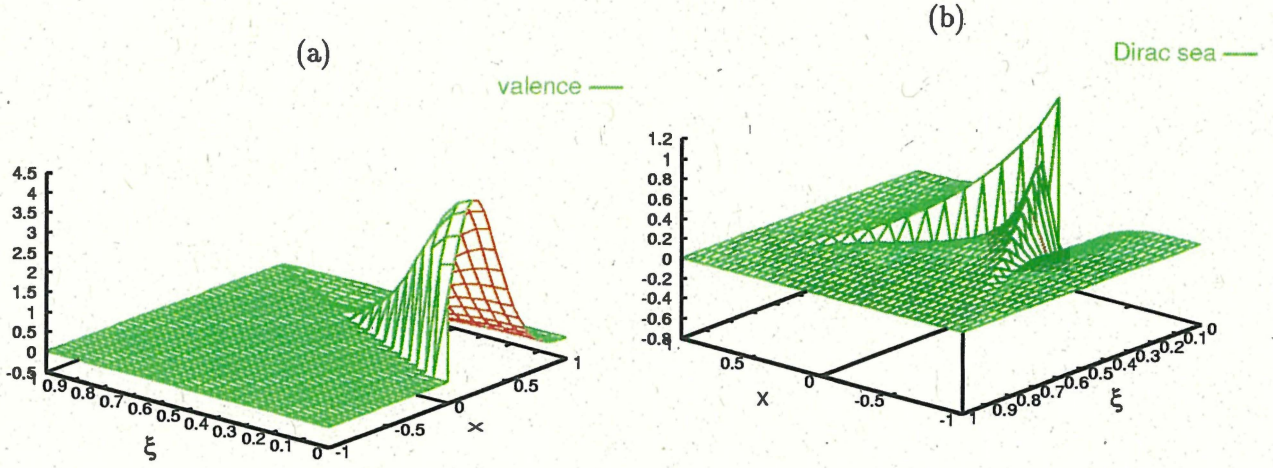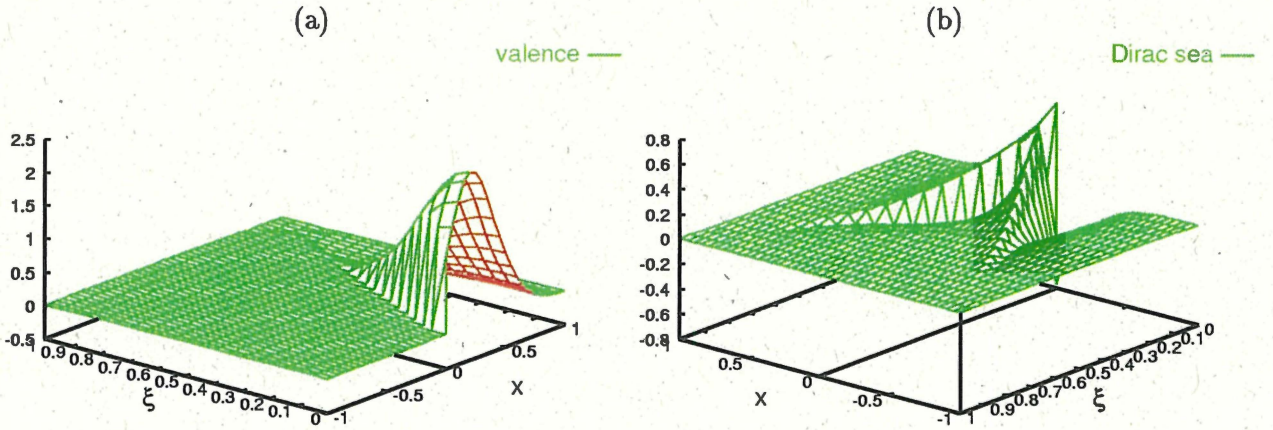
FIG. 26: The theoretical predictions for (a) the valence distribution $\mathcal{H}_{++}^{s-val.}(x,\xi,\Delta_{\perp}^2=0)$ and (b) the Dirac sea quark distribution $\mathcal{H}_{++}^{s-sea}(x,\xi,\Delta_{\perp}^2=0)$.

FIG. 27: The theoretical predictions for (a) the valence distribution $\widetilde{\mathcal{H}}_{++}^{u-val.}(x,\xi,\Delta_{\perp}^2=0)$ and (b) the Dirac sea quark distribution $\widetilde{\mathcal{H}}_{++}^{u-sea}(x,\xi,\Delta_{\perp}^2=0)$.

negative sign. In this framework, the size and sign of the D-term are thoroughly determined from the scalar part of the additional $Q\bar{Q}$ pair wave function generated due to the chiral mean field Eq.(182). As emphasized frequently until now, this Dirac sea contributions are closely related with the effect of the pion clouds. From dynamical point of view, the two pion exchange contributes to the D-term in the CQSM since the D-term consists of the scalar-isoscalar part only. Although D-term contribution is invisible in the forward limit, the second moments of the $H(x,\xi,t)$ and $E(x,\xi,t)$ have the contribution from the D-term, even its first moment have no D-term effects. For example, the second moment of $H^q(x,\xi,t)$

66
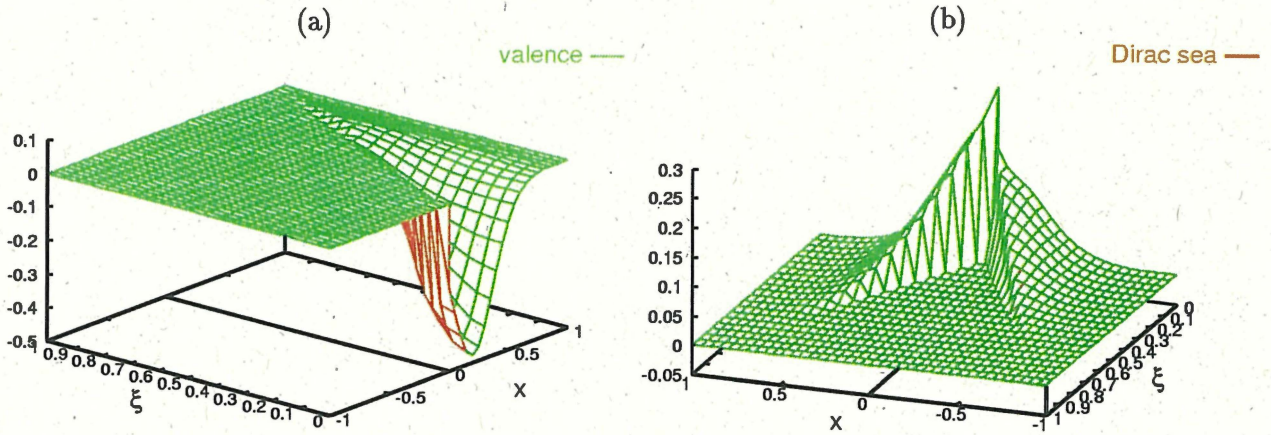
FIG. 28: The theoretical predictions for (a) the valence distribution $\widetilde{\mathcal{H}}_{++}^{d-val.}(x, \xi, \Delta_\perp^2 = 0)$ and (b) the Dirac sea quark distribution $\widetilde{\mathcal{H}}_{++}^{d-sea}(x, \xi, \Delta_\perp^2 = 0)$.
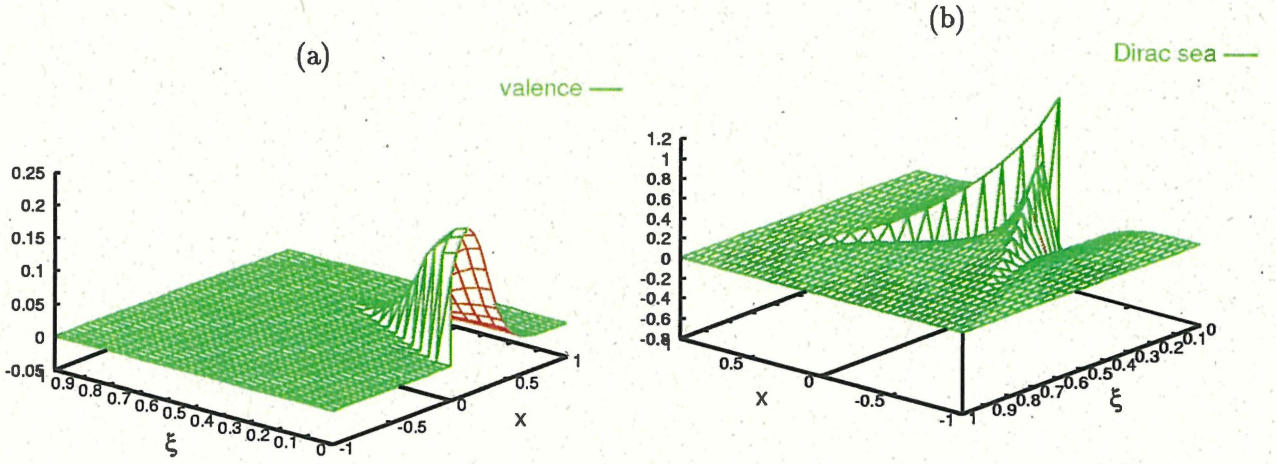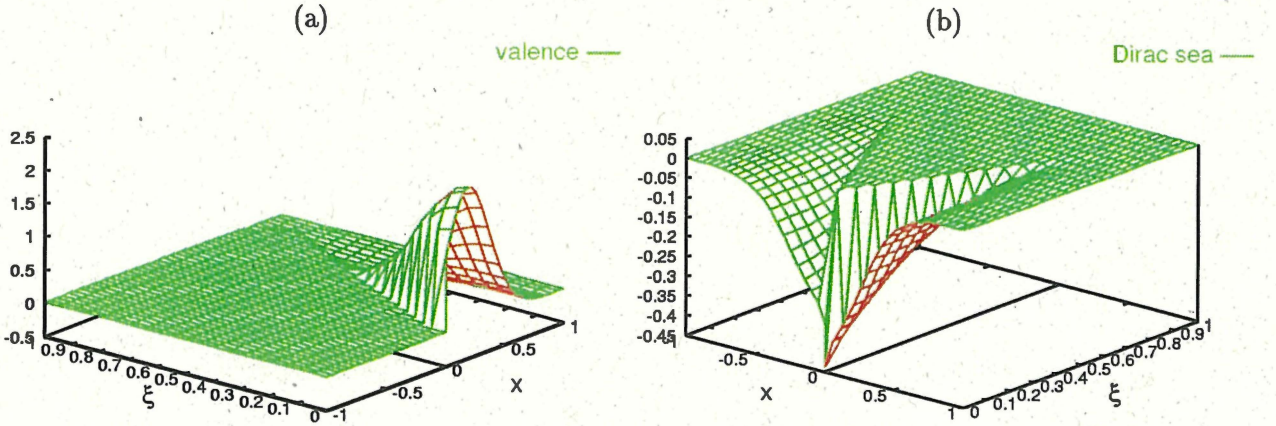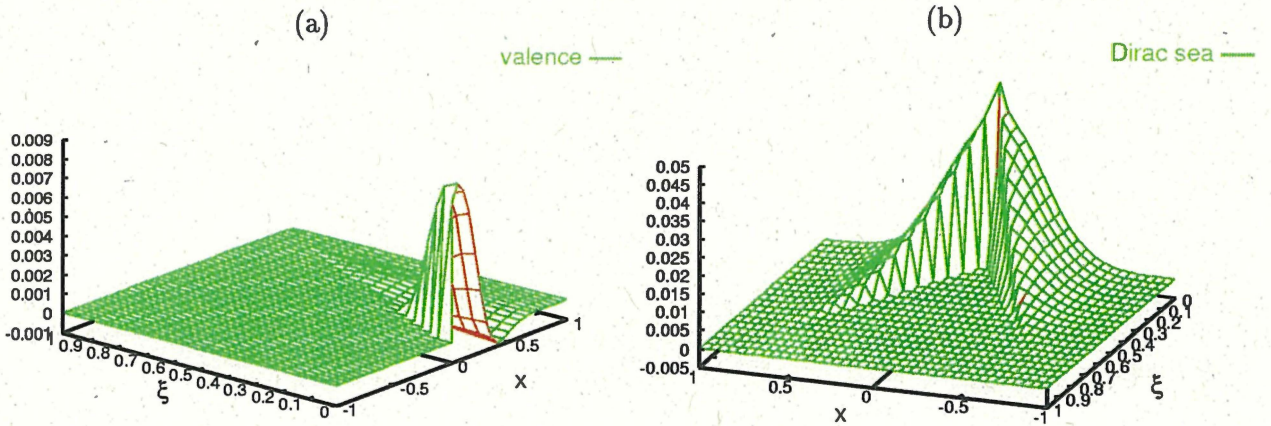

FIG. 29: The theoretical predictions for (a) the valence distribution $\widetilde{\mathcal{H}}_{++}^{s-val.}(x, \xi, \Delta_\perp^2 = 0)$ and (b) the Dirac sea quark distribution $\widetilde{\mathcal{H}}_{++}^{s-sea}(x, \xi, \Delta_\perp^2 = 0)$.

is expressed as [56]

$$\int_{-1}^{1} dx \, x \, H^q(x, \xi, t) = M_2^q(t) + \frac{4}{5} d^q(t) \xi^2. \tag{219}$$

Here, $M_2^q(t)$, that at $t = 0$ it is related to the momentum fraction carried by quarks, gives us information about the spatial distribution of quark momentum inside the nucleon. The constant $M_2^q(0)$ is related to the parton distributions via

$$M_2^q(0) = \int_0^1 dx \, x \, (q(x) + \bar{q}(x)) \,. \tag{220}$$

On the other hand, the form factor $d^q(t)$ is related to the traceless part of the energy-momentum tensor $\hat{T}_{i,j}^q(\boldsymbol{r}) = \frac{i}{2} \bar{\psi} \gamma_{\{i} \nabla_{j\}} \psi(\boldsymbol{r})$ which characterizes the spatial distribution of shear forces experienced by quarks in the nucleon. The form factor $d^q(t)$ contributes to the

67

x_{bj}-independent part of the real part of the DVCS amplitude, which is accessible through the beam charge asymmetry. Another interesting quantity related to the second moment is the generalized form factor, $A_q(t) + B_q(t)$

$$J_q(t) = \frac{1}{2}(A_q(t) + B_q(t)) = \int_{-1}^{1} dx\, x\, (H_q(x,\xi,t) + E_q(x,\xi,t)), \qquad (221)$$

which gives us information about the spatial distribution of the quark angular momentum inside the nucleon. The second moment of $E(x,\xi,t)$ is represented as

$$\int_0^1 dx\, x\, E(x,\xi,t) = B_q(t) - \frac{4}{5}d^q(t)\xi^2, \qquad (222)$$

where $B_q(t)$ is called the anomalous gravitomagnetic moment. Since the signs of the D-term involved in the second moments of $H(x,\xi,t)$ and $E(x,\xi,t)$ are opposite to each other, the Ji's sum rule Eq.(221) has no contribution from the D-term.

Next, we display the full x and ξ dependence of $\mathcal{H}^q_{++}(x,\xi,t)$ of each flavor in Figs.24-26. By moving along lines of constant ξ, one nicely sees how the sensitivity of the GPDs to the distribution in the $|x| < \xi/2$ region increases relative to the distribution in $|x| > \xi/2$ region when increasing the parameter ξ.

The polarized GPDs $\widetilde{\mathcal{H}}^q_{++}(x,\xi,t)$ of each flavor q are shown in Fig.27-29. As we have explained in Sec.IV, there is no contribution from the center region $|x| < \xi/2$ because we neglect the higher Fock components.

D.   Impact parameter space parton distribution $q(x,b_\perp)$

GPDs in the $\xi = 0$ limit, $\mathcal{H}_{++}(x,\xi,\Delta_\perp^2)$ and $\widetilde{\mathcal{H}}_{++}(x,\xi,\Delta_\perp^2)$ have very interesting information of the baryon structure. As shown from Eqs.(23)-(26), we can obtain only $H(x,0,\Delta_\perp^2)$ and $\widetilde{H}(x,0,\Delta_\perp^2)$, on the other hand $E(x,0,\Delta_\perp^2)$ and $\widetilde{E}(x,0,\Delta_\perp^2)$ decouple in the $\xi \to 0$ limit. We can get the impact parameter space parton distributions $q(x,b_\perp)$ by Fourier transform of $H(x,0,\Delta_\perp^2)$. $q(x,b_\perp)$ is the expectation value of the number operator, and its interpretation does not suffer from relativistic effects [88]. The variables $b_\perp$ and x live in different dimensions, and therefore there is no quantum mechanical uncertainty constraint. Indeed, $q(x,b_\perp)$ is a spatial-and-momentum-density hybrid in that it represents a spatial density in the transverse directions and momentum density in the longitudinal direction. In Figs.30, 31, and 32, we show the model prediction of the impact parameter space distributions for u, d, and s quarks

68
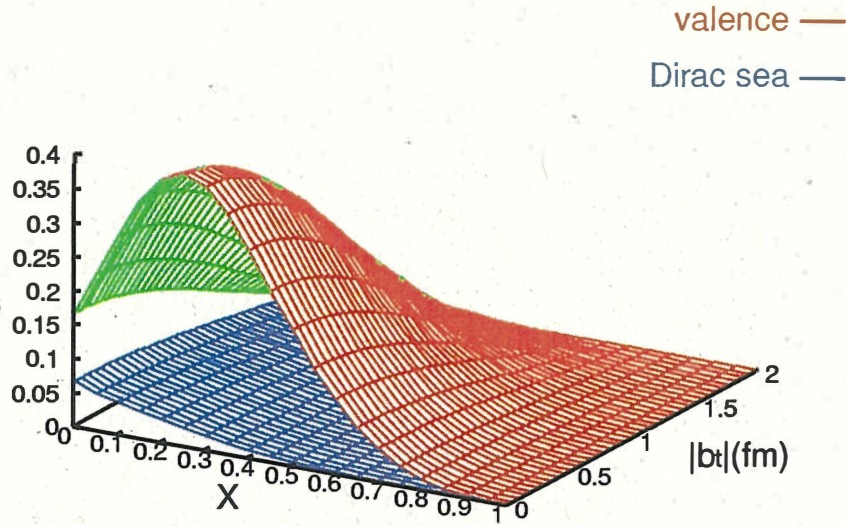
FIG. 30: The theoretical prediction for $u(x, |b_\perp|)$.
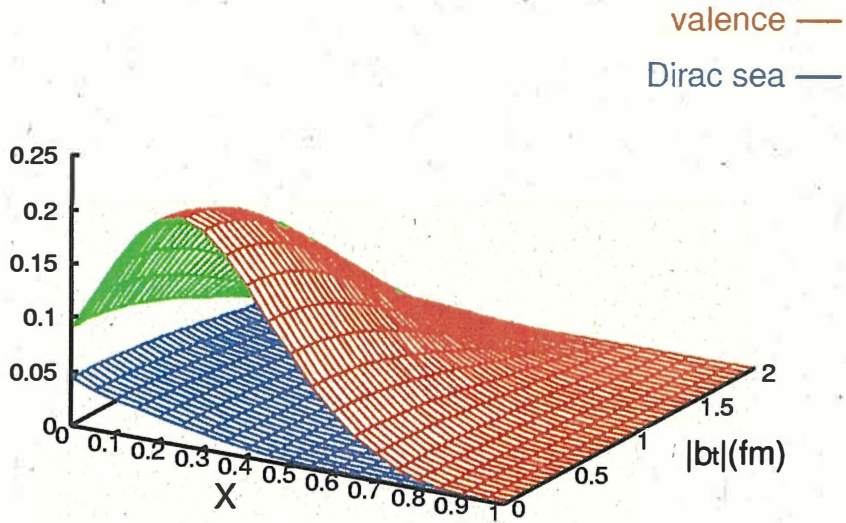
FIG. 31: The theoretical prediction for $d(x, |b_\perp|)$.

For u and d quarks, the contributions of the Dirac sea quarks are small compared with that of the valence quarks. But the Dirac sea quark contributions have long tails in the impact parameter space, and its contribution become dominant as x becomes small.. In order to sea this, we show the u quark distributions at various fixed x points. We can see from Figs.33 and 30 that although the valence contribution has a peak around $x = 0.3$, the Dirac sea contribution increases monotonously as x decreases. From Fig.33 (a), we can
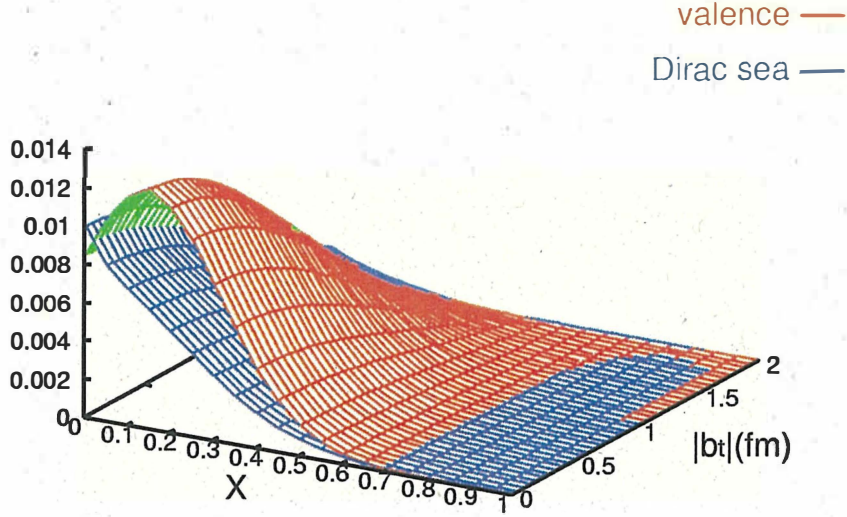
FIG. 32: The theoretical prediction for $s(x, |b_\perp|)$.

see that the contributions of the Dirac sea and valence quarks with small x are reversed bordering at $|b_\perp| = 1.8\,\text{fm}$. As we have mentioned repeatedly, the Dirac sea contributions would be more large if higher order Fock components are included. Therefore, the CQSM predicts that the partonic distribution have large spatial extension in the $b_\perp$ direction due to the long tail contributions of the Dirac sea contributions, This indicates that the $Q\bar{Q}$ pair contributions in this model are closely related to the pionic cloud srounding the three valence quark core.

A density interpretation of the distributions $E^q(x, \xi, t)$ at $\xi = 0$ is more subtle, since the corresponding matrix elements are still non-diagonal in the proton helicity (Eq.(24)). One can however diagonalize by the usual trick of changing basis from helicity states $|+\rangle_z$ and $|-\rangle_z$ to transversity states $|\pm\rangle_x = 1/\sqrt{2}(|+\rangle_z \pm |-\rangle_z)$. For a particle at rest the new basis states are polarized along the positive or negative x-axis, but for our fast-moving and transversely localized protons they are not eigenstates of the angular momentum operator J_1 along the x-axis, and their physical meaning is not quite clear. This reflects the notorious difficulty of defining transverse spin for relativistic particles and the complicated nature of transverse spin operators in the light-cone framework. Proceeding nevertheless along this line, Burkardt has obtained several physically intuitive results [88]. The Fourier transforms of $E^q(x, 0, t)$ describe a relative shift in the transverse density of partons along the y direction between the polarization states $|+\rangle_x$ and $|-\rangle_x$, or between the states $|+\rangle_x$ and $|+\rangle_z$. The second moment of $E^q(x, \xi, t)$ is called anomalous gravitomagnetic moment Eq.(222). In the
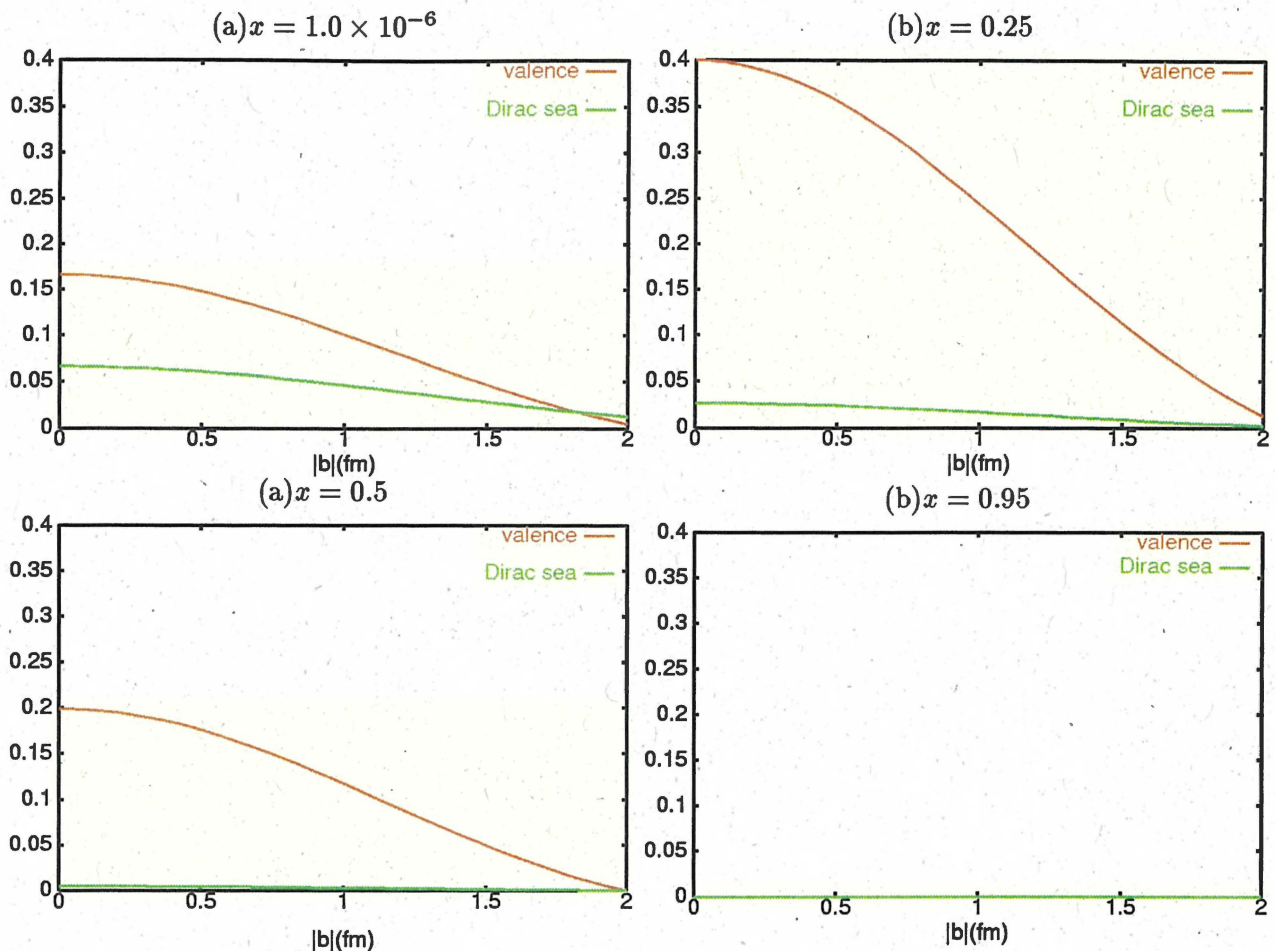
FIG. 33: x-dependence of the u quark impact parameter space distribution

chiral quark soliton model, it is shown that the isoscalar combination in the $t \to 0$ and $\xi \to 0$ limit identically vanishes [58]

$$B^{u+d}(0) = \sum_q \int_0^1 dx \, x E^q(x, 0, 0) = 0. \tag{223}$$

In terms of the impact parameter space, the moments $F_2^q(t) = \int dx E^q(x, \xi, t)$ and $\int dx x E^q(x, \xi, t)$ at $\xi = 0$ and $t = 0$ are also related with the corresponding averages $\langle b^y \rangle$ and $\langle x b^y \rangle$ for quarks. Conservation of the transverse center of momentum implies that the sum of $\langle x b^y \rangle$ over all parton species is zero in a hadron with zero center of momentum, which provides another derivation of the sum rule (223) for the distributions $E^q(x, \xi, t)$ in the forward limit. As we have denoted, in order to obtain $H(x, \xi, t)$ and $E(x, \xi, t)$ separately, we have to calculate the light-cone helicity flip amplitude $\mathcal{H}_{+-}$ in addition to the helicity non-flip one $\mathcal{H}_{++}$. To calculate E in the light-cone wave function is a task of future studies.

Next, we point out that there is another class of hadronic matrix elements that carries

information on both the transverse and longitudinal structure of partons, namely TMD parton distributions. In the present formalism, they can be obtained by leaving the transverse momentum unintegrated, and the predictions based on the CQSM were already shown in Figs.16-21. As we have explained in the Sec.II, in momentum space they have the meaning as the density of the transverse and longitudinal momentum space of the struck parton. The definition of the TMD parton distributions is

$$q(x, \mathbf{k}_\perp) = \int \frac{d^2 z_\perp dz^-}{16\pi^3} e^{ixP^+ z^- - i\mathbf{k}_\perp \cdot \mathbf{z}_\perp} \langle p|\bar{\psi}^q(0, -\frac{1}{2}z^-, -\frac{1}{2}\mathbf{z}_\perp)\gamma^+ \psi^q(0, \frac{1}{2}z^-, \frac{1}{2}\mathbf{z}_\perp)|p\rangle, \quad (224)$$

which is related to the usual quark density by $q(x) = \int d^2 k_\perp q(x, \mathbf{k}_\perp)$. This corresponds to different transverse positions of the emitted parton $(\mathbf{b}_\perp + 1/2 \mathbf{z}_\perp)$ and the reabsorbed parton $(\mathbf{b}_\perp - 1/2 \mathbf{z}_\perp)$. The Fourier transforms of unintegrated parton distributions with respect to the parton $\mathbf{k}_\perp$ thus describe correlations of the transverse location of partons in the nucleon, and never represent densities in impact parameter space. On the other hand, the impact parameter space PDF is the transverse space density measured from the transverse center of momentum of all partons $R_\perp = \sum_{i=q} x_i r_{\perp,i}$, where x_i is the momentum fraction carried by each parton and $r_{\perp,i}$ is their transverse position. Therefore, if the struck quark momentum $\mathbf{k}_\perp$ is left unintegrating in the GPDs in the $\xi \to 0$ limit, we have opportunity to get double information about the nucleon structure in the transverse direction. The Fourier transform of these GPDs over the $\boldsymbol{\Delta}_\perp$ contains a mean impact parameter space information $\bar{\mathbf{b}}_\perp = 1/2(\mathbf{b}_\perp^{in} + \mathbf{b}_\perp^{out})$ measured from the transverse center of momentum, and a correlation in the transverse direction $\mathbf{z}_\perp$ of the incoming and outgoing quarks.

VI. SUMMARY AND CONCLUSIONS

We have studied the generalized parton distribution functions (GPDs) through the light-cone wave function derived from the chiral quark soliton model, which is an effective model of baryons maximally incorporating the spontaneous chiral symmetry breaking of the QCD vacuum. In the relativistic mean field approximation in this model, one obtains a quantitative picture of baryons as localized states of constituent quarks bound by a self-consistent chiral filed. Simultaneously, the negative Dirac sea is distorted by the same chiral field, leading to the presence of an indefinite number of additional quark-antiquark pairs in the baryons. Then the baryon wave functions can be constructed as a product of $N_c = 3$ valence quark wave functions and the coherent exponent of quark-antiquark pairs.

The GPDs are denoted by $H, E, \widetilde{H}$ and $\widetilde{E}$, which depend on three variables; the light-cone momentum fraction x, light-cone momentum transfer ξ, and total squared momentum transfer $t = \Delta^2$. In the light-cone framework, these four type GPDs appear in the particular combinations according to the light-cone nucleon helicity flip or non-flip. In this thesis, we have concentrated on the spin unpolarized and polarized helicity non-flip combinations $\mathcal{H}_{++} = \sqrt{1 - \xi^2}H - \xi^2/\sqrt{1 - \xi^2}E$ and $\widetilde{\mathcal{H}}_{++} = \sqrt{1 - \xi^2}\widetilde{H} - \xi^2/\sqrt{1 - \xi^2}\widetilde{E}$, respectively.

We have clarified the expression of the GPDs in the light-cone frame using the light-cone wave function in this model. They are represented as the overlap integrals of the initial and final state Fock components. In the characteristic kinematical range in the expression of the GPDs, there arise non-diagonal Fock space matrix elements, which never appear in the case of ordinary Feynman quark distribution functions. Consequently, the GPDs contain quite new information on the nucleon structure.

In the $|x| < \xi/2$ region, where the nucleon emits a quark-antiquark pair, the initial $5Q$ and final $3Q$ Fock components are relevant. The GPDs in this region, called D-term, behave like a meson distribution amplitude. The physical content of the x-moment of this function is interpreted as the distribution of the shear forces experienced by quarks inside nucleon. In our model analysis, the GPDs in this region have contributions only from the Dirac sea continuum distorted by the presence of the chiral mean fields. The size and sign of the D-term are thoroughly determined by the scalar part of the chiral mean field.

We numerically investigate the GPDs under various limiting conditions. In the forward limit $t \to 0$, the GPDs reduce to the ordinary Feynman parton distribution. The model

73

predictions show that the valence contribution has a peak around $x = 1/3$, while the Dirac sea contribution has a rapidly growing peak near $x = 0$. The model also predicts the $\bar{u}(x) - \bar{d}(x)$, $s(x) - \bar{s}(x)$, $\Delta \bar{u}(x) - \Delta \bar{d}(x)$, and $\Delta s(x) - \Delta \bar{s}(x)$ asymmetries. We have point out that the predicted magnitude of $s(x) - \bar{s}(x)$ asymmetry is large enough to resolve the so-called NuTeV anomaly on the fundamental parameter $\sin^2 \theta_W$ in the standard model.

When one leave the transverse momentum of the struck quark unintegrated in the forward limit $t \to 0$, one can obtain the transverse momentum dependent quark distribution function. While the valence quark distribution has like a Gaussian shape in the transverse directions, the Dirac sea distribution has a long tail in that directions. This long tail contribution comes from the deep negative Dirac sea orbitals distorted by the presence of the chiral mean field. Recently, the transverse momentum dependent PDF have attracted much attention in the relation with the single spin asymmetry (SSA) measured in the semi-inclusive deep inelastic scatterings. Interestingly, these SSA phenomena can be explained by taking account of the "Sivers function" $f_{1T}^{\perp}(x, \boldsymbol{p}_{\perp})$ expected to be able to extract information from the HERMES data. In the data analysis, the unpolarized transverse momentum distributions $f(x, \boldsymbol{p}_{\perp})$ are needed, and the Gaussian ansatz in the transverse momentum directions for $f(x, \boldsymbol{p}_{\perp})$ are employed. Then the mean square and mean transverse momentum for $f(x, \boldsymbol{p}_{\perp})$ evaluated by the Gaussian ansatz are frequently used in the analysis. However, our analysis here shows that it is not the good assumption when the Dirac sea distribution has a long tail contribution in the transverse direction. Then, the mean square and mean transverse momentum are strongly influenced by the large $\boldsymbol{p}_{\perp}$ region, and would be drastically different from the ones obtained by the Gaussian ansatz. We emphasize that this Dirac sea contribution has to be taken more seriously into the analysis of the single spin asymmetry phenomena.

In the zero-transverse-momentum transfer case $\Delta_{\perp}^2 = 0$, we have shown the full x and ξ dependence of the GPDs $\mathcal{H}_{++}^q(x, \xi, t)$ and $\widetilde{\mathcal{H}}_{++}^q(x, \xi, t)$ of each flavor q. In the chiral quark soliton model, the large and negative sign contribution for the D-term in the $|x| < \xi/2$ region is given by the isoscalar part of the $Q\bar{Q}$ pair wave function. This Dirac sea contributions are closely connected with the effect of the pion clouds, and the negative sign of the nucleon D-term obtained by us coincides with that of the pion D-term evaluated by using the soft pion theorem. Therefore, we emphasize that the behavior of the D-term is related to the spontaneous chiral symmetry breaking of the QCD vacuum. From the dynamical point of view, the two pion exchange contributes to the D-term in the CQSM, since the D-term

consists of the scalar-isoscalar part only.

In the purely transverse momentum transfer case, GPDs become the probability density of both the longitudinal momentum direction and impact parameter space. The model predicts that quarks in low-x region have large spatial extension in the $\boldsymbol{b}_\perp$ direction. The $Q\bar{Q}$ pair contributions are essential in this result. It comes from the fact that the $Q\bar{Q}$ pair simulates to the pion cloud surrounding the three valence quark core.

We have point out that the impact parameter space quark distribution and transverse momentum dependent quark distribution have different information about transverse space directions. The TMD parton distributions have the meaning as the density of the transverse and longitudinal momentum space of the struck parton. The Fourier transforms of TMD parton distributions with respect to the parton $\boldsymbol{k}_\perp$ describe correlations of the transverse location of partons in the nucleon, and never represent densities in impact parameter space. On the other hand, the impact parameter space PDF is the transverse space density measured from the transverse center of momentum of all partons $R_\perp = \sum_{i=q} x_i r_{\perp,i}$. Therefore, if the struck quark momentum $\boldsymbol{k}_\perp$ is left unintegrating in the GPDs in the $\xi \to 0$ limit, we have opportunity to get double information about the nucleon structure in the transverse direction. The Fourier transform of these GPDs over the $\boldsymbol{\Delta}_\perp$ contains a mean impact parameter space information $\bar{\boldsymbol{b}}_\perp = 1/2(\boldsymbol{b}_\perp^{in} + \boldsymbol{b}_\perp^{out})$ measured from the transverse center of momentum, and a correlation in the transverse direction $\boldsymbol{z}_\perp$ of the incoming and outgoing quarks.

APPENDIX A: GENERAL CONVENTIONS

For completeness, notational conventions are collected in line with the standard textbooks.

Lorentz vectors. We have used

$$x^+ = \frac{1}{\sqrt{2}}(x^0 + x^3) \quad \text{and} \quad x^- = \frac{1}{\sqrt{2}}(x^0 - x^3), \tag{A1}$$

respectively, referred to as the "light-cone time" and "light-cone position". The covariant vectors are obtained by $x_\mu = g_{\mu\nu}x^\nu$, with the metric tensor

$$g^{\mu\nu} = g_{\mu\nu} = \begin{pmatrix} 0 & 1 & 0 & 0 \\ 1 & 0 & 0 & 0 \\ 0 & 0 & -1 & 0 \\ 0 & 0 & 0 & -1 \end{pmatrix} \tag{A2}$$

Scalar products are

$$x \cdot p = x^\mu p_\mu = x^+ p_+ + x^- p_- + x^1 p_1 + x^2 p_2 = x^+ p^- + x^- p^- - \boldsymbol{x}_\perp \cdot \boldsymbol{p}_\perp. \tag{A3}$$

All other four-vector including γ^μ are treated in the same way.

Dirac matrices. Up to unitary transformation, the 4×4 Dirac matrices γ^μ are defined by

$$\gamma^\mu \gamma^\nu + \gamma^\nu \gamma^\mu = 2g^{\mu\nu} \tag{A4}$$

γ^0 is hermitean and γ^k anti-hermitean. Useful combinations are $\beta = \gamma^0$ and $\alpha^k = \gamma^0 \gamma^k$, as well as

$$\sigma^{\mu\nu} = \frac{1}{2}i\left(\gamma^\mu\gamma^\nu - \gamma^\nu\gamma^\mu\right), \quad \gamma_5 = \gamma^5 = i\gamma^0\gamma^1\gamma^2\gamma^3. \tag{A5}$$

They are usually expressed in terms of the 2×2 Pauli matrices

$$I = \begin{bmatrix} 1 & 0 \\ 0 & 1 \end{bmatrix}, \sigma^1 = \begin{bmatrix} 0 & 1 \\ 1 & 0 \end{bmatrix}, \sigma^2 = \begin{bmatrix} 0 & -i \\ i & 0 \end{bmatrix}, \sigma^3 = \begin{bmatrix} 1 & 0 \\ 0 & -1 \end{bmatrix} \tag{A6}$$

In the Dirac representation the matrices are

$$\gamma^0 = \begin{pmatrix} I & 0 \\ 0 & -I \end{pmatrix}, \quad \gamma_k = \begin{pmatrix} 0 & \sigma^k \\ -\sigma^k & 0 \end{pmatrix},$$

$$\gamma_5 = \begin{pmatrix} 0 & I \\ I & 0 \end{pmatrix}, \quad \alpha^k = \begin{pmatrix} \sigma^k & 0 \\ 0 & -\sigma^k \end{pmatrix}, \quad \sigma^{ij} = \begin{pmatrix} \sigma^k & 0 \\ 0 & \sigma^k \end{pmatrix} \tag{A7}$$

Projection operators. The chiral representation of the γ-matrices is used, particularly

$$\gamma^+\gamma^+ = \gamma^-\gamma^- = 0. \tag{A8}$$

Alternating products are, for example,

$$\gamma^+\gamma^-\gamma^+ = 2\gamma^+ \quad \text{and} \quad \gamma^-\gamma^+\gamma^- = 2\gamma^- \tag{A9}$$

The projection matrices becomes

$$\Lambda_+ = \frac{1}{\sqrt{2}}\gamma^0\gamma^+ = \frac{1}{2}\gamma^-\gamma^+ \quad \text{and} \quad \Lambda_- = \frac{1}{\sqrt{2}}\gamma^0\gamma^- = \frac{1}{2}\gamma^+\gamma^- \tag{A10}$$

Dirac spinors. The spinors $u_\alpha(k,\lambda)$ and $v_\alpha(k,\lambda)$ are solutions of the Dirac equation

$$(\not{k} - m)\,u(k,\lambda) = 0, \quad (\not{k} + m)\,v(k,\lambda) = 0. \tag{A11}$$

They are prthonormal and complete:

$$u(k,\lambda)u(k,\lambda') = -v(k,\lambda)v(k,\lambda') = 2m\lambda_{\lambda,\lambda'}, \tag{A12}$$

$$\sum_\lambda u(k,\lambda)\bar{u}(k,\lambda) = \not{k} + m, \quad \sum_\lambda v(k,\lambda)\bar{v}(k,\lambda) = \not{k} - m. \tag{A13}$$

The Gordon decomposition of the currents is useful:

$$\bar{u}(p,\lambda)\gamma^\mu u(q,\lambda') = \bar{v}(q,\lambda)\gamma^\mu v(p,\lambda') = \frac{1}{2m}\bar{u}(p,\lambda)\left[(p+q)^\mu + i\sigma^{\mu\nu}(p-q)_\nu\right]u(q,\lambda'). \tag{A14}$$

We use as Dirac spinors

$$u(k,\uparrow) = \frac{1}{2^{1/4}\sqrt{k^+}}\begin{pmatrix} \sqrt{2}k^+ \\ k_x + ik_y \\ m \\ 0 \end{pmatrix}, \quad u(k,\downarrow) = \frac{1}{2^{1/4}\sqrt{k^+}}\begin{pmatrix} 0 \\ m \\ -k_x + ik_y \\ \sqrt{2}k^+ \end{pmatrix},$$

$$v(k,\uparrow) = \frac{1}{2^{1/4}\sqrt{k^+}}\begin{pmatrix} 0 \\ -m \\ -k_x + ik_y \\ \sqrt{2}k^+ \end{pmatrix}, \quad v(k,\downarrow) = \frac{1}{2^{1/4}\sqrt{k^+}}\begin{pmatrix} \sqrt{2}k^+ \\ k_x + ik_y \\ -m \\ 0 \end{pmatrix} \tag{A15}$$

APPENDIX B: GROUP INTEGRALS

In this appendix, we give a list of group integrals used in the main text, over the Haar measure of the SU(N) group, normalized to unity, $\int dR = 1$.

For any SU(N) one has

$$\int dR R_i^f = 0, \quad \int dR R_f^{\dagger i} = 0, \quad \int dR R_i^f R_g^{\dagger j} = \frac{1}{N} \delta_g^f \delta_i^j. \tag{B1}$$

For $N = 2$ the following group integral is non-zero:

$$\int dR R_i^f R_j^g = \frac{1}{2} \epsilon^{fg} \epsilon_{ij}. \tag{B2}$$

For $N > 2$ this integral is zero; its analog in SU(3) is

$$\int dR R_i^f R_j^g R_k^h = \frac{1}{6} \epsilon^{fgh} \epsilon_{ijk}. \tag{B3}$$

On the contrary, in SU(2) it is zero.

The general method of finding integrals of several matrices $R, R^\dagger$ is as follows. The result of an integration over the invariant measure can be only invariant tensors which, for the SU(N) group, can be built solely from the Kronecker δ and Levi-Civita ϵ tensors. One constructs the supposed tensor of a given rank as a combination of δ's and ϵ's, satisfying the symmetry relations following from the integral in question. The indefinite coefficients in the combination are then found from contracting both sides with various δ's and ϵ's and thus by reducing the integral to a previously derived one.

For any SU(N) group one has

$$\int dR R_{i_1}^{f_1} R_{g_1}^{\dagger j_1} R_{i_2}^{f_2} R_{g_2}^{\dagger j_2} = \frac{1}{N^2 - 1} \left[\delta_{g_1}^{f_1} \delta_{g_2}^{f_2} \left(\delta_{j_1}^{i_1} \delta_{j_2}^{i_2} - \frac{1}{N} \delta_{j_2}^{i_1} \delta_{j_1}^{i_2} \right) + \delta_{g_2}^{f_1} \delta_{g_1}^{f_2} \left(\delta_{j_2}^{i_1} \delta_{j_1}^{i_2} - \frac{1}{N} \delta_{j_1}^{i_1} \delta_{j_2}^{i_2} \right) \right] \tag{B4}$$

since its contraction with, say, $\delta_{f_1}^{g_1}$ must reduce it to Eq.(B1).

In SU(2) there is an identity

$$\delta_{j_3}^j \epsilon_{j_1 j_2} + \delta_{j_1}^j \epsilon_{j_2 j_3} + \delta_{j_2}^j \epsilon_{j_3 j_1} = 0, \tag{B5}$$

using which one finds that the following integral is non-zero:

$$\int dR R_{j_1}^{f_1} R_{j_2}^{f_2} R_{j_3}^{f_3} R_g^{\dagger j} = \frac{1}{6} \left(\delta_g^{f_1} \delta_{j_1}^j \epsilon^{f_2 f_3} \epsilon_{j_2 j_3} + \delta_g^{f_2} \delta_{j_2}^j \epsilon^{f_3 f_1} \epsilon_{j_3 j_1} + \delta_g^{f_3} \delta_{j_3}^j \epsilon^{f_1 f_2} \epsilon_{j_1 j_2} \right). \tag{B6}$$

In SU(3) and higher group, integral is zero. The analog of the identity (B5) in SU(3) is (notice the signs in the cyclic permutation!)

$$\delta^i_{j_1}\epsilon_{j_2 j_3 j_4} - \delta^i_{j_2}\epsilon_{j_3 j_4 j_1} + \delta^i_{j_3}\epsilon_{j_4 j_1 j_2} - \delta^i_{j_4}\epsilon_{j_1 j_2 j_3} = 0, \tag{B7}$$

and the analog of Eq.(B6) is

$$\int dR R^{f_1}_{j_1} R^{f_2}_{j_2} R^{f_3}_{j_3} R^{f_4}_{j_4} R^{\dagger j}_g \tag{B8}$$

$$= \frac{1}{24}\left(\delta^{f_1}_g \delta^j_{j_1}\epsilon^{f_2 f_3 f_4}\epsilon_{j_2 j_3 j_4} + \delta^{f_2}_g \delta^j_{j_2}\epsilon^{f_3 f_4 f_1}\epsilon_{j_3 j_4 j_1} + \delta^{f_3}_g \delta^j_{j_3}\epsilon^{f_4 f_1 f_2}\epsilon_{j_4 j_1 j_2} + \delta^{f_4}_g \delta^j_{j_4}\epsilon^{f_1 f_2 f_3}\epsilon_{j_1 j_2 j_3}\right)$$

This integral arises when one projects three quarks from the bound-state level onto the octet baryon.

To evaluate the SU(3) average of six matrices, one needs the identities

$$\epsilon_{i_1 j_2 j_3}\epsilon_{j_1 i_2 i_3} + \epsilon_{i_2 j_2 j_3}\epsilon_{i_1 j_1 i_3} + \epsilon_{i_3 j_2 j_3}\epsilon_{i_1 i_2 j_1} =$$

$$\epsilon_{j_1 j_1 j_3}\epsilon_{j_2 i_2 i_3} + \epsilon_{j_1 i_2 j_3}\epsilon_{i_1 j_2 i_3} + \epsilon_{j_1 i_3 j_3}\epsilon_{i_1 i_2 j_3} =$$

$$\epsilon_{j_1 j_2 i_1}\epsilon_{j_3 i_2 i_3} + \epsilon_{j_1 j_2 i_2}\epsilon_{i_1 j_3 i_3} + \epsilon_{j_1 j_2 i_3}\epsilon_{i_1 i_2 j_3} = \epsilon_{j_1 j_2 j_3}\epsilon_{i_1 i_2 i_3}. \tag{B9}$$

One gets

$$\int dR R^{f_1}_{j_1} R^{f_2}_{j_2} R^{f_3}_{j_3} R^{h_1}_{i_1} R^{h_2}_{i_2} R^{h_3}_{i_3} = \frac{1}{72}\left(\epsilon^{f_1 f_2 f_3}\epsilon^{h_1 h_2 h_3}\epsilon_{j_1 j_2 j_3}\epsilon_{i_1 i_2 i_3}\right. \tag{B10}$$

$$+ \epsilon^{h_1 f_2 f_3}\epsilon^{f_1 h_2 h_3}\epsilon_{i_1 j_2 j_3}\epsilon_{j_1 i_2 i_3} + \epsilon^{h_2 f_2 f_3}\epsilon^{h_1 f_1 h_3}\epsilon_{i_2 j_2 j_3}\epsilon_{i_1 j_1 i_3} + \epsilon^{h_3 f_2 f_3}\epsilon^{h_1 h_2 f_1}\epsilon_{i_3 j_2 j_3}\epsilon_{i_1 i_2 j_1}$$

$$+ \epsilon^{f_1 h_1 f_3}\epsilon^{f_2 h_2 h_3}\epsilon_{j_1 i_1 j_3}\epsilon_{j_2 i_2 i_3} + \epsilon^{f_1 h_2 f_3}\epsilon^{h_1 f_2 h_3}\epsilon_{j_1 i_2 j_3}\epsilon_{i_1 j_2 i_3} + \epsilon^{f_1 h_3 f_3}\epsilon^{h_1 h_2 f_2}\epsilon_{j_1 i_3 j_3}\epsilon_{i_1 i_2 j_2}$$

$$+ \epsilon^{f_1 f_2 h_1}\epsilon^{f_3 h_2 h_3}\epsilon_{j_1 j_2 i_1}\epsilon_{j_3 i_2 i_3} + \epsilon^{f_1 f_2 h_2}\epsilon^{h_1 f_3 h_3}\epsilon_{j_1 j_2 i_2}\epsilon_{i_1 j_3 i_3} + \epsilon^{f_1 f_2 h_3}\epsilon^{h_1 h_2 f_3}\epsilon_{j_1 j_2 i_3}\epsilon_{i_1 i_2 j_3}\left.\right).$$

The result for the next integral is rather lengthy. We give it for the general SU(N). For abbreviation, we use the notation

$$\delta^{f_1}_{h_2}\delta^{f_2}_{h_3}\delta^{f_3}_{h_1}\delta^{i_1}_{j_3}\delta^{i_2}_{j_1}\delta^{i_3}_{j_1} \equiv (231)(321), etc. \tag{B11}$$

One has

$$\int dR R^{f_1}_{j_1} R^{f_2}_{j_2} R^{f_3}_{j_3} R^{\dagger i_1}_{h_1} R^{\dagger i_2}_{h_2} R^{\dagger i_3}_{h_3} = \frac{1}{N(N^2-1)(N^2-4)} \tag{B12}$$

$$\{(N^2-2)[(123)(123) + (132)(132) + (321)(321) + (213)(213) + (312)(231) + (231)(312)]$$

$$- N[(123)((132) + (321) + (213)) + (132)((123) + (231) + (312)) + (321)((312) + (123) + (231))$$

$$+ (213)((231) + (312) + (123)) + (312)((213) + (132) + (321)) + (231)((321) + (213) + (132))]$$

$$+ 2[(123)((312) + (231)) + (132)((213) + (321)) + (321)((132) + (213))$$

$$+ (213)((321) + (132)) + (312)((123) + (312)) + (231)((231) + (123))]\}.$$

Apparently, at $N = 2$ something gets wrong. For $N = 2$ there is a formal identity following from the fact that at $N = 2$ one has $\epsilon^{f_1 f_2 f_3} \epsilon_{h_1 h_2 h_3} = 0$:

$$(123) - (132) - (321) - (213) + (312) + (231) = 0. \tag{B13}$$

Consequently, for SU(2) one obtains a shorter expression:

$$\int dR R_{j_1}^{f_1} R_{j_2}^{f_2} R_{j_3}^{f_3} R_{h_1}^{\dagger i_1} R_{h_2}^{\dagger i_2} R_{h_3}^{\dagger i_3} \tag{B14}$$

$$= \frac{1}{6} \{ [(123)(123) + (132)(132) + (321)(321) + (213)(213) + (312)(231) + (231)(312)]$$

$$- \frac{1}{4} [(123)((132) + (321) + (213)) + (132)((123) + (231) + (312)) + (321)((312) + (123) + (231))$$

$$+ (213)((231) + (312) + (123)) + (312)((213) + (132) + (321)) + (231)((321) + (213) + (132)))] \}$$

In case one is interested in the presence of an additional quark-antiquark pair in an octet baryon, one has to use the group integral

$$\int dR R_{j_1}^{f_1} R_{j_2}^{f_2} R_{j_3}^{f_3} (R_{j_4}^{f_4} R_{f_5}^{\dagger j_5}) R_g^{\dagger k} R_3^h = \frac{1}{360} \tag{B15}$$

$$\left\{ \epsilon^{f_1 f_2 h} \epsilon_{j_1 j_2} \left[\delta_g^{f_3} \delta_{f_5}^{f_4} \left(4 \delta_{j_4}^{j_5} \delta_{j_3}^{k} - \delta_{j_3}^{j_5} \delta_{j_4}^{k} \right) + \delta_g^{f_4} \delta_{f_5}^{f_3} \left(4 \delta_{j_3}^{j_5} \delta_{j_4}^{k} - \delta_{j_4}^{j_5} \delta_{j_3}^{k} \right) \right] \right.$$

$$+ \epsilon^{f_1 f_3 h} \epsilon_{j_1 j_3} \left[\delta_g^{f_2} \delta_{f_5}^{f_4} \left(4 \delta_{j_4}^{j_5} \delta_{j_2}^{k} - \delta_{j_2}^{j_5} \delta_{j_4}^{k} \right) + \delta_g^{f_4} \delta_{f_5}^{f_2} \left(4 \delta_{j_2}^{j_5} \delta_{j_4}^{k} - \delta_{j_4}^{j_5} \delta_{j_2}^{k} \right) \right]$$

$$+ \epsilon^{f_1 f_4 h} \epsilon_{j_1 j_4} \left[\delta_g^{f_2} \delta_{f_5}^{f_3} \left(4 \delta_{j_3}^{j_5} \delta_{j_2}^{k} - \delta_{j_2}^{j_5} \delta_{j_3}^{k} \right) + \delta_g^{f_3} \delta_{f_5}^{f_2} \left(4 \delta_{j_2}^{j_5} \delta_{j_3}^{k} - \delta_{j_3}^{j_5} \delta_{j_2}^{k} \right) \right]$$

$$+ \epsilon^{f_2 f_3 h} \epsilon_{j_2 j_3} \left[\delta_g^{f_1} \delta_{f_5}^{f_4} \left(4 \delta_{j_4}^{j_5} \delta_{j_1}^{k} - \delta_{j_1}^{j_5} \delta_{j_4}^{k} \right) + \delta_g^{f_4} \delta_{f_5}^{f_1} \left(4 \delta_{j_1}^{j_5} \delta_{j_4}^{k} - \delta_{j_4}^{j_5} \delta_{j_1}^{k} \right) \right]$$

$$+ \epsilon^{f_2 f_4 h} \epsilon_{j_2 j_4} \left[\delta_g^{f_1} \delta_{f_5}^{f_3} \left(4 \delta_{j_3}^{j_5} \delta_{j_1}^{k} - \delta_{j_1}^{j_5} \delta_{j_3}^{k} \right) + \delta_g^{f_3} \delta_{f_5}^{f_1} \left(4 \delta_{j_1}^{j_5} \delta_{j_3}^{k} - \delta_{j_3}^{j_5} \delta_{j_1}^{k} \right) \right]$$

$$+ \left. \epsilon^{f_3 f_4 h} \epsilon_{j_3 j_4} \left[\delta_g^{f_1} \delta_{f_5}^{f_2} \left(4 \delta_{j_2}^{j_5} \delta_{j_1}^{k} - \delta_{j_1}^{j_5} \delta_{j_2}^{k} \right) + \delta_g^{f_2} \delta_{f_5}^{f_1} \left(4 \delta_{j_1}^{j_5} \delta_{j_2}^{k} - \delta_{j_2}^{j_5} \delta_{j_1}^{k} \right) \right] \right\}$$

This tensor defines, in particular, the five-quark wave function of the nucleon.

For finding the quark structure of the antidecuplet, the following group integrals are relevant. The rotational wave function of the antidecuplet is

$$A_k^{*\{h_1 h_2 h_3\}}(R) = \frac{1}{3} \left(R_3^{h_1} R_3^{h_2} R_k^{h_3} + R_3^{h_3} R_3^{h_1} R_k^{h_2} + R_3^{h_2} R_3^{h_3} R_k^{h_1} \right). \tag{B16}$$

Projecting it on three quarks and using Eq.(B11) we get an identical zero because all terms in Eq.(B11) are antisymmetric in a pair of flavor indices while the tensor (B16) is symmetric. It reflects the fact that one cannot build an antidecuplet from three quarks:

$$\int dR R_{j_1}^{f_1} R_{j_2}^{f_2} R_{j_3}^{f_3} A_k^{*\{h_1 h_2 h_3\}}(R) = 0. \tag{B17}$$

However, a similar group integral with an additional quark-antiquark pair is non-zero:

$$\int dR R_{j_1}^{f_1} R_{j_2}^{f_2} R_{j_3}^{f_3} (R_{j_4}^{f_4} R_{f_5}^{\dagger j_5}) A_k^{*\{h_1 h_2 h_3\}}(R) = \frac{\delta_k^{J_5}}{1080} \left\{ \epsilon_{j_1 j_2} \epsilon_{j_3 j_4} \left[\delta_{f_5}^{h_3} (\epsilon^{f_1 f_2 h_1} \epsilon^{f_3 f_4 h_2} + \epsilon^{f_1 f_2 h_2} \epsilon^{f_3 f_4 h_1}) \right. \right.$$

$$+ \; \delta_{f_5}^{h_1} (\epsilon^{f_1 f_2 h_2} \epsilon^{f_3 f_4 h_3} + \epsilon^{f_1 f_2 h_3} \epsilon^{f_3 f_4 h_2}) + \delta_{f_5}^{h_2} (\epsilon^{f_1 f_2 h_1} \epsilon^{f_3 f_4 h_3} + \epsilon^{f_1 f_2 h_3} \epsilon^{f_3 f_4 h_1}) \Big]$$

$$+ \; \epsilon_{j_2 j_3} \epsilon_{j_1 j_4} \left[\delta_{f_5}^{h_3} (\epsilon^{f_2 f_3 h_1} \epsilon^{f_1 f_4 h_2} + \epsilon^{f_2 f_3 h_2} \epsilon^{f_1 f_4 h_1}) + \delta_{f_5}^{h_1} (\epsilon^{f_2 f_3 h_2} \epsilon^{f_1 f_4 h_3} + \epsilon^{f_2 f_3 h_3} \epsilon^{f_1 f_4 h_2}) \right.$$

$$+ \; \delta_{f_5}^{h_2} (\epsilon^{f_2 f_3 h_1} \epsilon^{f_1 f_4 h_3} + \epsilon^{f_2 f_3 h_3} \epsilon^{f_1 f_4 h_1}) \Big] + \epsilon_{j_1 j_3} \epsilon_{j_2 j_4} \left[\delta_{f_5}^{h_3} (\epsilon^{f_1 f_3 h_1} \epsilon^{f_2 f_4 h_2} + \epsilon^{f_1 f_3 h_2} \epsilon^{f_2 f_4 h_1}) \right.$$

$$+ \; \delta_{f_5}^{h_1} (\epsilon^{f_1 f_3 h_2} \epsilon^{f_2 f_4 h_3} + \epsilon^{f_1 f_3 h_3} \epsilon^{f_2 f_4 h_2}) + \delta_{f_5}^{h_2} (\epsilon^{f_1 f_3 h_1} \epsilon^{f_2 f_4 h_3} + \epsilon^{f_1 f_3 h_3} \epsilon^{f_2 f_4 h_1}) \Big] \right\} \tag{B18}$$

In particular, for the Θ^+ baryon being the 333-component of the antidecuplet we have

$$\Theta_k^*(R) = \sqrt{30} A_k^{*\{333\}}(R) = \sqrt{30} R_3^3 R_3^3 R_k^3, \quad \Theta^k(R) = \sqrt{30} R_3^{\dagger 3} R_3^{\dagger 3} R_3^{\dagger k} \tag{B19}$$

The projection of five quarks onto to the Θ^+ rotational wave function (B19) gives the tensor

$$T_{j_1 j_2 j_3 j_4, f_5, k}^{f_1 f_2 f_3 f_4, j_5}(\Theta) = \int dR R_{j_1}^{f_1} R_{j_2}^{f_2} R_{j_3}^{f_3} (R_{j_4}^{f_4} R_{f_5}^{\dagger j_5}) \Theta_k^*(R) \tag{B20}$$

$$= \frac{\delta_{f_5}^3 \delta_k^{j_5} \sqrt{30}}{180} \left(\epsilon_{j_1 j_2} \epsilon_{j_3 j_4} \epsilon^{f_1 f_2} \epsilon^{f_3 f_4} + \epsilon_{j_2 j_3} \epsilon_{j_1 j_4} \epsilon^{f_2 f_3} \epsilon^{f_1 f_4} + \epsilon_{j_1 j_3} \epsilon_{j_2 j_4} \epsilon^{f_1 f_3} \epsilon^{f_2 f_4} \right).$$

APPENDIX C: CONTRIBUTIONS OF THE DISTORTED DIRAC SEA EFFECTS TO THE DISCRETE WAVE FUNCTION

The discrete wave function $F(p)$ consists of three terms, i.e., upper component, lower component and sea quark effect:

$$F^{j\sigma}(p) = F^{j\sigma}_{up}(p) + F^{j\sigma}_{low}(p) + F^{j\sigma}_{sea}(p) \equiv F^{j\sigma}_{lev}(p) + F^{j\sigma}_{sea}(p). \tag{C1}$$

In order to evaluate the spin unpolarized and polarized observables, one needs the products of the level and sea wave functions

$$F^\dagger_{j\sigma}(p)F^{j\sigma'}(p)\delta^\sigma_{\sigma'} = |F_{lev}(p)|^2 + F^\dagger_{lev}(p) \cdot F_{sea}(p) + F_{lev}(p) \cdot F^\dagger_{sea}(p) + |F_{sea}(p)|^2 \tag{C2}$$

$$F^\dagger_{j\sigma}(p)F^{j\sigma'}(p)(\sigma_3)^\sigma_{\sigma'} = |\Delta F_{lev}(p)|^2 + \Delta F^\dagger_{lev} \cdot (p)F_{sea}(p) + \Delta F_{lev}(p) \cdot F^\dagger_{sea}(p) + |\Delta F_{sea}(p)|^2. \tag{C3}$$

The sea effect independent parts $|F_{lev}(p)|^2$ and $|\Delta F_{lev}(p)|^2$ can be expressed in terms of the $L = 0$ and $L = 1$ wave functions $h(p)$ and $j(p)$, and these representations have been shown in Eq.(156) and Eq.(157). In this section, we will show the complete representations including the sea effect $F_{sea}(p)$ in the proton case.

1. Interference terms of $F_{lev}(p)$ and $F_{sea}(p)$

For saving space, we will express spin polarized and unpolarized case together. In the following equation, upper sign denotes unpolarized case and lower sign denotes polarized case:

$$9\left(F^\dagger_{lev}(p) \cdot F_{sea}(p) + F_{lev}(p) \cdot F^\dagger_{sea}(p)\right) \text{ or } 9\left(\Delta F^\dagger_{lev} \cdot (p)F_{sea}(p) + \Delta F_{lev}(p) \cdot F^\dagger_{sea}(p)\right)$$

$$= -\left(\frac{\mathcal{M}_N}{2\pi}\right)^2 M \int dz' \frac{d^2 p'_\perp}{(2\pi)^2} \frac{1}{\mathcal{Z}} \left[\left(h(p) + \frac{p_z}{|p|}j(p)\right) \cdot \left(h(p') - \frac{p'_z}{|p'|}j(p')\right)\right.$$

$$\times \left\{18\Sigma(q)M(z'-z) \pm 18\Pi(q)\left(\frac{q_3}{|q|}M(z'+z) - \frac{q_\perp \cdot Q_\perp}{q}\right)\right\}$$

$$+ \left(h(p) + \frac{p_z}{|p|}j(p)\right)\left(-\frac{j(p')}{|p'|}\right) \cdot \left\{18 p'_\perp \cdot Q_\perp \Sigma(q) - 18\frac{p'_\perp \cdot q_\perp + q_z p'_\perp \cdot Q_\perp}{|q|}M(z'+z)\Pi(q)\right\}$$

$$+ \left(h(p') - \frac{p'_z}{|p'|}j(p')\right) \cdot \left(\frac{j(p)}{|p|}\right) \cdot \left\{\mp 18 p_\perp \cdot Q_\perp \Sigma(q) \mp 18\frac{p_\perp \cdot q_\perp \pm q_z p_\perp \cdot Q_\perp}{|q|}M(z'+z)\Pi(q)\right\}$$

82

$$+ \; \frac{j(p)}{|p|}\frac{j(p')}{|p'|} \cdot \left\{ \pm 18 \boldsymbol{p}_\perp \cdot \boldsymbol{p}'_\perp M(z'-z)\Sigma(q) \pm \boldsymbol{p}_\perp \cdot \boldsymbol{p}'_\perp \frac{q_3}{|q|} M(z'+z)\Pi(q) \right.$$

$$\mp \; 18\frac{\Pi(q)}{|q|} \cdot \left(p_{\perp 2} Q_{\perp 2}(\boldsymbol{p}'_\perp \cdot \boldsymbol{q}_\perp) + p_{\perp 1} q_{\perp 1}(\boldsymbol{p}'_\perp \cdot \boldsymbol{Q}_\perp) \right.$$

$$\left. \left. + \; p_{\perp 2} Q_{\perp 1}(\epsilon_{\alpha\beta} \boldsymbol{p}'_{\perp\alpha} \cdot \boldsymbol{q}_{\perp\beta}) + p_{\perp 1} q_{\perp 2}(\epsilon_{\alpha\beta} \boldsymbol{Q}_{\perp\alpha} \cdot \boldsymbol{q}_{\perp\beta})\right)\right\} \Bigg],$$

$$\text{(C4)}$$

where

$$\mathcal{Z} = \mathcal{M}_N^2 z z'(z'+z) + z(\boldsymbol{p}'^{2}_\perp + M^2) + z'(\boldsymbol{p}^2_\perp + M^2), \tag{C5}$$

and

$$\boldsymbol{q} = ((\boldsymbol{p}_\perp + \boldsymbol{p}'_\perp), (z+z')\mathcal{M}_N), \quad Q_{\perp\alpha} = z p'_{\perp\alpha} - z' p_{\perp\alpha}, \quad \alpha = 1,2. \tag{C6}$$

2. Square terms of $F_{sea}(p)$

The unpolarized and polarized square parts of $F_{sea}(p)$ in Eq.(C2) and Eq.(C3) in the proton case are written as:

$$9|F_{sea}(p)|^2 \; \text{or} \; 9|\Delta F_{sea}(p)|^2$$

$$= \frac{\mathcal{M}_N}{2\pi} \int \frac{dz' d^2 \boldsymbol{p}'_\perp}{(2\pi)^2} \int \frac{dz'' d^2 \boldsymbol{p}''_\perp}{(2\pi)^2} \left(\frac{M\mathcal{M}_N}{2\pi}\right)^2 \frac{1}{\mathcal{Z}''\mathcal{Z}'} \cdot \left[\left(h(p'') - \frac{p''_z}{|p''|}j(p'') \right) \left(h(p') - \frac{p'_z}{|p'|}j(p') \right) \right.$$

$$\left\{ \Sigma(q'')\Sigma(q') \left(9M^2(z''-z)(z'-z) \pm 9\boldsymbol{Q}''_\perp \cdot \boldsymbol{Q}'_\perp \right) - \Sigma(q'')\frac{\Pi(q')}{|q'|} \left(9M^2(z''-z)(z''+z)q'_z \right. \right.$$

$$+ \; 9M(z''-z)\boldsymbol{q}'_\perp \cdot \boldsymbol{Q}'_\perp \mp 9M(z'+z)\boldsymbol{q}'_\perp \cdot \boldsymbol{Q}''_\perp \pm 9q'_z\boldsymbol{Q}'_\perp \cdot \boldsymbol{Q}''_\perp \Big) - \Sigma(q')\frac{\Pi(q'')}{|q''|}$$

$$\left(9M^2(z''+z)(z''-z)q''_z \mp 9M(z''+z)\boldsymbol{q}''_\perp \cdot \boldsymbol{Q}'_\perp + 9M(z'-z)\boldsymbol{q}''_\perp \cdot \boldsymbol{Q}''_\perp \pm 9q''_z\boldsymbol{Q}'_\perp \cdot \boldsymbol{Q}''_\perp \right)$$

$$+ \; \frac{\Pi(q'')\Pi(q')}{|q''||q'|} \left(\pm 9M^2(z''+z)(z'+z) \left(\boldsymbol{q}''_\perp \cdot \boldsymbol{q}'_\perp \pm q''_z q'_3 \right) \mp 9M(z''+z)q'_z\boldsymbol{q}''_\perp \cdot \boldsymbol{Q}'_\perp \right.$$

$$+ \; 9M(z''+z)q''_z\boldsymbol{q}'_\perp \cdot \boldsymbol{Q}'_\perp \mp 9M(z'+z)q''_z\boldsymbol{q}'_\perp \cdot \boldsymbol{Q}''_\perp + 9M(z''+z)q'_z\boldsymbol{q}''_\perp \cdot \boldsymbol{Q}''_\perp$$

$$\left. + \; 9 \left\{ \left(\boldsymbol{Q}''_\perp \cdot \boldsymbol{Q}'_\perp \right) \left(\boldsymbol{q}''_\perp \cdot \boldsymbol{q}'_\perp \pm q''_z q'_z \right) + \epsilon_{\alpha\beta}\epsilon_{\alpha'\beta'} \left(Q''_{\perp\alpha}Q'_{\perp\beta} \right) \left(q''_{\perp\alpha'}q'_{\perp\beta'} \right) \right\} \right) \right\}$$

$$- \; \left(h(p'') - \frac{p''}{|p''|}j(p'') \right) \frac{j(p')}{|p'|} \cdot \left(9\Sigma(q'')\Sigma(q') \left(M(z''-z)\boldsymbol{p}'_\perp \cdot \boldsymbol{Q}'_\perp \mp M(z'-z)\boldsymbol{p}_\perp \cdot \boldsymbol{Q}''_\perp \right) \right.$$

$$- \; 9\Sigma(q'')\frac{\Pi(q')}{|q'|} \cdot \left(M^2(z''-z)(z'+z)\boldsymbol{p}'_\perp \cdot \boldsymbol{q}'_\perp - M(z''-z)q'_z\boldsymbol{p}'_\perp \cdot \boldsymbol{Q}'_\perp \mp M(z'+z)q'_z\boldsymbol{p}_\perp \cdot \boldsymbol{Q}''_\perp \right.$$

$$\left. \mp \; \left(\boldsymbol{p}'_\perp \cdot \boldsymbol{q}'_\perp \right) \left(\boldsymbol{Q}'_\perp \cdot \boldsymbol{Q}''_\perp \right) \mp \epsilon_{\alpha\beta}\epsilon_{\alpha'\beta'} \left(p'_{\perp\alpha}q'_{\perp\beta} \right) \left(Q'_{\perp\alpha'}Q''_{\perp\beta'} \right) \right) - 9\Sigma(q')\frac{\Pi(q'')}{|q''|}$$

$$\left(M^2(z''+z)(z'-z)\boldsymbol{p}'_\perp \cdot \boldsymbol{q}''_\perp + M(z''+z)q''_z \boldsymbol{p}'_\perp \cdot \boldsymbol{Q}'_\perp \mp M(z'-z)q''_z \boldsymbol{p}'_\perp \cdot \boldsymbol{Q}''_\perp \right.$$

$$\pm \left(\boldsymbol{p}'_\perp \cdot \boldsymbol{q}''_\perp \right) \left(\boldsymbol{Q}'_\perp \cdot \boldsymbol{Q}''_\perp \right) \pm \epsilon_{\alpha\beta}\epsilon_{\alpha'\beta'} \left(p'_{\perp\alpha}q''_{\perp\beta} \right) \left(Q'_{\perp\alpha'}Q''_{\perp\beta'} \right) \right)$$

$$+ \frac{9\Pi(q')\Pi(q'')}{|q'||q''|} \left(\mp M^2(z''+z)(z'+z)q'_z \boldsymbol{q}''_\perp \cdot \boldsymbol{p}'_\perp + M^2(z''+z)(z'+z)q''_z \boldsymbol{q}'_\perp \cdot \boldsymbol{p}'_\perp \right.$$

$$\mp M(z''+z)\left\{ \left(\boldsymbol{q}'_\perp \cdot \boldsymbol{q}''_\perp \right) \left(\boldsymbol{Q}'_\perp \cdot \boldsymbol{p}'_\perp \right) \pm \epsilon_{\alpha\beta}\epsilon_{\alpha'\beta'} \left(q'_{\perp\alpha}q''_{\perp\beta} \right) \left(Q'_{\perp\alpha'}p'_{\perp\beta'} \right) \right\}$$

$$+ M(z''+z)\left\{ \left(\boldsymbol{q}'_\perp \cdot \boldsymbol{q}''_\perp \right) \left(\boldsymbol{Q}''_\perp \cdot \boldsymbol{p}'_\perp \right) + \epsilon_{\alpha\beta}\epsilon_{\alpha'\beta'} \left(q''_{\perp\alpha}q'_{\perp\beta} \right) \left(Q''_{\perp\alpha'}p'_{\perp\beta'} \right) \right\}$$

$$- q'_z \left\{ \left(\boldsymbol{p}'_\perp \cdot \boldsymbol{q}''_\perp \right) \left(\boldsymbol{Q}''_\perp \cdot \boldsymbol{p}'_\perp \right) + \epsilon_{\alpha\beta}\epsilon_{\alpha'\beta'} \left(q''_{\perp\alpha}p'_{\perp\beta} \right) \left(Q''_{\perp\alpha'}Q'_{\perp\beta'} \right) \right\}$$

$$\left. \left(\pm q''_z \left\{ \left(\boldsymbol{p}'_\perp \cdot \boldsymbol{q}'_\perp \right) \left(\boldsymbol{Q}''_\perp \cdot \boldsymbol{p}'_\perp \right) + \epsilon_{\alpha\beta}\epsilon_{\alpha'\beta'} \left(q'_{\perp\alpha}p'_{\perp\beta} \right) \left(Q''_{\perp\alpha'}Q'_{\perp\beta'} \right) \right\} \right) \right)$$

$$- \left(h(p') - \frac{p'}{|p'|}j(p') \right) \frac{j(p'')}{|p''|} \cdot \left(9\Sigma(q')\Sigma(q'') \left(M(z'-z)\boldsymbol{p}''_\perp \cdot \boldsymbol{Q}''_\perp \mp M(z''-z)\boldsymbol{p}''_\perp \cdot \boldsymbol{Q}'_\perp \right) \right.$$

$$- 9\Sigma(q')\frac{\Pi(q'')}{|q''|} \cdot \left(M^2(z'-z)(z''+z)\boldsymbol{p}''_\perp \cdot \boldsymbol{q}'_\perp - M(z'-z)q'_z \boldsymbol{p}''_\perp \cdot \boldsymbol{Q}''_\perp \mp M(z''+z)q'_z \boldsymbol{p}''_\perp \cdot \boldsymbol{Q}'_\perp \right.$$

$$\mp \left(\boldsymbol{p}''_\perp \cdot \boldsymbol{q}'_\perp \right) \left(\boldsymbol{Q}''_\perp \cdot \boldsymbol{Q}'_\perp \right) \mp \epsilon_{\alpha\beta}\epsilon_{\alpha'\beta'} \left(p''_{\perp\alpha}q'_{\perp\beta} \right) \left(Q''_{\perp\alpha'}Q'_{\perp\beta'} \right) \right) - 9\Sigma(q'')\frac{\Pi(q')}{|q'|}$$

$$\left(M^2(z'+z)(z''-z)\boldsymbol{p}''_\perp \cdot \boldsymbol{q}'_\perp + M(z'+z)q'_z \boldsymbol{p}''_\perp \cdot \boldsymbol{Q}'_\perp \mp M(z''-z)q'_z \boldsymbol{p}''_\perp \cdot \boldsymbol{Q}'_\perp \right.$$

$$\left. \pm \left(\boldsymbol{p}''_\perp \cdot \boldsymbol{q}'_\perp \right) \left(\boldsymbol{Q}''_\perp \cdot \boldsymbol{Q}'_\perp \right) \pm \epsilon_{\alpha\beta}\epsilon_{\alpha'\beta'} \left(p''_{\perp\alpha}q'_{\perp\beta} \right) \left(Q''_{\perp\alpha'}Q'_{\perp\beta'} \right) \right)$$

$$+ \frac{9\Pi(q'')\Pi(q')}{|q''||q'|} \left(\mp M^2(z'+z)(z''+z)q''_z \boldsymbol{q}'_\perp \cdot \boldsymbol{p}''_\perp + M^2(z'+z)(z''+z)q'_z \boldsymbol{q}''_\perp \cdot \boldsymbol{p}''_\perp \right.$$

$$\mp M(z'+z)\left\{ \left(\boldsymbol{q}''_\perp \cdot \boldsymbol{q}'_\perp \right) \left(\boldsymbol{Q}''_\perp \cdot \boldsymbol{p}''_\perp \right) \pm \epsilon_{\alpha\beta}\epsilon_{\alpha'\beta'} \left(q''_{\perp\alpha}q'_{\perp\beta} \right) \left(Q''_{\perp\alpha'}p'_{\perp\beta'} \right) \right\}$$

$$+ M(z'+z)\left\{ \left(\boldsymbol{q}''_\perp \cdot \boldsymbol{q}'_\perp \right) \left(\boldsymbol{Q}'_\perp \cdot \boldsymbol{p}''_\perp \right) + \epsilon_{\alpha\beta}\epsilon_{\alpha'\beta'} \left(q'_{\perp\alpha}q''_{\perp\beta} \right) \left(Q'_{\perp\alpha'}p''_{\perp\beta'} \right) \right\}$$

$$- q''_z \left\{ \left(\boldsymbol{p}''_\perp \cdot \boldsymbol{q}'_\perp \right) \left(\boldsymbol{Q}'_\perp \cdot \boldsymbol{p}''_\perp \right) + \epsilon_{\alpha\beta}\epsilon_{\alpha'\beta'} \left(q'_{\perp\alpha}p''_{\perp\beta} \right) \left(Q'_{\perp\alpha'}Q''_{\perp\beta'} \right) \right\}$$

$$\left. \left(\pm q'_z \left\{ \left(\boldsymbol{p}''_\perp \cdot \boldsymbol{q}''_\perp \right) \left(\boldsymbol{Q}'_\perp \cdot \boldsymbol{p}''_\perp \right) + \epsilon_{\alpha\beta}\epsilon_{\alpha'\beta'} \left(q''_{\perp\alpha}p''_{\perp\beta} \right) \left(Q'_{\perp\alpha'}Q''_{\perp\beta'} \right) \right\} \right) \right)$$

$$+ \frac{j(p'')j(p')}{|p''||p'|} \left\{ \Sigma(q'')\Sigma(q') \left(\pm 9M^2(z''-z)(z'-z) \left(\boldsymbol{p}'_\perp \cdot \boldsymbol{p}''_\perp \right) + \left(\boldsymbol{Q}'_\perp \cdot \boldsymbol{Q}''_\perp \right) \left(\boldsymbol{p}'_\perp \cdot \boldsymbol{p}''_\perp \right) \right. \right.$$

$$+ \epsilon_{\alpha\beta}\epsilon_{\alpha'\beta'} \left(Q''_{\perp\alpha}Q'_{\perp\beta} \right) \left(p''_{\perp\alpha'}p'_{\perp\beta'} \right) \Big) - \Sigma(q'')\frac{\Pi(q')}{|q'|} \left\{ \mp M^2(z''-z)(z'+z)q'_z \left(\boldsymbol{p}'_\perp \cdot \boldsymbol{p}''_\perp \right) \right.$$

$$+ M(z''-z) \left(\mp q'_1 Q'_1 p'_1 p'_1 \pm q'_1 Q'_1 p'_2 p'_2 \pm q'_2 Q'_2 p'_1 p'_1 \mp q'_2 Q'_2 p'_2 p'_2 \pm q'_1 Q'_2 p'_1 p'_2 \pm q'_1 Q'_2 p'_2 p'_1 \right.$$

$$\left. \mp q'_2 Q'_1 p'_2 p'_1 \mp q'_2 Q'_1 p'_1 p'_2 \right) + M(z'+z) \left(\left(\boldsymbol{Q}''_\perp \cdot \boldsymbol{p}'_\perp \right) \left(\boldsymbol{p}'_\perp \cdot \boldsymbol{q}'_\perp \right) + \epsilon_{\alpha\beta}\epsilon_{\alpha'\beta'} \left(Q''_{\perp\alpha}p'_{\perp\beta} \right) \left(p'_{\perp\alpha'}q'_{\perp\beta'} \right) \right)$$

$$\left. - q'_z \left(\left(\boldsymbol{Q}''_\perp \cdot \boldsymbol{Q}'_\perp \right) \left(\boldsymbol{p}''_\perp \cdot \boldsymbol{p}'_\perp \right) + \epsilon_{\alpha\beta}\epsilon_{\alpha'\beta'} \left(Q''_{\perp\alpha}Q'_{\perp\beta} \right) \left(p''_{\perp\alpha'}p'_{\perp\beta'} \right) \right) \right\}$$

$$- \Sigma(q')\frac{\Pi(q'')}{|q''|} \left\{ \mp M^2(z'-z)(z''+z)q''_z \left(\boldsymbol{p}''_\perp \cdot \boldsymbol{p}'_\perp \right) \right.$$

$$+ M(z'-z) \left(\mp q''_1 Q''_1 p'_1 p''_1 \pm q''_1 Q''_1 p'_2 p''_2 \pm q''_2 Q''_2 p'_1 p''_1 \mp q''_2 Q''_2 p'_2 p''_2 \pm q''_1 Q''_2 p'_1 p''_2 \pm q''_1 Q''_2 p'_2 p''_1 \right.$$

$$\left. \mp q''_2 Q''_1 p'_2 p''_1 \mp q''_2 Q''_1 p'_1 p''_2 \right) + M(z''+z) \left(\left(\boldsymbol{Q}'_\perp \cdot \boldsymbol{p}'_\perp \right) \left(\boldsymbol{p}''_\perp \cdot \boldsymbol{q}''_\perp \right) + \epsilon_{\alpha\beta}\epsilon_{\alpha'\beta'} \left(Q'_{\perp\alpha}p'_{\perp\beta} \right) \left(p''_{\perp\alpha'}q''_{\perp\beta'} \right) \right)$$

$$- q_z'' \left(\left(\boldsymbol{Q}_\perp' \cdot \boldsymbol{Q}_\perp'' \right) \left(\boldsymbol{p}_\perp' \cdot \boldsymbol{p}_\perp'' \right) + \epsilon_{\alpha\beta}\epsilon_{\alpha'\beta'} \left(Q_{\perp\alpha}' Q_{\perp\beta}'' \right) \left(p_{\perp\alpha'}' p_{\perp\beta'}'' \right) \right) \Big\}$$

$$+ \; \frac{\Pi(q'')\Pi(q')}{|q''||q'|} \left(M^2(z''+z)(z'+z) \left\{ \left(\boldsymbol{q}_\perp' \cdot \boldsymbol{q}_\perp'' \right) \left(\boldsymbol{p}_\perp' \cdot \boldsymbol{p}_\perp'' \right) + \epsilon_{\alpha\beta}\epsilon_{\alpha'\beta'} \left(q_{\perp\alpha}' q_{\perp\beta}'' \right) \left(p_{\perp\alpha'}' p_{\perp\beta'}'' \right) \right\} \right.$$

$$\pm \; M(z''+z)q_z'' \left\{ \left(\boldsymbol{p}_\perp'' \cdot \boldsymbol{q}_\perp' \right) \left(\boldsymbol{Q}_\perp' \cdot \boldsymbol{p}_\perp' \right) + \epsilon_{\alpha\beta}\epsilon_{\alpha'\beta'} \left(p_{\perp\alpha}'' q_{\perp\beta}' \right) \left(Q_{\perp\alpha'}' p_{\perp\beta'}' \right) \right\}$$

$$- \; M(z''+z)q_z' \left\{ \left(\boldsymbol{p}_\perp'' \cdot \boldsymbol{q}_\perp'' \right) \left(\boldsymbol{Q}_\perp' \cdot \boldsymbol{p}_\perp' \right) + \epsilon_{\alpha\beta}\epsilon_{\alpha'\beta'} \left(q_{\perp\alpha}'' p_{\perp\beta}'' \right) \left(p_{\perp\alpha'}' Q_{\perp\beta'}' \right) \right\}$$

$$\pm \; M(z'+z)q_z' \left\{ \left(\boldsymbol{p}_\perp' \cdot \boldsymbol{q}_\perp'' \right) \left(\boldsymbol{Q}_\perp'' \cdot \boldsymbol{p}_\perp'' \right) + \epsilon_{\alpha\beta}\epsilon_{\alpha'\beta'} \left(p_{\perp\alpha}' q_{\perp\beta}'' \right) \left(Q_{\perp\alpha'}'' p_{\perp\beta'}'' \right) \right\}$$

$$- \; M(z'+z)q_z'' \left\{ \left(\boldsymbol{p}_\perp' \cdot \boldsymbol{q}_\perp' \right) \left(\boldsymbol{Q}_\perp'' \cdot \boldsymbol{p}_\perp'' \right) + \epsilon_{\alpha\beta}\epsilon_{\alpha'\beta'} \left(q_{\perp\alpha}' p_{\perp\beta}' \right) \left(p_{\perp\alpha'}'' Q_{\perp\beta'}'' \right) \right\}$$

$$\pm \; \left(\boldsymbol{q}_\perp'' \cdot \boldsymbol{q}_\perp' \pm q_z'' q_z' \right) \left(\left(\boldsymbol{p}_\perp'' \cdot \boldsymbol{p}_\perp' \right) \left(\boldsymbol{Q}_\perp'' \cdot \boldsymbol{Q}_\perp' \right) + \epsilon_{\alpha\beta}\epsilon_{\alpha'\beta'} \left(p_{\perp\alpha}'' p_{\perp\beta}' \right) \left(Q_{\perp\alpha'}'' Q_{\perp\beta'}' \right) \right)$$

$$\pm \; \left(\boldsymbol{p}_\perp'' \cdot \boldsymbol{p}_\perp' \right) \left(\epsilon_{\alpha\beta}\epsilon_{\alpha'\beta'} \left(q_{\perp\alpha}'' q_{\perp\beta}' \right) \left(Q_{\perp\alpha'}'' Q_{\perp\beta'}' \right) \right) \pm \left(\boldsymbol{Q}_\perp'' \cdot \boldsymbol{Q}_\perp' \right) \left(\epsilon_{\alpha\beta}\epsilon_{\alpha'\beta'} \left(q_{\perp\alpha}'' q_{\perp\beta}' \right) \left(p_{\perp\alpha'}'' p_{\perp\beta'}' \right) \right) \right) \Big\} \Big] ,$$

$$\tag{C7}$$

where

$$\mathcal{Z}^{l'} \; = \; \mathcal{M}_N^2 zz'(z'+z) + z(\boldsymbol{p}_\perp'^2 + M^2) + z'(\boldsymbol{p}_\perp^2 + M^2), \tag{C8}$$

$$\mathcal{Z}'' \; = \; \mathcal{M}_N^2 zz''(z''+z) + z(\boldsymbol{p}_\perp''^2 + M^2) + z''(\boldsymbol{p}_\perp^2 + M^2), \tag{C9}$$

and

$$\boldsymbol{q}' \; = \; \left((\boldsymbol{p}_\perp + \boldsymbol{p}_\perp'), (z+z')\mathcal{M}_N \right), \quad Q_{\perp\alpha}' = z p_{\perp\alpha}' - z' p_{\perp\alpha}, \quad \alpha = 1,2, \tag{C10}$$

$$\boldsymbol{q}'' \; = \; \left((\boldsymbol{p}_\perp + \boldsymbol{p}_\perp''), (z+z'')\mathcal{M}_N \right), \quad Q_{\perp\alpha}'' = z p_{\perp\alpha}'' - z'' p_{\perp\alpha}, \quad \alpha = 1,2. \tag{C11}$$

References

[1] D.J.Gross and Frack Wilczek, *Phys. Rev.*, D8:3633, 1973.

[2] D.J.Gross and Frack Wilczek, *Phys. Rev. Lett.* 30:1343, 1973.

[3] H.David Politzer, *Phys. Rept.* 14:129, 1974.

[4] EMC Collaboration : J. Ashman et al. *Phys. Lett.* B206:364, 1988.

[5] EMC Collaboration : J. Ashman et al. *Nucl. Phys.* B328:1, 1989.

[6] SMC Collaboration :B. Adeva et al. *Phys. Rev.* D58:112001, 1998.

[7] R. L. Jaffe and Aneesh Manohar, *Nucl. Phys.* B337:509, 1990.

[8] Xiang-Dong Ji, *Phys. Rev. Lett.* 78:610, 1997.

[9] Stanley J. Brodsky, John Ellis and Marek Karliner, *Phys. Lett.* B206:309, 1988.

[10] B.W. Filippone and Xiang-Dong Ji, *Adv. Nucl. Phys.* 26:1, 2001.

[11] Hai-Yang Cheng, *Int. J. Mod. Phys.* A11:5109, 1996.

[12] Stevev D. Bass, *hep-ph*/0411005.

[13] K. Goeke, Maxim V Polyakov and M. Vanderhaeghen, *Prog. Part. Nucl. Phys.* 47:401, 2001.

[14] M. Diehl, *Phys. Rept.* 388:41, 2003.

[15] A. V. Belitsky and A. V. Radyushkin, *Phys. Rept.* 418:1, 2005.

[16] Xiang-Dong Ji, *J. Phys.* G24:1181, 1998.

[17] A. V. Radyushkin, *Phys. Rev.* D56:5524, 1997.

[18] V. L. Chernyak, A. R. Zhitnitsky, *JETP Lett.* 25:510, 1977.

[19] G. Peter Lepage and Stanly J. Brodsky, *Phys. Lett.* B87:359, 1979.

[20] A. V. Efremov and A. V. Radyushikin, *Phys. Lett.* B94:245, 1980.

[21] Stanly J. Brodsky, Hans-Christian Pauli and Stephen S. Pinsky, *Phys. Rept.* 301:299, 1998.

[22] G. Peter Lepage and Stanley J. Brodsky. *Phys. Rev.* D22:2157, 1980.

[23] M. Diehl, T. Feldmann, R. Jakob and P. Kroll, *Nucl. Phys.* B596:33, 2001.

[24] Stanley J. Brodsky, Markus Diehl, and Dae Sung Hwang, *Nucl. Phys.* B596:99, 2001.

[25] V. Yu. Petrov and Maxim V. Polyakov, *hep-ph*/0307077, 2003.

[26] Dmitri Diakonov and V. Yu. Petrov, *Nucl. Phys.* B245:259, 1984.

[27] Dmitri Diakonov and V. Yu. Petrov, *Nucl. Phys.* B272:457, 1986.

[28] Dmitri Diakonov, V. Yu. Petrov, and P. V. Pobylitsa, *Nucl. Phys.* B306:809, 1988.

[29] M. Wakamatsu and H.Yoshiki, *Nucl. Phys.* A524:600, 1991.

[30] Dmitri Diakonov, *hep-ph*/0408219, 2004.

[31] Dmitri Diakonov, *Annalen Phys.* 12:637, 2004.

[32] Dmitri Diakonov and Victor Petrov, *Phys. Rev.* D72:074009, 2005.

[33] Hai-Yan Gao, *Int. J. Mod. Phys.* E12:1, 2003.

[34] Xiang-Dong Ji, *J. Phys.* G24:1181, 1998.

[35] Dennis W. Sivers, *Phys. Rev.* D41:83, 1990.

[36] P. J. Mulders and R. D. Tangerman, *Nucl. Phys.* B461:197, 1996.

[37] Daniel Boer and P. J. Mulders, Phys. Rev. D57:5780, 1996.

[38] Daniel Boer, P. J. Mulders, and F.Pijlman, *Nucl. Phys.* B667:201, 2003.

[39] Xiang-Dong Ji, *Phys. Rev.* D55:7114, 1997.

[40] Davison E. Soper, *Phys. Rev.* D15:1141, 1977.

[41] John P. Ralston and Bernard Pire, *Phys. Rev.* D66:111501, 2002.

[42] M. Diehl, *Eur. Phys. J.* C25:223, 2002.

[43] Andrei V. Belitsky and Dieter Muller, *Nucl. Phys.* A711:118, 2002.

[44] HERMES Collaboration: A. Airapetian et al., *Phys. Rev. Lett.* 87:182001, 2001.

[45] CLAS Collaboration : S. Stepanyan et al., *Phys. Rev. Lett.* 87:182002, 2001.

[46] H1 Collaboration: C. Adloff et al., *Phys. Lett.* B517:47, 2001.

[47] ZEUS Collaboration: P. R. B. Saull et al., *hep-ex*/0003030, 1999.

[48] Dieter Mueller, D. Robaschik, B. Geyer, F. M. Dittes, and J. Horejsi, *Fortsch. Phys.* 42:101, 1994.

[49] A. V. Radyushkin, *Phys. Lett.* B380:417, 1996.

[50] A. V. Radyushkin, *Phys. Rev.* D56:5524, 1997.

[51] A. V. Radyushkin, *hep-ph*/0101225, 2001.

[52] Andrei V. Belitsky, Dieter Mueller, A. Kirchner, and A. Schafer, *Phys. Rev.* D64:116002, 2001.

[53] O. V. Teryaev, *Phys. Lett.* B510:125, 2001.

[54] Maxim V. Polyakov and C.Weiss, *Phys. Rev.* D60:114017, 1999.

[55] G. S. Danilov, I. T. Dyatlov, and V. Yu. Petrov, *Nucl. Phys.* B174:68, 1980.

[56] M. V. Polyakov, *Phys. Lett.* B555:57, 2003.

[57] V. Yu. Petrov, P. V. Pobylitsa, Maxim V. Polyakov, I. Bornig, K. Goeke, and C. Weiss, *Phys. Rev.* D57:4325, 1988.

[58] J. Ossmann, M. V. Polyakov, P. Schweitzer, D. Urbao, and K. Goeke, *Phys. Rev.* D71:034011, 2005.

[59] M. Wakamatsu and H. Tsujimoto, *Phys. Rev.* D71:074001, 2005.

[60] M. Wakamatsu, *Phys. Rev.* D72:074006, 2005.

[61] M. Wakamatsu, T. Watabe, *Phys. Lett.* B312:184, 1993.

[62] M. Wakamatsu and T. Kubota, *Phys. Rev.* D60:034020, 1999.

[63] M. Wakamatsu and T. Watabe, *Phys. Rev.* D62:017506, 2000.

[64] M. Wakamatsu and T. Watabe, *Phys. Rev.* D62:054009, 2000.

[65] M. Wakamatsu, *Phys. Lett.* B487:118, 2000.

[66] Y. Ohnishi and M. Wakamatsu *Phys. Rev.* D69:114002, 2004.

[67] M. Wakamatsu and Y. Ohnishi *Phys. Rev* D67:114011, 2003.

[68] Dmitri Diakonov, V. Petrov, P. Pobilitsa and Maxim V. Polyakov, *Nucl. Phys.* B480:341, 1996.

[69] Dmitri Diakonov, V. Yu. Petrov, P. V. Pobilitsa, Maxim V. Polyakov and C. Weiss, *Phys. Rev.* D56:4069, 1997.

[70] M. Wakamatsu, *Phys. Rev.* D67:034005, 2003.

[71] M. Wakamatsu, *Phys. Rev.* D67:034006, 2003.

[72] NuTeV Collaboration, G. P. Zeller et al., *Phys. Rev. Lett.* 88:091802, 2002.

[73] NuTeV Collaboration, G. P. Zeller et al., *Phys. Rev.* D65:111103, 2002.

[74] F. Olness, J. Pumplin, D. Stump, J. Huston, P. Nadolsky, H.-L. Lai, S. Kretzer, J. Fowens, and W. K. Tung, *hep-ph*/0312323, 2003.

[75] S. Kretzer, F. Olness, J. Pumplin, D. Stump, W. K. Tung, and M. H. Peno, *Phys. Rev. Lett.* 93:041802, 2004.

[76] M. Wakamatsu, *Phys. Rev.* D71:057504, 2005.

[77] NMC Collaboration, P. Amaudruz et al., *Phys. Rev. Lett.* 66:2712, 1991.

[78] E. M. Henley and G. A. Miller, *Phys. Lett.* B251:453, 1990.

[79] HERMES Collaboration, A. Airapetian et al., *Phys. Rev.* D64:097101, 2001.

[80] Fermilab E704 Collaboration, A. Bravar et al., *Phys. Rev. Lett.* 77:2626, 1996.

[81] A. V. Efremov, K. Goeke, S. Menzel, A. Metz, and P. Schweitzer, *Phys. Lett.* B612:233, 2005.

[82] J. C. Collins, A. V. Efremov, K. Goeke, M. Gross Perdekamp, S. Menzel,B. Meredith, A. Metz, and P. Schweitzer, *hep-ph*/0510342, 2005.

[83] P. V. Pobilitsa, *hep-ph*/0212027, 2002.

[84] P. V. Pobilitsa, *hep-ph*/0301236, 2003.

[85] M. Wakamatsu, *Phys. Lett.* B269:394, 1991.

[86] M. Wakamatsu, *Phys. Rev.* D46:3762, 1992.

[87] HERMES Collaboration, F. Ellinghaus et al., *Nucl. Phys.* A711:171, 2002.

[88] Mattias Burkardt, *Int. J. Mod. Phys.* A18:173, 2003.

研究業績

学会誌等における誌上発表

- Masashi Wakamatsu and Youichi Ohnishi,

  "The nonperturbative origin of delta function singularity in the chirally odd twist three distribution function $e(x)$"

  Physical Review D 誌、67 号、114011、2003 年 6 月

- Youichi Ohnishi and Masashi Wakamatsu,

  "pi N sigma term and chiral-odd twist-3 distribution function $e(x)$ of the nucleon in the chiral quark soliton model"

  Physical Review D 誌、69 号、114002、2004 年 6 月

- Y. Ohnishi and M. Wakamatsu

  "The chiral-odd twist-3 distribution $e(x)$ of the nucleon"

  Nuclear　Physics A 誌、755C 号、341 項 - 344 項

学会等における口頭発表

- Youichi Ohnishi and Masashi Wakamatsu

  10th International Conference BARYONS04

  France 　palaiseau 　2004 年 10 月 28 日

  "The chiral-odd twist-3 distribution $e(x)$ of the nucleon"

- Youichi Ohnishi and Masashi Wakamatsu

  The 5th Circum-Pan-Pacific Symposium on 'High Energy Spin Physics'

  Tokyo Institute of Technology, Tokyo, Japan, on July 5-8, 2005

  "Chiral-odd twist-3 distribution $e(x)$ of the nucleon"

- 大西陽一　若松正志

  日本物理学会　第５８回年次大会

  　於東北学院大学土樋キャンパス 2003 年 3 月 30 日

  「カイラル・クォーク・ソリトン模型に基づくカイラリティ奇，ツイスト３分布関数 $e(x)$ 」

- 大西陽一　若松正志

  日本物理学会 秋季大会

  於宮崎ワールドコンベンションセンター・サミット　　2003年9月9日

  「カイラリティ奇・ツイスト3の分布関数 $e(x)$ とその和則」

- 大西陽一　若松正志―

  日本物理学会　第59回年次大会

  於九州大学箱崎キャンパス　2004年3月29日

  「The scalar form factor on the basis of the chiral quark soliton model」

- 大西陽一　若松正志

  日本物理学会 第60回年次大会

  於東京理科大野田キャンパス　2005年3月27日

  「カイラル・クォーク・ソリトン模型に基づくエキゾチックバリオンのクォーク構造」

- 大西陽一　若松正志

  「原子核理論呑舟研究会」

  at KEK 2005年3月22日

  「Quark strcuture of the exotic antidecuplte in the chiral quark soliton model」